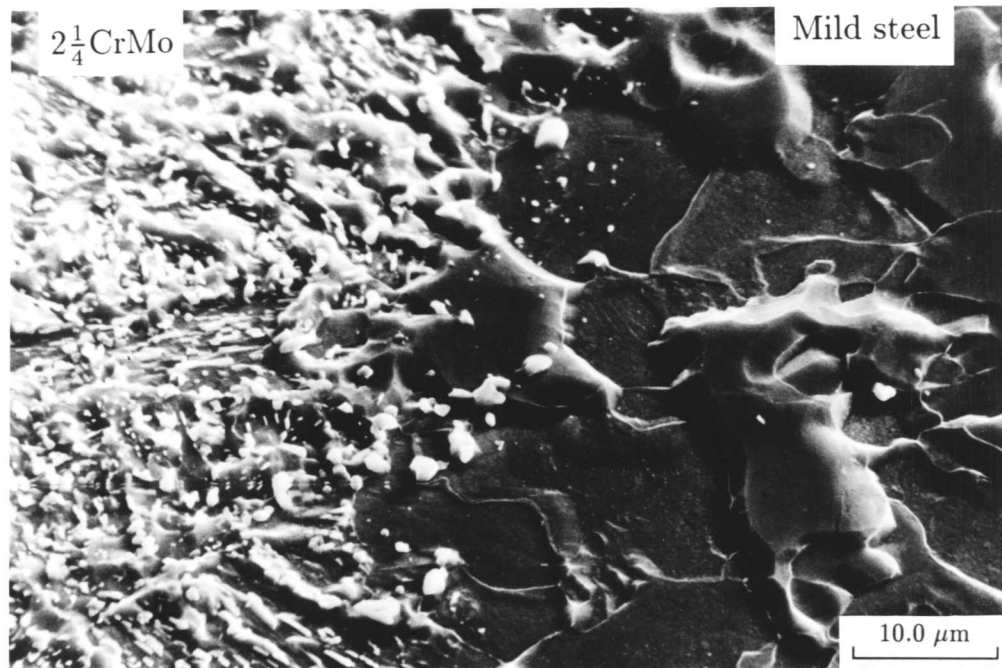


a) Parent plate



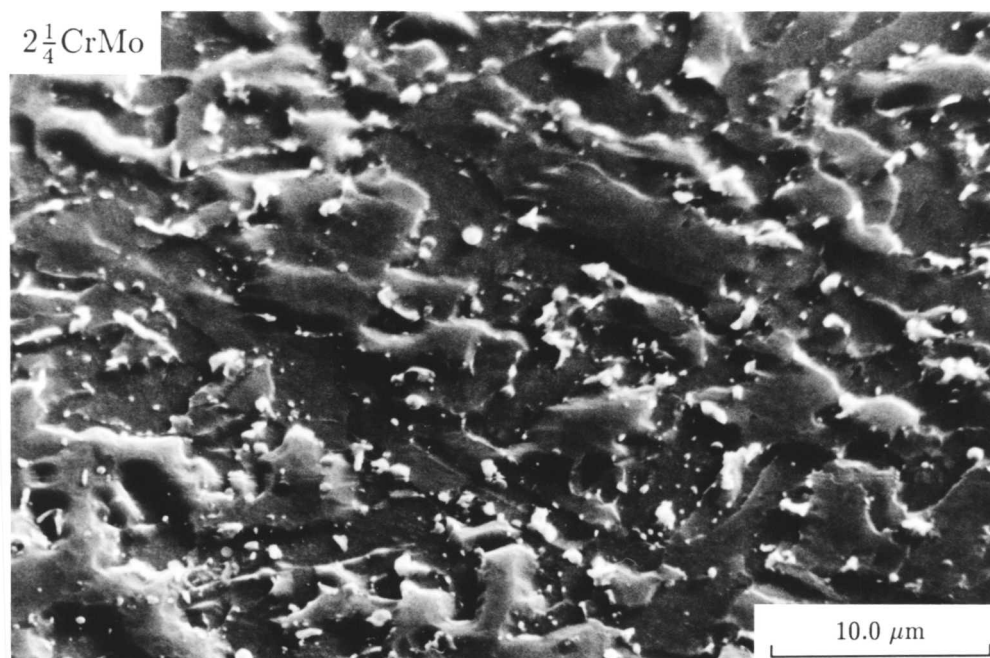
b) Interface region

Figure 6.12: SEM micrographs of mild steel/ $2\frac{1}{4}$ CrMo joint heat treated at 700°C for 1024 hours





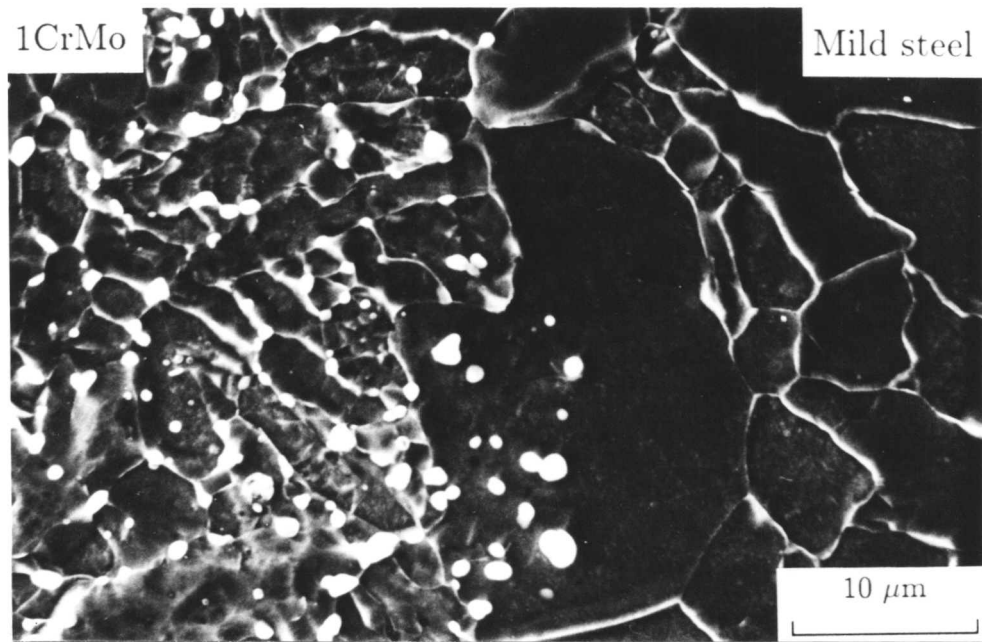
c) Detail of carbides in the interface region



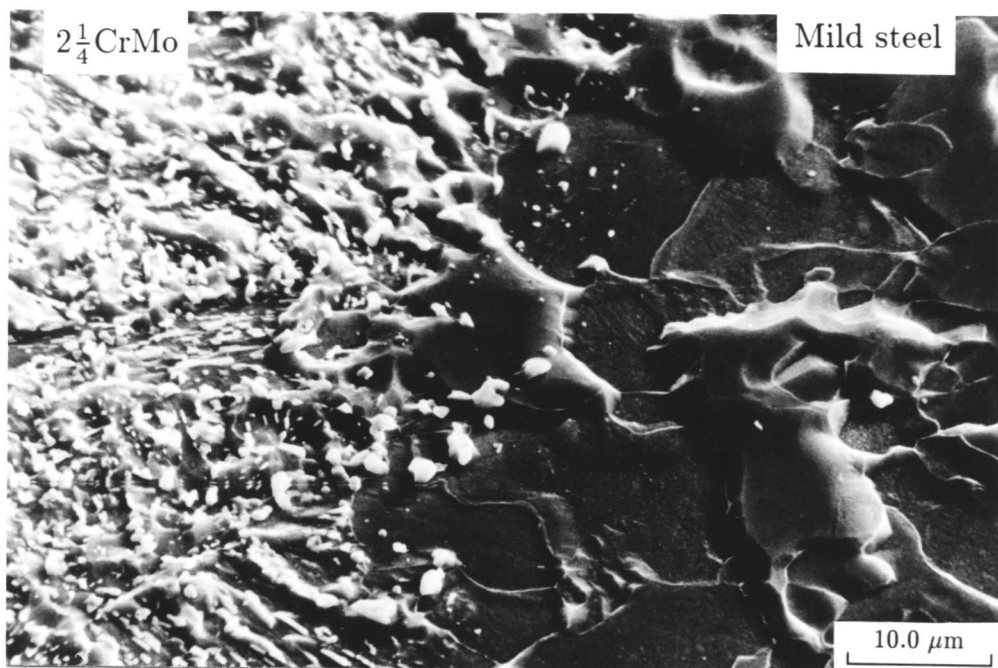
d) Weld metal

Figure 6.12: SEM micrographs of mild steel/ $2\frac{1}{4}\text{CrMo}$ joint heat treated at 700°C for 1024 hours





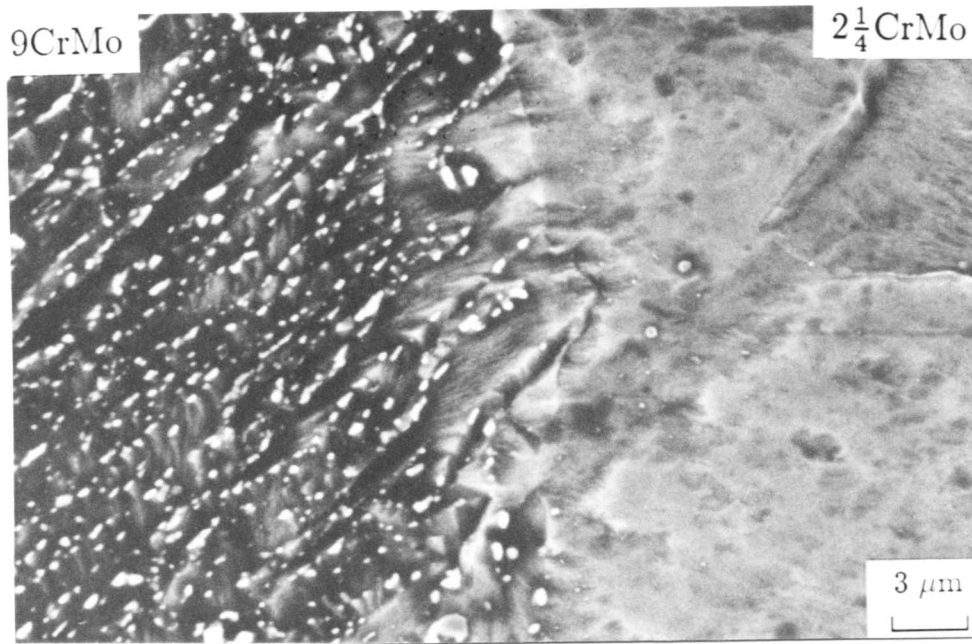
a) Mild steel/1CrMo - 700°C



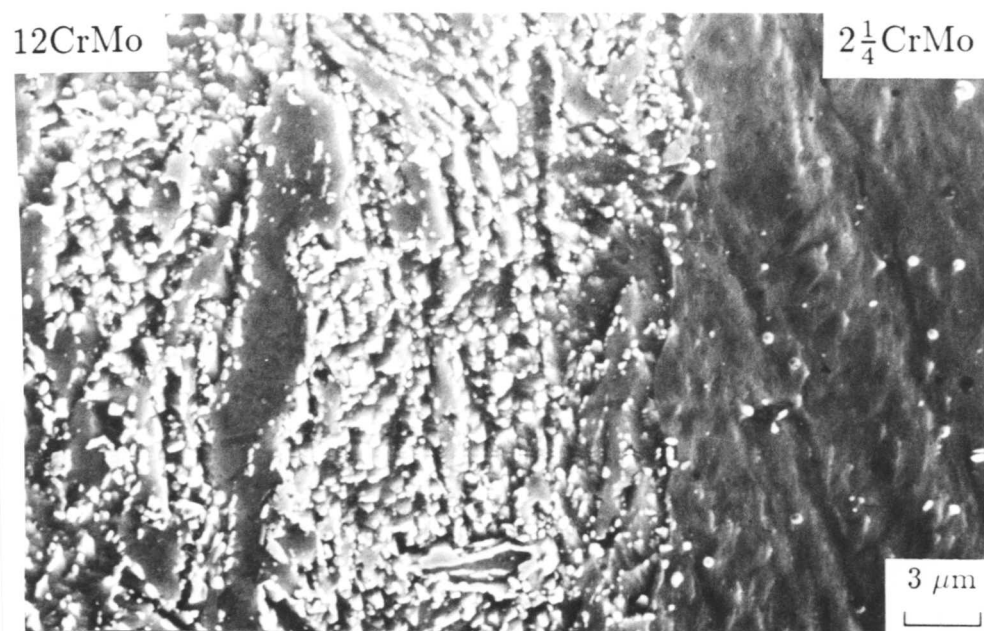
b) Mild steel/2 $\frac{1}{4}$ CrMo - 700°C

Figure 6.13: SEM micrographs of all joints heat treated at the post weld heat treatment temperature for 1024 hours





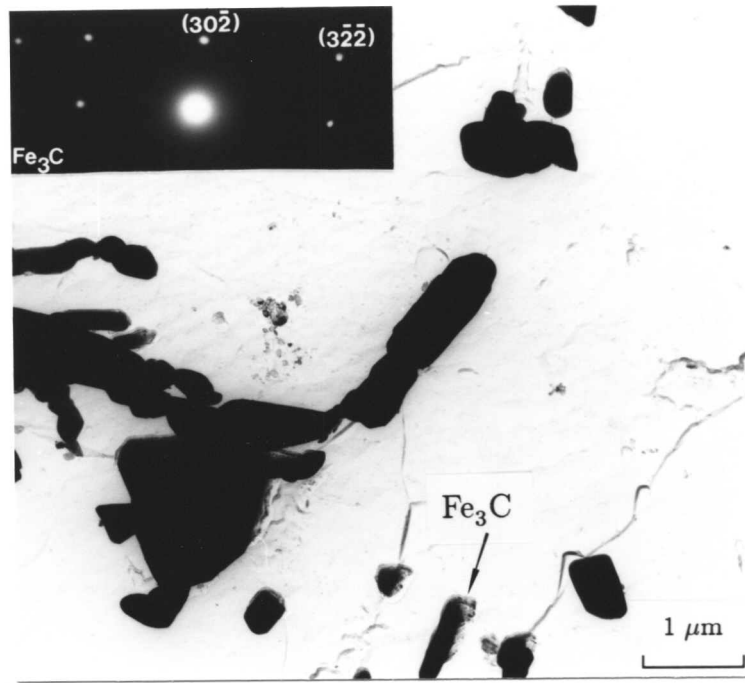
c) 2 1/4CrMo/9CrMo - 730°C



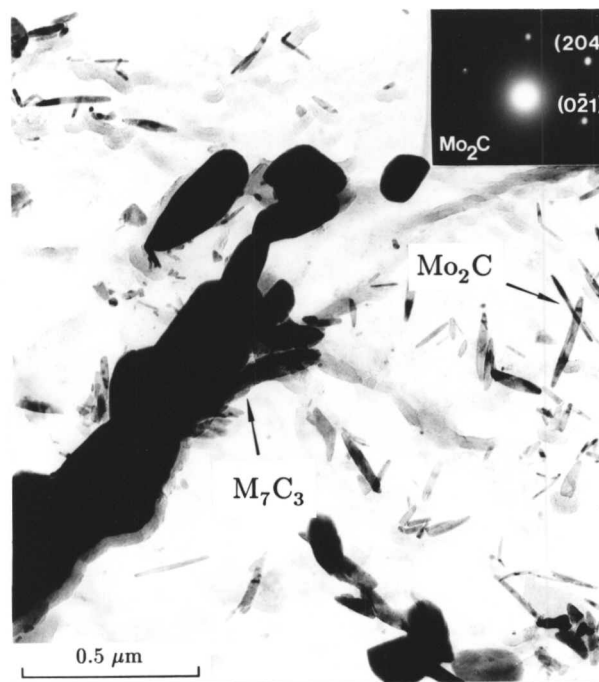
d) 2 1/4CrMo/12CrMo - 730°C

Figure 6.13: SEM micrographs of all joints heat treated at the post weld heat treatment temperature for 1024 hours





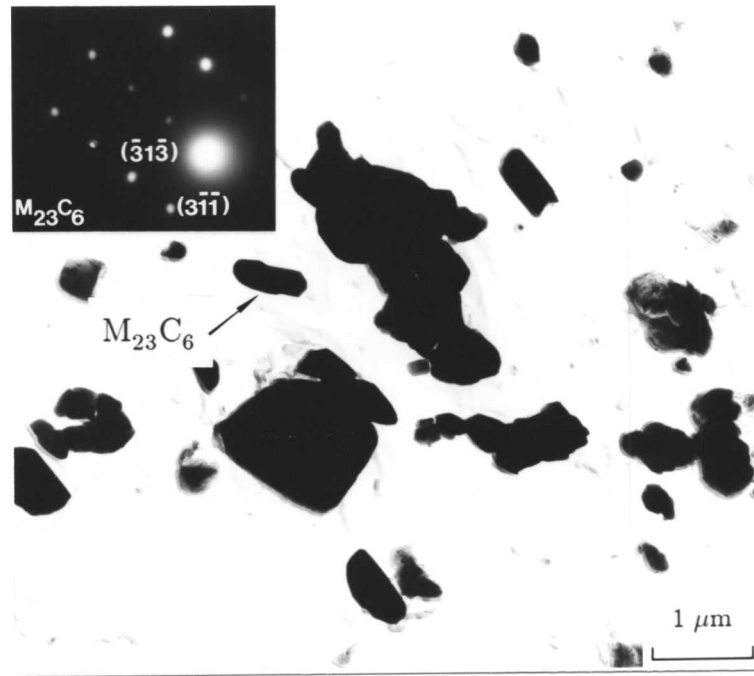
a) Morphology of Fe_3C particle in $2\frac{1}{4}\text{CrMo}$



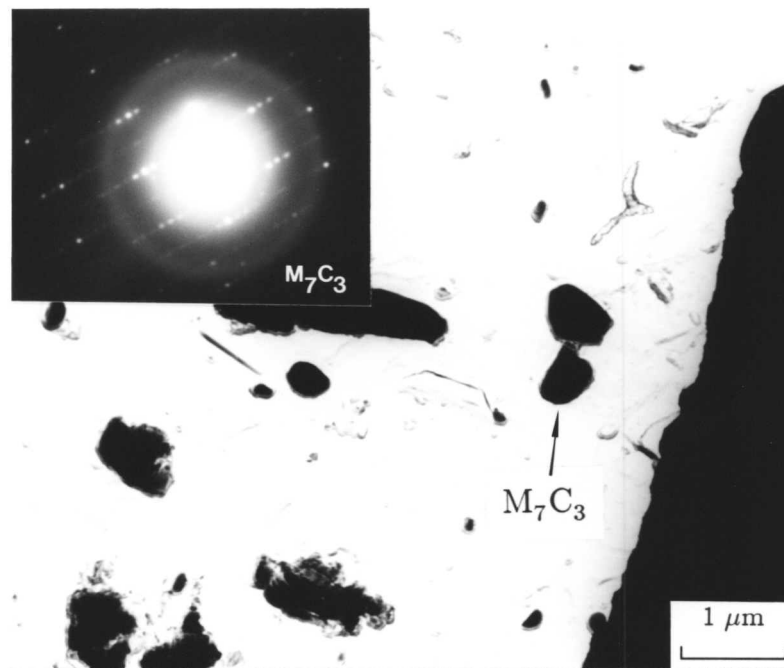
b) Morphology of Mo_2C particle in $2\frac{1}{4}\text{CrMo}$

Figure 6.14: TEM micrographs of $2\frac{1}{4}\text{CrMo}$ joint heat treated at 700°C



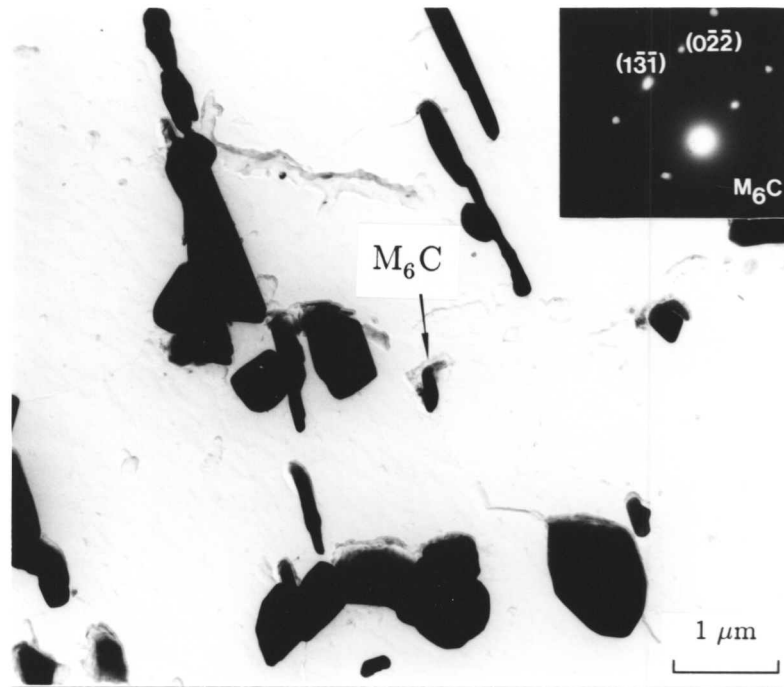


c) Morphology of $M_{23}C_6$ particle in $2\frac{1}{4}CrMo$



d) Morphology of M_7C_3 particle in $2\frac{1}{4}CrMo$

Figure 6.14: TEM micrographs of $2\frac{1}{4}CrMo$ joint heat treated at $700^\circ C$



e) Morphology of M_6C in $2\frac{1}{4}CrMo$

Figure 6.14: TEM micrographs of $2\frac{1}{4}CrMo$ joint heat treated at $700^\circ C$



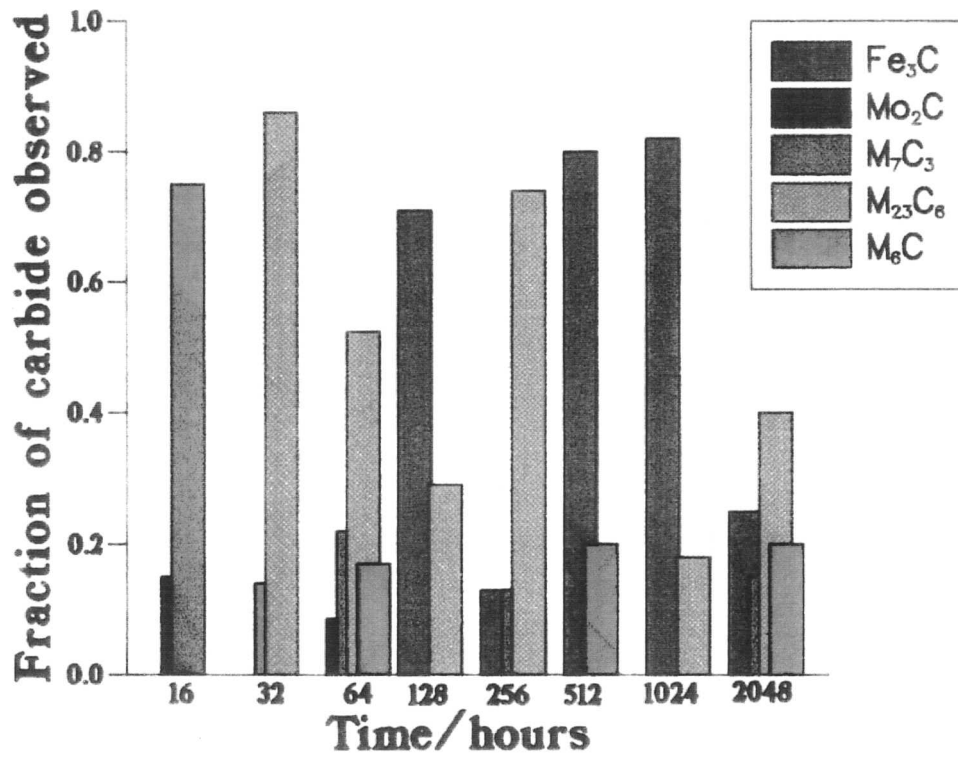


Figure 6.15: Fraction of each carbide type found at the various heat treatment times in $2\frac{1}{4}$ CrMo heat treated at 700°C

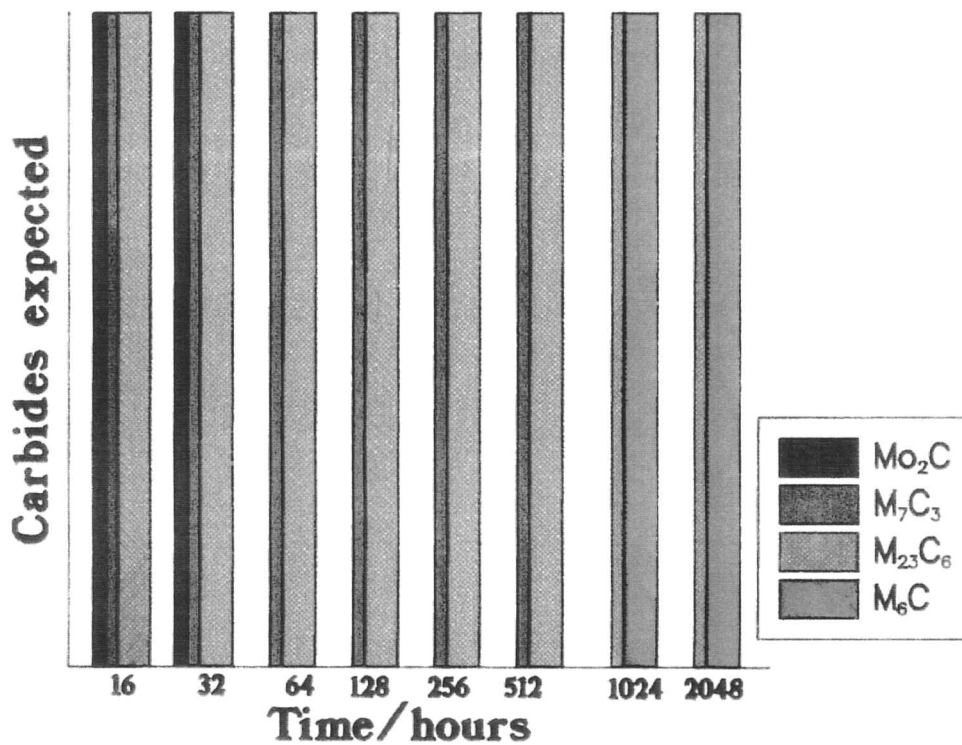


Figure 6.16: Predicted carbides in $2\frac{1}{4}$ CrMo heat treated at 700°C from the work of Baker and Nutting (1959)

cementite in a ferrite matrix up until the longest times. The carbide present in the 12CrMo was $M_{23}C_6$ for all of the specimens up until 10,000 hours. The 9CrMo side of the $2\frac{1}{4}$ CrMo/9CrMo joint showed varying proportions of $M_{23}C_6$ and M_7C_3 as illustrated in Figure 6.18. The presence of M_7C_3 is consistent with MTDATA calculations for this joint (Section 2.8.3) but no other authors have reported the presence of $M_{23}C_6$ and M_7C_3 concurrently in the microstructure even at the longest tempering times.

Carbide	Carbide composition /wt%			
	Fe	Cr	Mn	Mo
Fe_3C	65.1	24.8	9.8	0.3
Mo_2C	–	18.0	–	82.0
$M_{23}C_6$	40.6	51.1	7.8	0.5
M_7C_3	54.2	33.4	6.3	0.1
M_6C	39.0	17.0	40.0	4.0

Table 6.2: Typical EDX compositions of the carbides found in $2\frac{1}{4}$ CrMo heat treated at 700°C. It should be noted that this table neglects carbon which cannot be detected on the equipment used which has a Be window on the EDX detector.

The size and distribution of the carbides in the joints varied with time and temperature as illustrated in Figure 6.19 and Figure 6.20. These micrographs are of the 12CrMo joint in which the carbide type remained as $M_{23}C_6$. It can be seen that with increasing time at the same temperature there is an increase in the particle size and a decrease in the particle volume fraction. With increasing temperature the particle size increases and the volume fraction decreases.

6.6 Summary of results presented

The salient results from this experimental work are:-

1. The decarburised zone width levels off on a plot against root time where parabolic growth theory would predict linear behaviour.
2. The precipitation sequences on the high alloy side of the weld are changed, reverting back to carbide phases which had previously dissolved.



These results require discussion and explanation in order that they may be incorporated into any successful model.

Consider what is occurring during the diffusion of carbon across the interface. Effectively, the average carbon concentration in the interface region is decreasing on the low alloy side and increasing on the high alloy side. This results in local changes in the bulk carbon concentration. If MTDATA calculations are made for the $2\frac{1}{4}$ CrMo steel by increasing the carbon concentration of the alloy then the volume fractions and types of carbide depicted in Figure 6.21 are predicted. Thus it can be seen that the lower order carbides become stable again as the carbon concentration is increased. This is what is effectively occurring in the welded joint together with the normal precipitation sequence of Figure 6.16 superimposed. The reason that the 12CrMo side remains as $M_{23}C_6$ is that MTDATA calculations predict that the average carbon concentration in the joint would have to rise to 3wt% in order to reprecipitate cementite (Figure 6.22). The conclusion is that the change in precipitation sequences on the high alloy side of dissimilar metal welds is a result of the local increase in carbon concentration. This, in turn, is going to affect the driving force for diffusion across the joint as will be described in Section 7.7.4 and will influence the decarburised zone width plot.

Other results that need to be able to be predicted are:-

1. The decarburised zone width increases with both time and temperature.
2. The effect of alloy content on the extent of decarburisation.
3. The extent of carburisation.

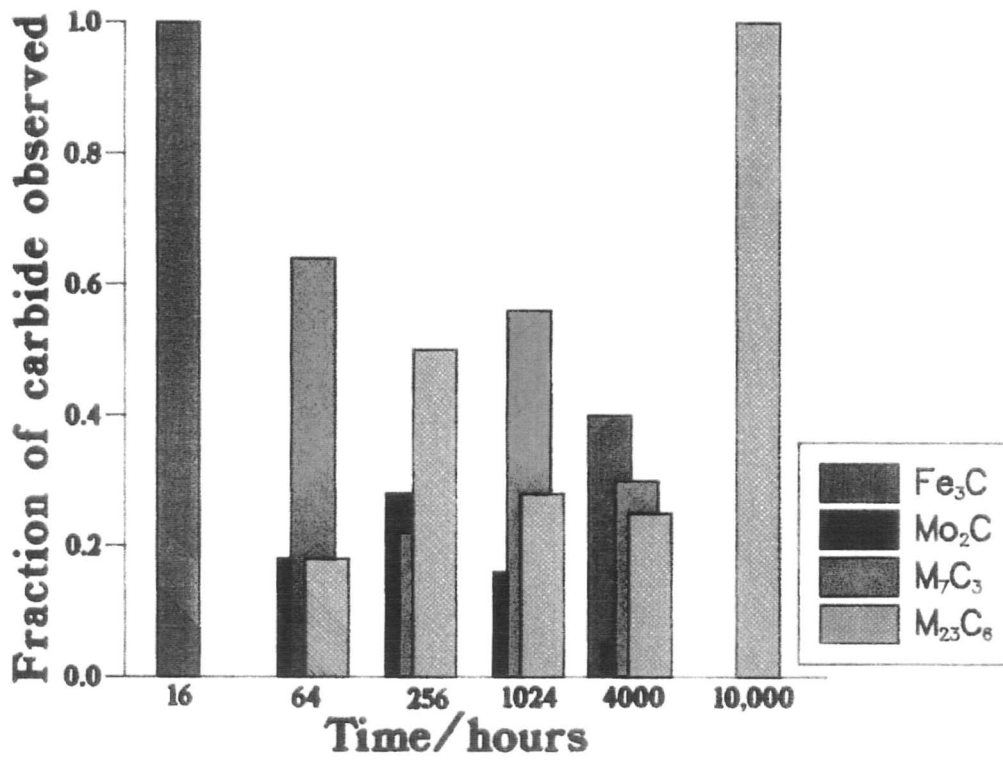


Figure 6.17: Fraction of each carbide type found at the various heat treatment times in 2 $\frac{1}{4}$ CrMo heat treated at 620°C

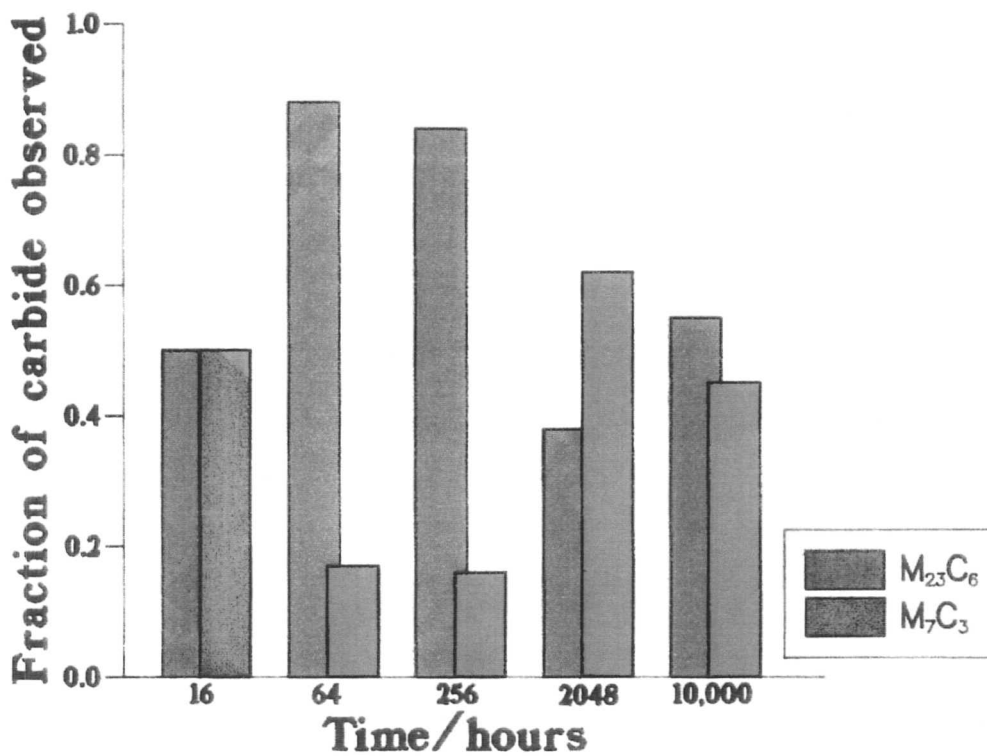
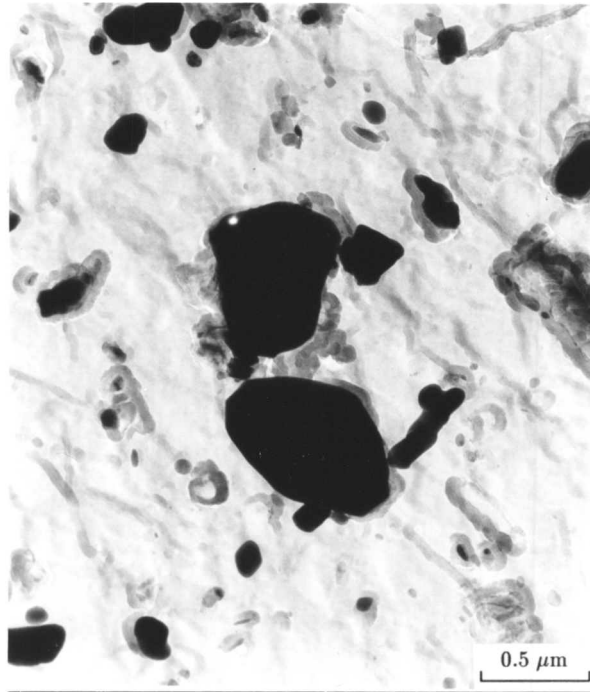
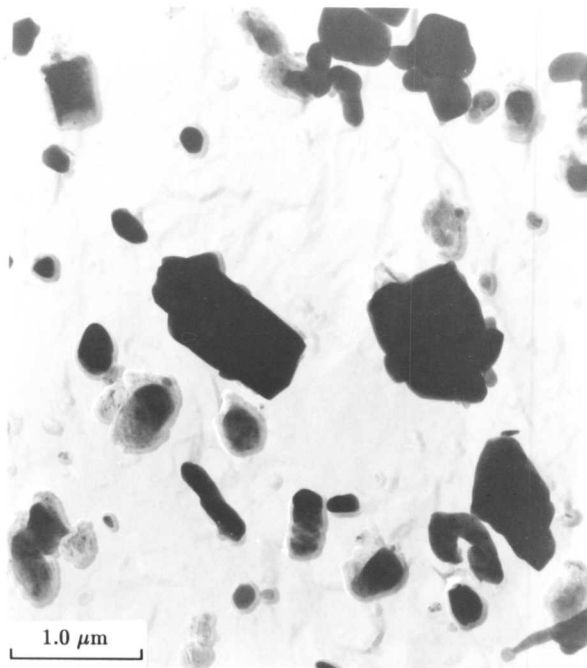


Figure 6.18: Fraction of each carbide type found at the various heat treatment times in 9CrMo heat treated at 730°C

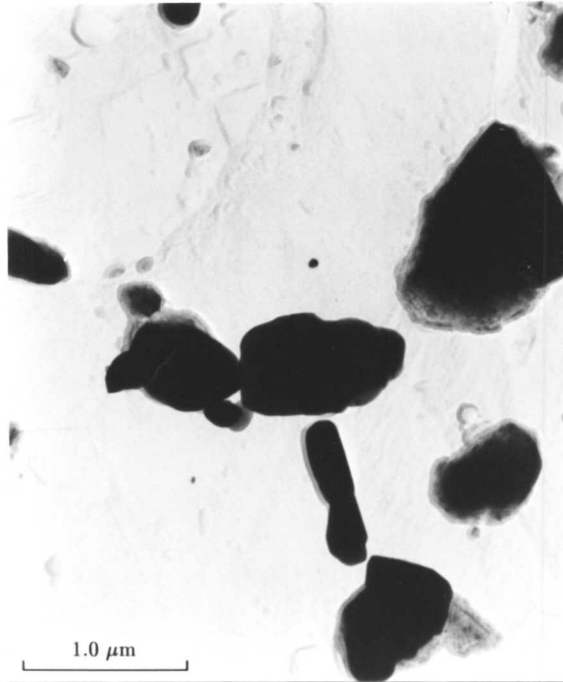


a) 16 hours



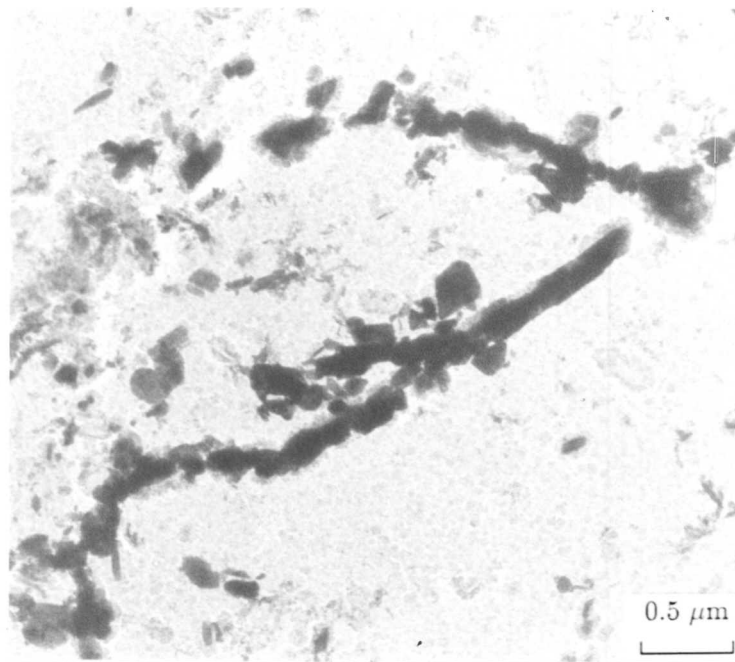
b) 256 hours

Figure 6.19: Carbon extraction replicas from 12CrMo heat treated at 730°C for various times



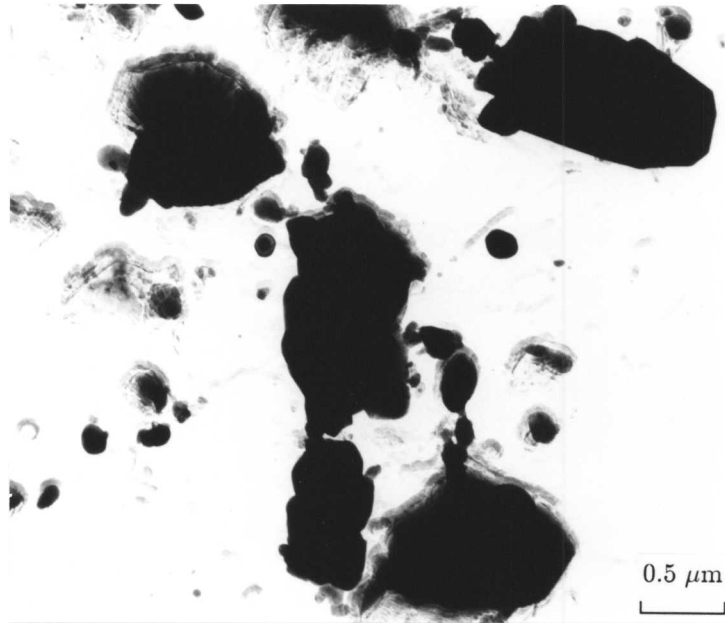
c) 2048 hours

Figure 6.19: Carbon extraction replicas from 12CrMo heat treated at 730°C for various times

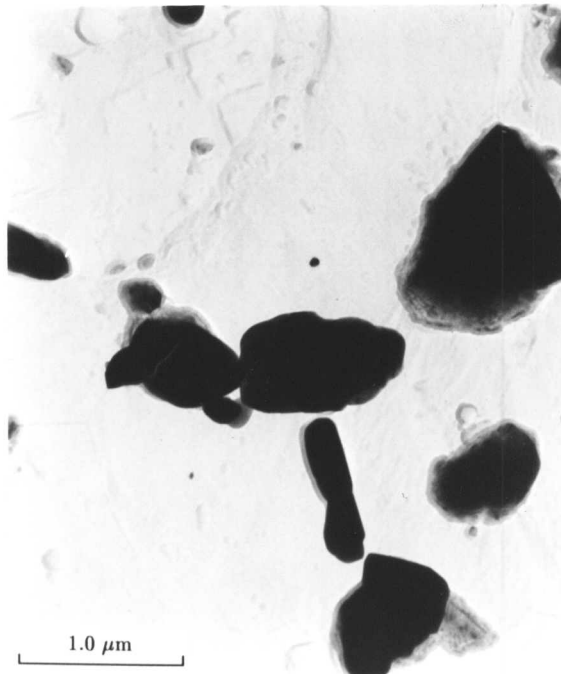


a) 565°C

Figure 6.20: Carbon extraction replicas from 12CrMo heat treated for 2048 hours at various temperatures



b) 620°C



c) 730°C

Figure 6.20: Carbon extraction replicas from 12CrMo heat treated for 2048 hours at various temperatures

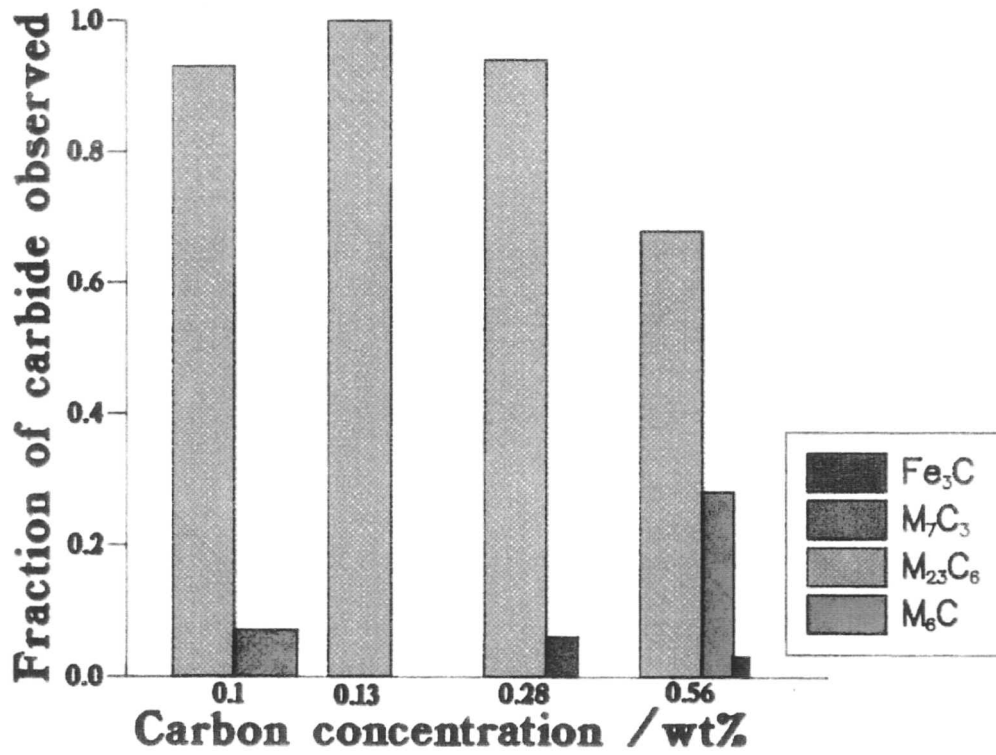


Figure 6.21: MTDATA predictions of carbon types and volume fraction in 2 $\frac{1}{4}$ CrMo with increasing carbon concentration

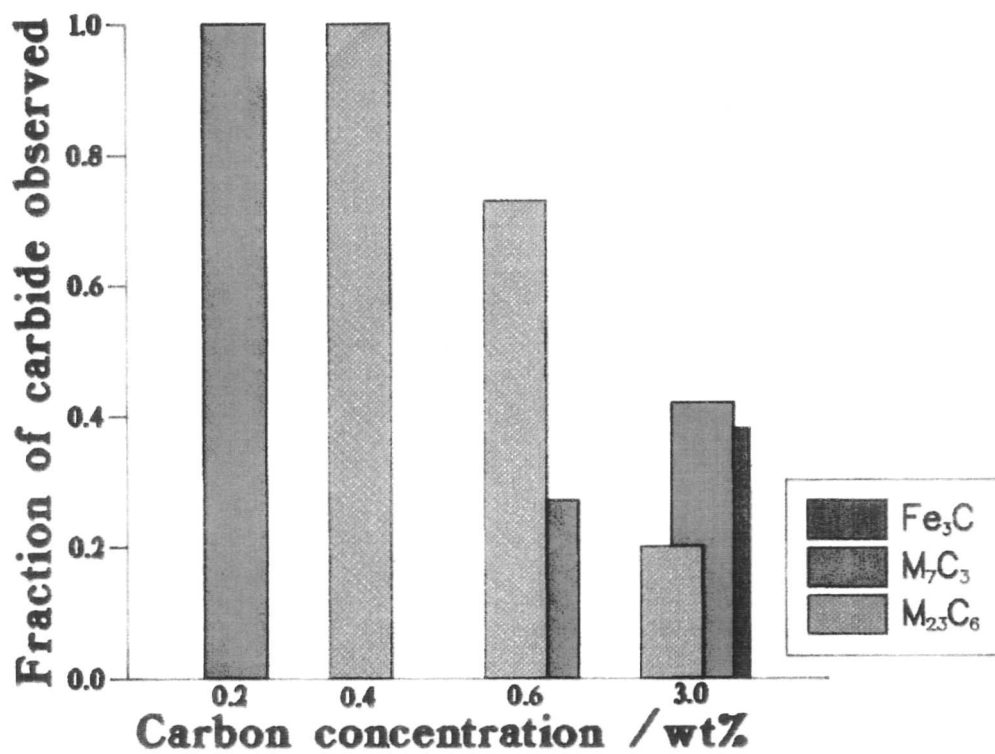


Figure 6.22: MTDATA predictions of carbon types and volume fraction in 12CrMo with increasing carbon concentration

CHAPTER 7

Modelling of carbon diffusion across dissimilar metal welds in ferrite

7.1 Model for the determination of the decarburised zone width

A search of the literature has revealed no model which can successfully predict decarburised zone widths in the ferrite phase field because none of the models takes into account the dissolution and precipitation of carbides which occurs on either side of the interface. In this work, a theory has been developed which attempts to account for these processes.

The carbides on either side of the weld interface are represented as particles of carbide in a ferrite matrix as illustrated in Figure 7.1. The substitutional alloy content is such that diffusion will occur from the α to the β side of the weld interface.

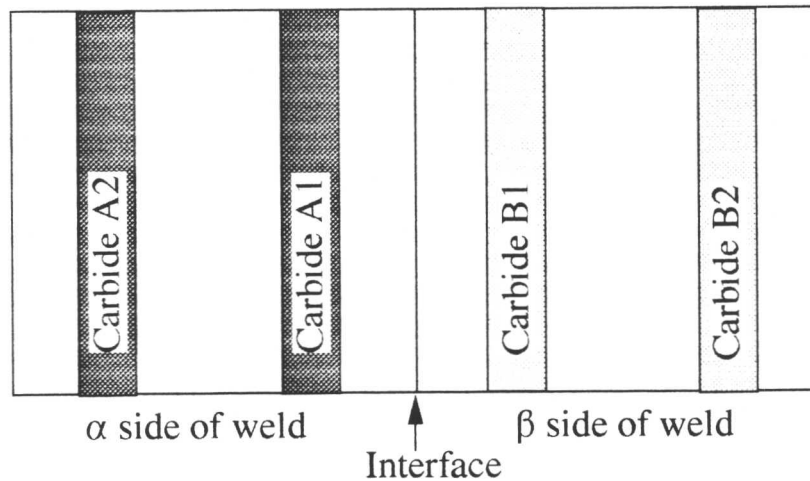


Figure 7.1: Illustration of the particulate nature of the model.

The decarburised zone width is defined as the distance from the weld interface to the carbide particle that is dissolving at any time t after diffusion has been allowed to occur. The initial distance from the interface is z_o^A (as illustrated in Figure 7.2). With increasing time, the particle, A1, will progressively dissolve so that the distance z_o^A increases to z_i^A . The decarburised zone width, η^α , is therefore given by:-

$$\eta^\alpha = z_i^A \quad (7.1)$$

There are two models that have been developed to determine a value of z_i^A ; one which approximates constant concentration gradients in the ferrite and another which is based on

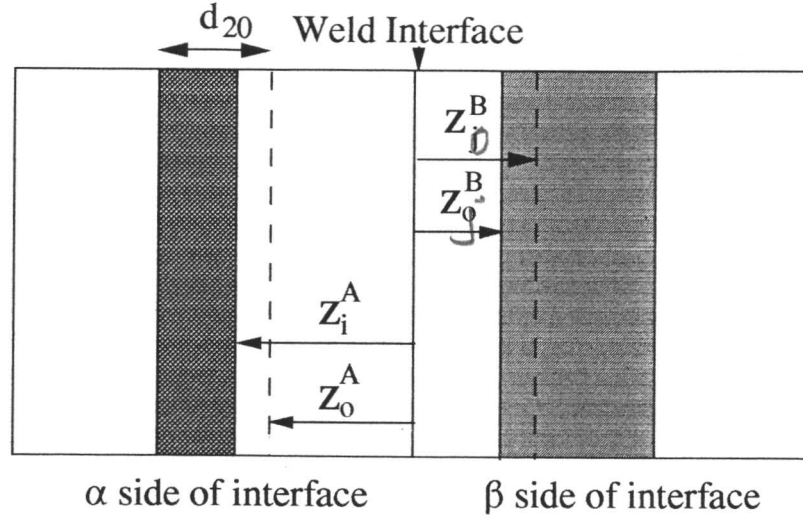


Figure 7.2: Illustration of the diffusion distances in the model.

exponential profile. Both of these profiles are illustrated in Figure 7.3 together with the variety of carbon concentration terms. Thus $x^{A\alpha}$ is the carbon concentration of the carbide which is in equilibrium with the ferrite on the low alloy side of the weld interface and $x^{\alpha A}$ is the carbon concentration of the ferrite which is in equilibrium with the carbide on the low alloy side of the weld interface. Similarly on the high alloy side of the weld $x^{B\beta}$ is the carbon concentration in the carbide which is in equilibrium with ferrite and $x^{\beta B}$ is the carbon concentration in the ferrite which is in equilibrium with the carbide. These carbon concentrations can be calculated using MTDATA (1989). The interface carbon concentrations, $x^{\alpha\beta}$ and $x^{\beta\alpha}$ are also illustrated in Figure 7.3. $x^{\alpha\beta}$ is therefore the concentration of carbon in α at the α/β interface and similarly $x^{\beta\alpha}$ is the carbon concentration in β at the α/β interface.

7.1.1 Constant concentration gradient model

If a linear concentration profile is assumed as illustrated in Figure 7.3(a) then mass conservation requires that for the i th particle A,

$$V_i^A(x^{A\alpha} - x^{\alpha A}) = \frac{(x^{\alpha A} - x^{\alpha\beta})D_\alpha}{z_i^A} \quad (7.2)$$

where $V_i = \frac{\partial z_i^A}{\partial t}$, so that

$$\frac{\partial z_i^A}{\partial t}(x^{A\alpha} - x^{\alpha A}) = \frac{(x^{\alpha A} - x^{\alpha\beta})D_\alpha}{z_i^A} \quad (7.3)$$

Integrating this expression:-

$$\int_{z_0^A}^{z_i^A} z_i^A \partial z_i^A = \int_0^t D_\alpha \frac{(x^{\alpha A} - x^{\alpha\beta})}{(x^{A\alpha} - x^{\alpha A})} \partial t \quad (7.4)$$

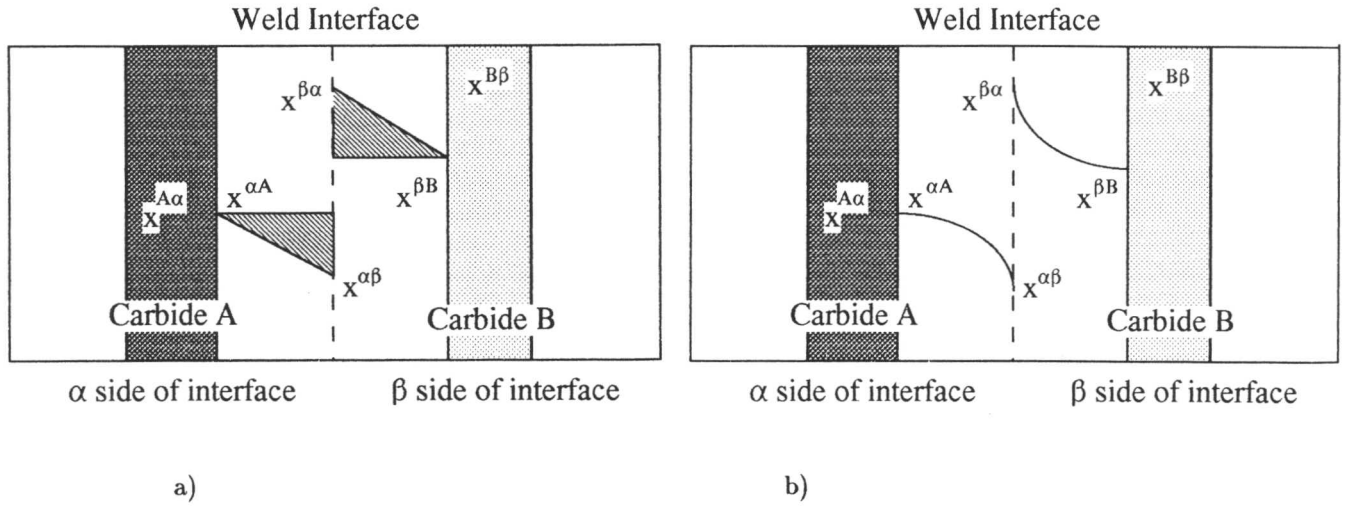


Figure 7.3: Illustration of the two concentration gradients assumed : a) linear
b) exponential.

Thus

$$\frac{1}{2} \{ (z_i^A)^2 - (z_o^A)^2 \} = D_\alpha \frac{(x^{\alpha A} - x^{\alpha\beta})}{(x^{A\alpha} - x^{\alpha A})} t \quad (7.5)$$

For the other side of the weld, the expression is similarly:-

$$\frac{1}{2} \{ (z_j^B)^2 - (z_o^B)^2 \} = D_\beta \frac{(x^{\beta\alpha} - x^{\beta B})}{(x^{B\beta} - x^{\beta B})} t \quad (7.6)$$

where z_o^B is the initial distance from the interface to particle B and z_j^B is the distance to the growing particle at some time t . Rearrangement of these equations yields the following expressions for z_i^A and z_j^B ,

$$z_i^A = \sqrt{\frac{2D_\alpha(x^{\alpha A} - x^{\alpha\beta})t}{(x^{A\alpha} - x^{\alpha A})} + z_o^A{}^2} \quad (7.7)$$

$$z_j^B = \sqrt{\frac{2D_\beta(x^{\beta\alpha} - x^{\beta B})t}{(x^{B\beta} - x^{\beta B})} + z_o^B{}^2} \quad (7.8)$$

Now, for mass balance to be satisfied, the area of the two shaded triangles in Figure 7.3(a) must be equal. Therefore,

$$\frac{1}{2} z_i^A (x^{\alpha A} - x^{\alpha\beta}) = \frac{1}{2} z_j^B (x^{\beta\alpha} - x^{\beta B}) \quad (7.9)$$

$$\frac{(x^{\alpha A} - x^{\alpha\beta})}{(x^{\beta\alpha} - x^{\beta B})} = \frac{z_j^B}{z_i^A} \quad (7.10)$$

A partition coefficient, k can be defined such that

$$k = \frac{x^{\beta\alpha}}{x^{\alpha\beta}} \quad (7.11)$$

which rearranges to

$$x^{\beta\alpha} = k \cdot x^{\alpha\beta} \quad (7.12)$$

Therefore, equations 7.12 and 7.10 can be solved simultaneously to calculate the interface compositions $x^{\alpha\beta}$ viz.,

$$x^{\alpha\beta} = \frac{(z_i^A x^{\alpha A} + z_j^B x^{\beta B})}{k z_j^B + z_i^A} \quad (7.13)$$

7.1.2 Exponential concentration profile

It was shown from the previous section that the flux of carbon from the i th particle is given by:-

$$\frac{\partial z_i^A}{\partial t} (x^{A\alpha} - x^{\alpha A}) = D \left[\frac{\partial x}{\partial z} \right]_{z=0} \quad (7.14)$$

and for the other side of the interface:-

$$\frac{\partial z_j^B}{\partial t} (x^{B\beta} - x^{\beta B}) = -D \left[\frac{\partial x}{\partial z} \right]_{z=0} \quad (7.15)$$

If an exponential concentration profile is assumed as shown in Figure 7.3(b) then an expression for $\frac{\partial x}{\partial z}$ can be obtained from the Laplace solution for Ficks second law.

$$x_\alpha = A_1 + B_1 \operatorname{erf} \left(\frac{z}{2\sqrt{D_\alpha t}} \right) \quad (7.16)$$

$$x_\beta = A_2 + B_2 \operatorname{erf} \left(\frac{|z|}{2\sqrt{D_\beta t}} \right) \quad (7.17)$$

where A_1, B_1, A_2 and B_2 are constants determined by the boundary conditions. Details of the calculation of the constants are given in Chapter 3.

Therefore, from equation (7.14):

$$D_\alpha \left[\frac{\partial x_\alpha}{\partial z} \right]_{z=0} = D_\alpha \frac{\partial \left(B_1 \operatorname{erf} \left\{ \frac{z}{2\sqrt{D_\alpha t}} \right\} \right)}{\partial z} \quad (7.18)$$

so,

$$D_\alpha \left[\frac{\partial x_\alpha}{\partial z} \right]_{z=0} = \frac{2}{\sqrt{\pi}} D_\alpha B_1 \exp \left\{ \frac{z^2}{4D_\alpha t} \right\} \frac{1}{2\sqrt{D_\alpha t}} \quad (7.19)$$

when $z = 0$

$$D_\alpha \left[\frac{\partial x_\alpha}{\partial z} \right]_{z=0} = \frac{2}{\sqrt{\pi}} D_\alpha B_1 \frac{1}{2\sqrt{D_\alpha t}} \quad (7.20)$$

$$D_\alpha \left[\frac{\partial x_\alpha}{\partial z} \right]_{z=0} = \frac{D_\alpha B_1}{\sqrt{\pi D_\alpha t}} \quad (7.21)$$

therefore, substituting into (7.14)

$$(x^{A\alpha} - x^{\alpha A}) \frac{\partial z_i^A}{\partial t} = \frac{D_\alpha B_1}{\sqrt{\pi D_\alpha t}} \quad (7.22)$$

Rearrangement yields:-

$$(x^{A\alpha} - x^{\alpha A}) \partial z = \frac{D_\alpha B_1}{\sqrt{\pi D_\alpha t}} \partial t \quad (7.23)$$

and on integration

$$(x^{A\alpha} - x^{\alpha A}) \int_{z_0^A}^{z_i^A} \partial z = \int_0^t \frac{D_\alpha B_1}{\sqrt{\pi D_\alpha t}} \partial t \quad (7.24)$$

$$(x^{A\alpha} - x^{\alpha A}) (z_i^A - z_0^A) = \frac{2\sqrt{D_\alpha t} B_1}{\sqrt{\pi}} \quad (7.25)$$

therefore,

$$z_i^A = 2\sqrt{\frac{D_\alpha t}{\pi}} \frac{B_1}{(x^{A\alpha} - x^{\alpha A})} + z_0^A \quad (7.26)$$

where from Chapter 3,

$$A_1 = \frac{x^{\beta B} (-x^{\alpha A})}{k+1} = x^{\alpha\beta} \quad + \quad \text{see ch. 3}$$

and

$$B_1 = x^{\alpha A} - A_1$$

Similarly, for the other side of the weld:-

$$z_j^B = 2\sqrt{\frac{D_\beta t}{\pi}} \frac{-B_2}{(x^{B\beta} - x^{\beta B})} + z_0^B \quad (7.27)$$

where

$$B_2 = -B_1$$

therefore

$$z_j^B = 2\sqrt{\frac{D_\beta t}{\pi}} \frac{(x^{\alpha A} - x^{\alpha\beta})}{(x^{B\beta} - x^{\beta B})} + z_0^B \quad (7.28)$$

7.2 Summary of calculations.

The following equations are a summary of the relevant equations for each model as derived in the previous sections. These are the equations that are utilised in the computer model.

Constant concentration gradient

$$z_i^A = \sqrt{\frac{2D_\alpha (x^{\alpha A} - x^{\alpha\beta}) t}{(x^{A\alpha} - x^{\alpha A})}} + z_0^A \quad (7.29)$$

$$z_j^B = \sqrt{\frac{2D_\beta(x^{\beta\alpha} - x^{\beta B})t}{(x^{B\beta} - x^{\beta B})} + z_o^B} \quad (7.30)$$

$$x^{\alpha\beta} = \frac{(z_i^A x^{\alpha A} + z_j^B x^{\beta B})}{kz_j^B + z_i^A} \quad (7.31)$$

$$x^{\beta\alpha} = k \cdot x^{\alpha\beta} \quad (7.32)$$

Exponential concentration gradient

$$z_i^A = 2\sqrt{\frac{D_\alpha t}{\pi} \frac{(x^{\alpha A} - x^{\alpha\beta})}{(x^{A\alpha} - x^{\alpha A})}} + z_0^A \quad (7.33)$$

$$z_j^B = 2\sqrt{\frac{D_\beta t}{\pi} \frac{(x^{\alpha A} - x^{\alpha\beta})}{(x^{B\beta} - x^{\beta B})}} + z_0^B \quad (7.34)$$

$$x^{\alpha\beta} = \frac{x^{\beta B} - x^{\alpha A}}{k + 1} \quad (7.35)$$

$$x^{\beta\alpha} = k \cdot x^{\alpha\beta} \quad (7.36)$$

In order to solve these equations knowledge is required of the diffusion coefficient of carbon in ferrite, D_α and D_β and the partition coefficient, k .

7.3 Calculation of the carbon diffusion coefficient in ferrite

The model used in this analysis is due to M^cLellan *et al.* (1965). The carbon is assumed to occupy both the tetrahedral and octahedral sites in the ferrite lattice. The observed diffusivity is therefore a weighted sum of the three possible diffusion paths:

- i) from an octahedral (O) site to another O site will be via a tetrahedral (T) hole, giving $O-T-O$;
- ii) an atom on a position T has two alternative paths $T-O-T$ and $T-T$.

The diffusion coefficient is given by :-

$$D = \phi D^{O-T-O} + (1 - \phi) f D^{T-T} + (1 - \phi)(1 - f) D^{T-O-T} \quad (7.37)$$

where ϕ is the fraction of the total interstitial atoms in the octahedral sites and f is the fraction of the remaining interstitial atoms which jump via the $T - T$ route. The superscripts in the diffusion coefficients indicate the particular jump paths for the carbon atoms. M^cLellan *et al.* (1965) give the following expressions for ϕ and f :-

$$\phi = 1 - \left(\frac{1}{2} e^{\frac{\Delta E}{kT}} e^{-\frac{\Delta S}{k}} + 1 \right)^{-1}$$



and

$$f = 0.86$$

In this expression, $\Delta E = E_u^T - E_u^O$ where E_u^T is the change in Gibbs free energy when a solute atom is placed in a tetrahedral site and E_u^O is the change in Gibbs free energy when a solute atom is placed in an octahedral site. Similarly $\Delta S = S_u^T - S_u^O$ where S_u^T is the change in vibrational entropy when a solvent atom is inserted in a tetrahedral site and S_u^O is the change in vibrational entropy on insertion of a solute atom into an octahedral site.

7.4 Calculation of the partition coefficient

For the linear model, the following equation was derived for calculating the interfacial carbon concentration, $x^{\alpha\beta}$:-

$$x^{\alpha\beta} = \frac{(z_i^A x^{\alpha A} + z_j^B x^{\beta B})}{kz_j^B + z_i^A}$$

In order for there to be any diffusion at all, $x^{\alpha A}$ must be greater than $x^{\alpha\beta}$, as Figure 7.3 illustrates. Therefore, from the above equation, for diffusion to start:-

$$x^{\alpha A} > \frac{(z_i^A x^{\alpha A} + z_j^B x^{\beta B})}{kz_j^B + z_i^A}$$

Rearrangement of this equation yields the following condition for diffusion using the linear gradient model:-

$$x^{\alpha A} k > x^{\beta B} \quad (7.38)$$

This provides a criterion for predicting a value of k that:-

$$k > \frac{x^{\beta B}}{x^{\alpha A}}$$

which enables the best estimate to be made of the methods available to be made. In general it has been found that the models of Wagner and Wada *et al.* give very similar values for the lower chromium concentration systems (mild steel/1CrMo and mild steel/2 $\frac{1}{4}$ CrMo) but that the Wagner model gives a better estimate for the higher chromium concentrations. These models are exactly as have been described previously in Chapter 4.

7.5 Carburised zone width.

On the high alloy side of the weld, the situation is as illustrated in Figure 7.4. Carbon is diffusing away from the low alloy side of the weld causing the carbide B1 to grow. The value of z_j^B (*i.e.* the distance to which the particle B1 has grown in time t) is increasing with time as

the carbide grows and therefore a carburised zone is forming on this side of the interface. In a similar manner to the decarburised zone, a carburised zone width can also be defined as:-

$$\eta^\beta = (z_j^B - z_o^B) + d_{20} \quad (7.39)$$

i.e. the gain in size of the particle as a result of diffusion from the low alloy side ($z_j^B - z_o^B$) plus the original size of the particle, d_{20} .

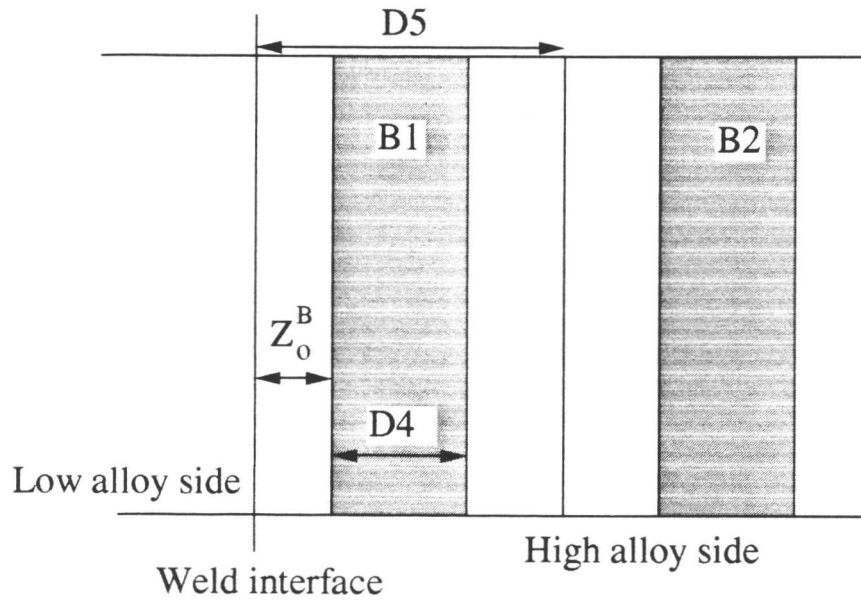


Figure 7.4: Schematic representation of the high alloy side of the weld.

7.6 Calculation of diffusion away from the interface.

Consider what is happening on the high alloy side of the interface. A carbon concentration gradient builds up in this region due to the diffusion of carbon from the low alloy side. Thus, it would be expected that carbon would diffuse away from the interface on the high alloy side of the weld under the influence of this carbon gradient. Figure 7.5 outlines the equilibrium carbon concentrations present between the matrix and alloy carbides on the high alloy side of the interface. Now mass balance requires that:-

$$-(x^{B_2\beta} - x^{\beta B_2}) \frac{\partial z}{\partial t} = \frac{D(x^{\beta B_1} - x^{\beta B_2})}{z} \quad (7.40)$$

i.e. the mass absorbed by the carbide must be equal to the mass arriving by diffusion. In this expression the subscript 1 refers to the first slice and the subscript 2 to the second slice, therefore $x^{B_2\beta}$ is the equilibrium carbon concentration in the carbide B_2 in equilibrium with ferrite and $x^{\beta B_2}$ is the equilibrium concentration in the ferrite in equilibrium with the carbide



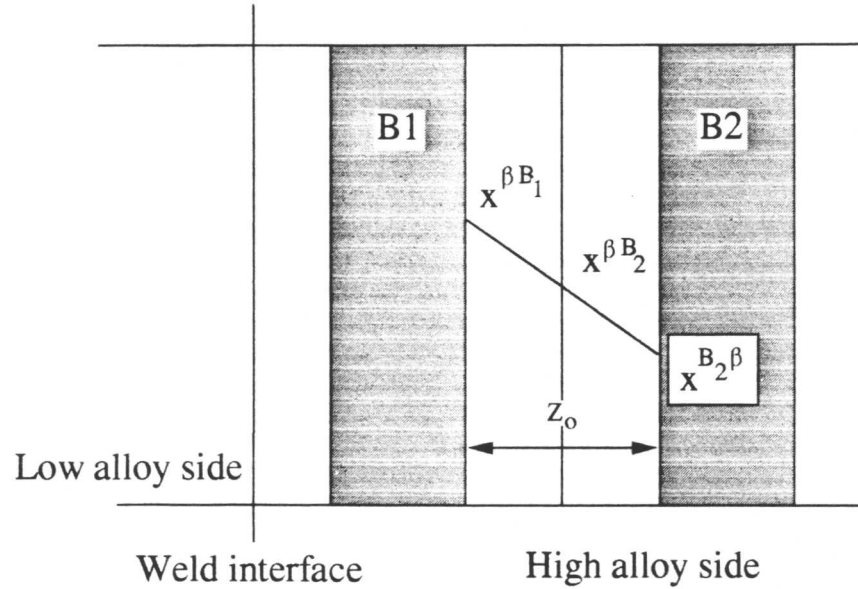


Figure 7.5: Equilibrium concentrations between the matrix and carbides on the high alloy side of the weld.

B_2 . Similarly, B_1 refers to the carbide in the first slice from the interface.

Integrating the above expression:-

$$\int_{z=z_0}^z z \partial z = \int_0^t \partial t \left(\frac{x^{\beta B_1} - x^{\beta B_2}}{x^{\beta B_2} - x^{B_2 \beta}} D \right) \quad (7.41)$$

z_0 is the initial distance between the carbides and z is the distance between carbides at some time t after the particle B_2 has been allowed to grow (*i.e.* z decreases with time).

Therefore,

$$\frac{1}{2} z^2 - \frac{1}{2} z_0^2 = \frac{(x^{\beta B_1} - x^{\beta B_2})}{(x^{\beta B_2} - x^{B_2 \beta})} Dt \quad (7.42)$$

$$z^2 = \frac{(x^{\beta B_1} - x^{\beta B_2})}{(x^{\beta B_2} - x^{B_2 \beta})} 2Dt + z_0^2 \quad (7.43)$$

therefore

$$z = \left(\frac{(x^{\beta B_1} - x^{\beta B_2})}{(x^{\beta B_2} - x^{B_2 \beta})} 2Dt + z_0^2 \right)^{\frac{1}{2}} \quad (7.44)$$

The amount of carbon transferred, Δc , in time t is therefore given by:-

$$\Delta c = (z_0 - z)(x^{B_2 \beta} - x^{\beta B_2}) \quad (7.45)$$



This amount is then subtracted from \bar{x}_β to give a new value for the average carbon concentration on the high alloy side.

7.7 Application of the theory to a computer model

The basic set-up for the computer model is illustrated in Figure 7.6.

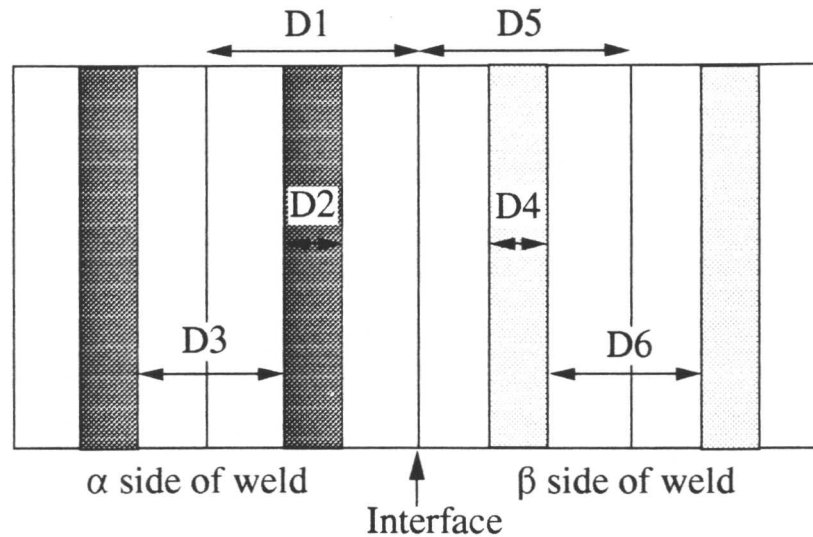


Figure 7.6: Set-up dimensions for the computer model.

It is assumed that the diffusion is only occurring in one dimension perpendicular to the weld interface, so the carbide particles are considered to dissolve or grow in this direction. The dimensions of the model are also illustrated in Figure 7.6. D1 and D5 are the widths of the ferrite slabs on the α and β sides of the interface respectively, D3 is the inter-particle spacing on the α side and D6 is the inter-particle spacing in β . D2 is the particle size on the α side and D4 the particle size on the β side of the weld interface. As diffusion occurs from α to β , particle A1 will dissolve and particle B1 will grow. With reference to Figure 7.2, particle A1 will decrease by an amount $(z_i^A - z_o^A)$ in any time interval, whilst particle B1 will grow by an amount $(z_j^B - z_o^B)$. As the particles dissolve and D2, the particle size, decreases, there comes a point when D2=0 and the particle has dissolved. When this occurs the program will step to the next particle, A2, on the low alloy side as illustrated in Figure 7.7. The decarburised zone width will therefore increase in a step-like fashion by an amount $D1 + \frac{D3}{2}$ as far as the calculations are concerned.

7.7.1 Calculation of the modelled dimensions

For this model, it is initially assumed that each ferrite slab contains the equilibrium volume fraction of carbide. Therefore, on the α side, there is v_α volume fraction of carbide and on the β



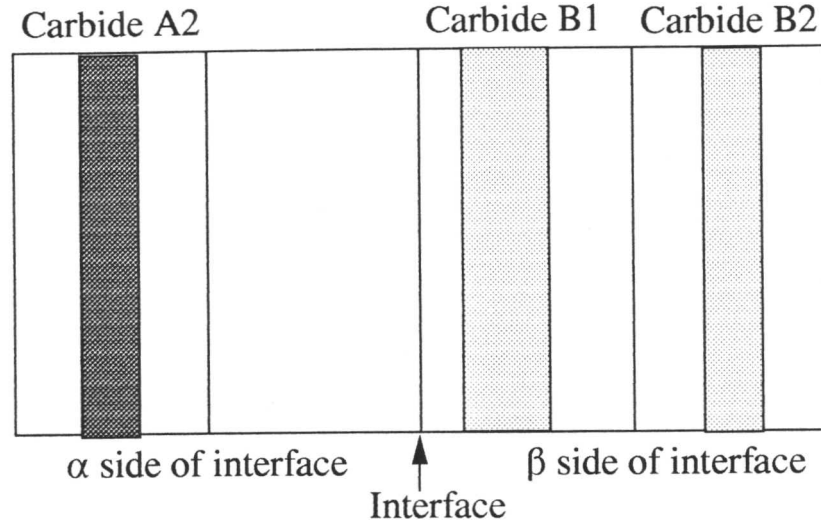


Figure 7.7: Dissolution of particles on the low alloy side of the interface.

side, v_β volume fraction of carbide. These equilibrium volume fractions can be calculated using MTDATA. The value of D2 and D4, the particle sizes, are initially set at an arbitrary value of $5\mu\text{m}$ and thus all of the other distances can be determined from the input volume fractions, v_α and v_β , viz.,

$$D1 = \frac{D2}{v_\alpha} \quad \text{and} \quad D5 = \frac{D4}{v_\beta} \quad (7.46)$$

$$D3 = D1 - D2 \quad \text{and} \quad D6 = D5 - D4 \quad (7.47)$$

The particle size of $5\mu\text{m}$ was chosen as it was fairly representative of actual particle sizes taking into account the clustering of the particles found experimentally. As the particles on the low alloy side of the weld start dissolving, then obviously the particle is getting smaller and D2 is decreasing by an amount $(z_i^A - z_o^A)$ for every time increment. Conversely on the high alloy side of the weld, the particle size, D4, increases with time. Now, the volume fractions of carbide on either side of the interface can be calculated using a rearrangement of equations (7.46). Thus,

$$v_\alpha = \frac{D2}{D1} \quad \text{and} \quad v_\beta = \frac{D4}{D5}$$

and therefore, as D1 and D5 are constant until a particle has dissolved completely (see section 7.10), the value of v_α will decrease and the value of v_β will correspondingly increase.

7.7.2 Calculation of the average carbon concentrations

A consequence of the change in volume fractions of carbide on either side of the interface is that the average carbon concentrations in each of the slabs are also going to change; decreasing



on the low alloy side of the interface and increasing on the high alloy side. These changes can be calculated using the formulae:-

$$\bar{x}_\alpha = x^{A\alpha}v_\alpha + x^{\alpha A}(1 - v_\alpha) \quad (7.48)$$

$$\bar{x}_\beta = x^{B\beta}v_\beta + x^{\beta B}(1 - v_\beta) \quad (7.49)$$

That is, the average carbon concentration in α , \bar{x}_α , is equal to the equilibrium carbon concentration in the carbide, $x^{A\alpha}$, multiplied by the volume fraction of carbide present (v_α), plus the equilibrium carbon concentration in the ferrite, $x^{\alpha A}$, multiplied by the volume fraction of ferrite ($1-v_\alpha$), and similarly for the β side of the interface.

7.7.3 Calculation of the partition coefficient.

If the average carbon concentration changes then the change must affect the calculation of the partition coefficient. Consequently, a new value has to be calculated at the end of every time step using one of the methods previously outlined.

7.7.4 Changes in equilibrium carbon concentrations.

As the diffusion of carbon proceeds there is a change in the bulk carbon concentration on either side of the interface. This, in turn, means that the equilibrium carbon concentrations between the carbides and the matrix are constantly changing. However, if MTDATA calculations are run allowing for changes in bulk carbon concentration, then the changes in $x^{\alpha A}$, $x^{\beta B}$, $x^{A\alpha}$ and $x^{B\beta}$ can be plotted as functions of the carbon concentration. An example plot for $x^{A\alpha}$ for mild steel is shown in Figure 7.8 for three different temperatures. Equations can be produced, by this method, for every alloy at every temperature so that the equilibrium carbon concentrations can be recalculated as the carbon concentration changes. When calculating curves such as these, it is important to ensure that the carbon concentration calculated in the program does not exceed the limit of the carbon concentrations for which data points have been calculated. For this reason the plots cover a wide range of carbon concentrations to ensure that accurate values of the equilibrium carbon concentrations are calculated. The equations for all of the alloys are given with the program listing in Appendix III.

Another consequence of the change in bulk carbon concentration is that the carbide that is precipitating also changes as has been observed experimentally. This change in carbide precipitation sequence can also be predicted by MTDATA. Table 7.1 shows that as the carbon concentration is increased there is a reversion in the sequence to carbides that have previously dissolved. This will cause another change in the equilibrium carbon concentrations which can be accounted for in the program by allowing the equations for calculation of $x^{\beta B}$ and $x^{B\beta}$ to



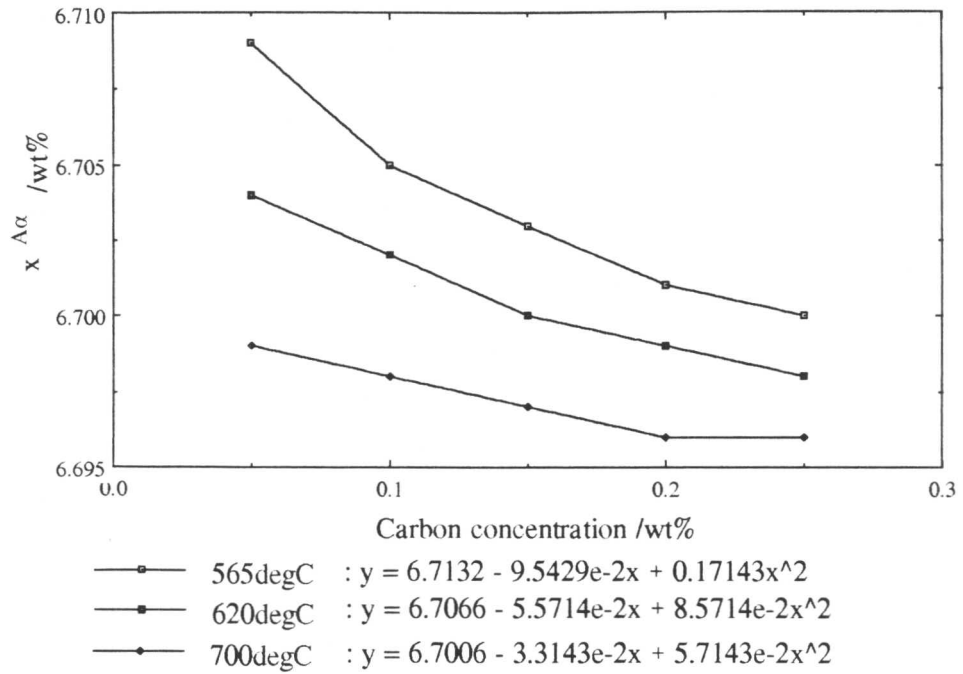


Figure 7.8: Plots of $x^{A\alpha}$ as a function of the bulk carbon concentration for mild steel at 700°C, 620°C and 565°C.

	Fe_3C	M_2C	M_7C_3	$M_{23}C_6$	M_6C
0.1 wt% C				0.0214	0.00155
0.12 wt% C				0.0226	0.00035
0.13 wt% C				0.0286	
0.27 wt% C				0.0593	
0.28 wt% C			0.00367	0.0598	
0.55 wt% C			0.0286	0.0709	
0.56 wt% C	0.00245		0.0275	0.0712	
0.57 wt% C	0.00495		0.0294	0.0714	

Table 7.1: MTDATA predictions showing the change in type of carbide with increasing carbon content. The numbers in the boxes indicate the equilibrium volume fractions.

change once the average carbon concentration (predicted by MTDATA) has exceeded that required for lower order carbide precipitation.

The effect of this can be seen in Figure 7.9. This shows that the profiles level off after cementite precipitation and therefore it would be expected that the rate of diffusion or the width of the decarburised zone would also tend to increase at a slower rate, as observed experimentally.



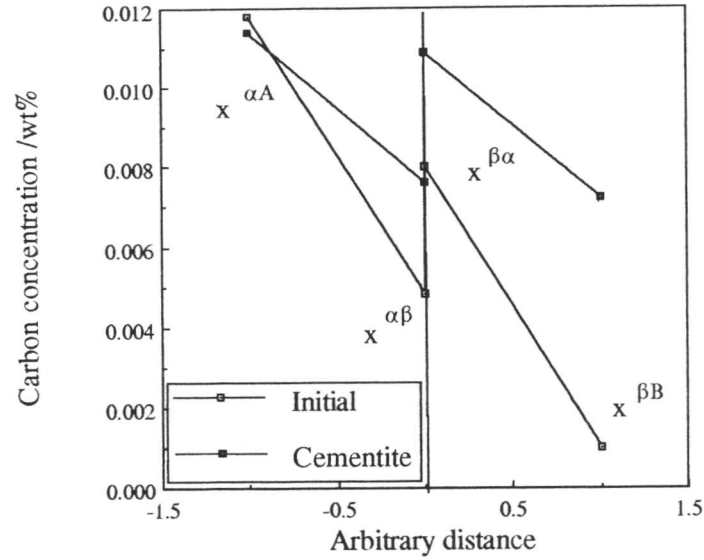


Figure 7.9: Profiles produced for the mild steel/ $2\frac{1}{4}$ CrMo weld before and after cementite precipitation.

7.8 Testing the model

The model was tested for four experimental joints, mild steel/1CrMo, mild steel/ $2\frac{1}{4}$ CrMo, $2\frac{1}{4}$ CrMo/9CrMo and $2\frac{1}{4}$ CrMo/12CrMo. The exact steel compositions used in the calculations are given in Table 7.2.

Material	Composition /wt%									
	C	Si	Mn	P	S	Cr	Mo	Ni	V	N
Mild steel/1CrMo weld										
Mild steel plate	0.20	0.26	0.76	0.010	0.016	0.035	0.015	0.015	0.000	0.0
1CrMo weld	0.056	0.40	0.77	0.010	0.012	1.11	0.44	0.035	0.015	0.0
Mild steel/ $2\frac{1}{4}$ CrMo weld										
Mild steel plate	0.23	0.26	0.77	0.011	0.016	0.037	0.015	0.017	0.000	0.0
$2\frac{1}{4}$ CrMoweld	0.079	0.43	0.98	0.011	0.012	2.17	0.99	0.053	0.025	0.0
$2\frac{1}{4}$ CrMo/9CrMo weld										
9CrMo pipe	0.108	0.44	0.46	0.017	0.001	8.74	0.94	0.19	0.24	0.049
$2\frac{1}{4}$ CrMoweld	0.08	0.43	1.01	0.011	0.003	2.42	1.00	0.064	0.028	0.0
$2\frac{1}{4}$ CrMo/12CrMo weld										
12CrMo pipe	0.20	0.37	0.58	0.035	0.003	11.5	0.92	0.74	0.31	0.0
$2\frac{1}{4}$ CrMoweld	0.08	0.43	1.01	0.011	0.003	2.42	1.00	0.064	0.028	0.0

Table 7.2: Chemical compositions of all of the weld joints.



The convention adopted for all of these joints is that the low alloy (α) side of the weld combination will be written first followed by the high alloy (β) side *i.e.* mild steel/ $2\frac{1}{4}$ CrMo. Table 7.3 illustrates this further as well as giving the carbides expected in each combination and the change of carbide, if any, that would be expected as the carbon concentration is increased.

Alloy combination	α side	β side	carbide A	carbide B	Change in carbide B to
mild steel/1CrMo	mild steel	1CrMo	Fe ₃ C	M ₂₃ C ₆	Fe ₃ C
mild steel/ $2\frac{1}{4}$ CrMo	mild steel	$2\frac{1}{4}$ CrMo	Fe ₃ C	M ₂₃ C ₆	Fe ₃ C
$2\frac{1}{4}$ CrMo/9CrMo	$2\frac{1}{4}$ CrMo	9CrMo	M ₂₃ C ₆	M ₇ C ₃	no change
$2\frac{1}{4}$ CrMo/12CrMo	$2\frac{1}{4}$ CrMo	12CrMo	M ₂₃ C ₆	M ₂₃ C ₆	no change

Table 7.3: Classification of alloy combinations.

The volume fractions of carbide phases present are calculated from the weight fraction of phase output by MTDATA and using the density of that phase to calculate the resultant volume fractions. The weight fractions and volume fractions of the equilibrium carbide present are tabulated in Table 7.4 for each alloy combination. It is assumed in this model that only one carbide is present at any time. In the case of $2\frac{1}{4}$ CrMo, more than one carbide is expected at equilibrium. The carbide with the largest volume fraction, M₂₃C₆ is therefore chosen. Similarly, as the increase in carbon content causes a change in the carbide precipitating, it is assumed that Fe₃C is the sole carbide present.

Temperature	Alloy combination	carbide A	carbide B	wt. frac A	wt. frac B	v_α	v_β
700°C	mild steel/ $2\frac{1}{4}$ CrMo	Fe ₃ C	M ₂₃ C ₆	0.0326	0.0155	0.0337	0.0178
700°C	mild steel/1CrMo	Fe ₃ C	M ₂₃ C ₆	0.0326	0.0109	0.0337	0.0111
730°C	$2\frac{1}{4}$ CrMo/9CrMo	M ₂₃ C ₆	M ₇ C ₃	0.0153	0.0209	0.0175	0.0240
730°C	$2\frac{1}{4}$ CrMo/12CrMo	M ₂₃ C ₆	M ₂₃ C ₆	0.0153	0.0385	0.0175	0.0450

Table 7.4: Input data for volume fractions for all the weld combinations. The density of M₂₃C₆ is taken to be 6.996 g/cm³, the density of Fe₃C as 7.704 g/cm³ and the density of M₇C₃ as 6.965 g/cm³, Andrews *et al.* (1967)

7.9 One particle system

In order to illustrate clearly what the program is doing, the first results presented are for a one particle system (*i.e.* there is one particle dissolving and one growing on either side of



the interface). All of these calculations were carried out using the exponential model and the experimental joint mild steel/ $2\frac{1}{4}$ CrMo at a temperature of 700°C . As a recap, mild steel is the α side of the interface with the carbide Fe_3C dissolving and $2\frac{1}{4}$ CrMo is the β side of the interface with the carbide M_{23}C_6 precipitating. For a one particle system the carbon concentration on the β side does not increase sufficiently to cause precipitation of Fe_3C . Figure 7.10 illustrates the variations in the particle sizes.

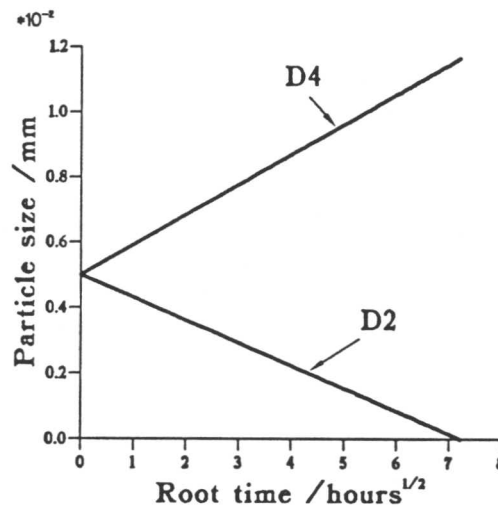


Figure 7.10: Change in D2 and D4 with root time for a one particle system using the exponential model : mild steel/ $2\frac{1}{4}$ CrMo, carbide A= Fe_3C , carbide B= M_{23}C_6 , 700°C

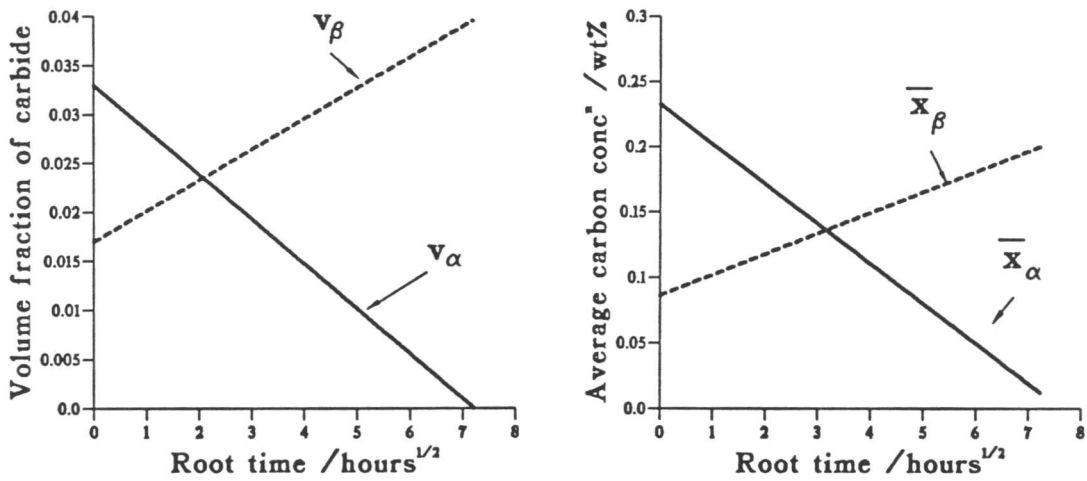
Both D2 and D4 start at the initial value set (*i.e.* $5\mu\text{m}$), D2 decreases until the particle size reaches zero when it has dissolved and D4 increases in a linear fashion. As a result of the changes in particle size, the volume fractions of carbide (Figure 7.11(a)) and the average carbon content (Figure 7.11b) in the slice also behave in a similar manner.

The reason that the average carbon content in the low alloy side does not reach zero when the carbide has dissolved is due to the carbon concentration in the ferrite, from equation 7.48, contributing to the average carbon concentration. For the one particle system, the value of z_i^A and z_j^B are also increasing giving rise to the corresponding graphs for carburised and decarburised zone widths (Figure 7.12 and Figure 7.13).

7.10 Multi-particle system

During the dissolution of one particle all of the other variables discussed earlier remain constant. However, once a particle has dissolved the value of D1 is stepped as shown in Figure 7.14 and the value of D2 is reset to the original value. It is at this point that all of the





a) b)
Figure 7.11: a) Change in v_α and v_β with root time for a one particle system
 b) Change in \bar{x}_α and \bar{x}_β with root time for a one particle system using the exponential model : mild steel/ $2\frac{1}{4}$ CrMo, carbide A= Fe_3C , carbide B= M_{23}C_6 , 700°C

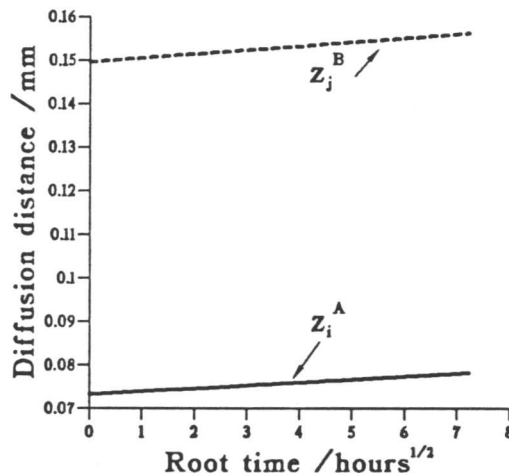


Figure 7.12: Change in z_i^A and z_j^B with root time for a one particle system using the exponential model : mild steel/ $2\frac{1}{4}$ CrMo, carbide A= Fe_3C , carbide B= M_{23}C_6 , 700°C.

equilibrium carbide concentrations, volume fractions of carbides and average carbon concentrations are recalculated.

In the following calculations the same conditions have been used as for the one particle system calculations (*i.e.* mild steel/ $2\frac{1}{4}$ CrMo, carbide A= Fe_3C , carbide B= M_{23}C_6 , 700°C). However, once the average carbon concentration \bar{x}_β has exceeded 0.4 wt%, the carbide B becomes



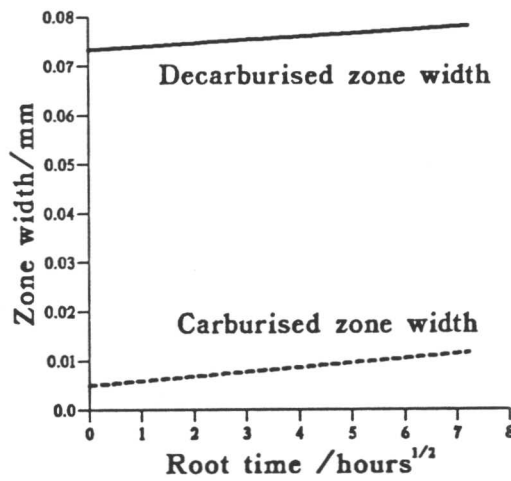


Figure 7.13: Change in carburised and decarburised zone widths between initial and final conditions for a one particle system using the exponential model : mild steel/ $2\frac{1}{4}$ CrMo, carbide A= Fe_3C , carbide B= M_{23}C_6 , 700°C .

Fe_3C . The carbon concentration at which the cementite appears was calculated using MTDATA. Figure 7.15 illustrates the changes that occur in the interfacial concentrations $x^{\alpha A}$ and $x^{\beta B}$.

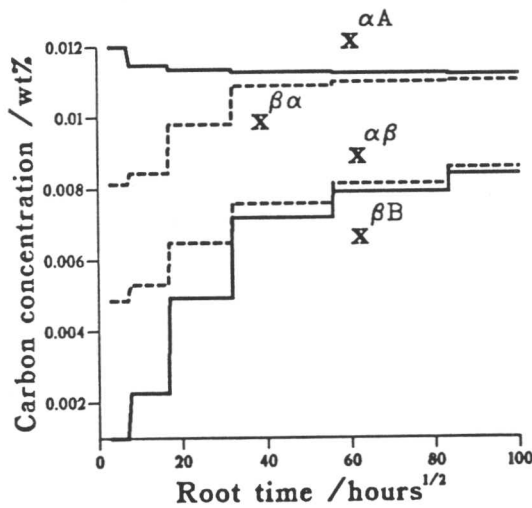


Figure 7.15: Change in interfacial carbon concentrations with root time : mild steel/ $2\frac{1}{4}$ CrMo, carbide A= Fe_3C , carbide B= $\text{M}_{23}\text{C}_6 \rightarrow \text{Fe}_3\text{C}$ when $\bar{x}_\beta \geq 0.4\text{wt}\%$, 700°C .

It can be seen from these diagrams that the values of these variables are converging as successive particles are dissolved. This translates to a levelling off of the respective concentration gradients as illustrated in Figure 7.16.

The 'flattening' of the carbon concentration gradients accounts for the levelling off of the decarburised zone width against root time plots observed experimentally, because the driving



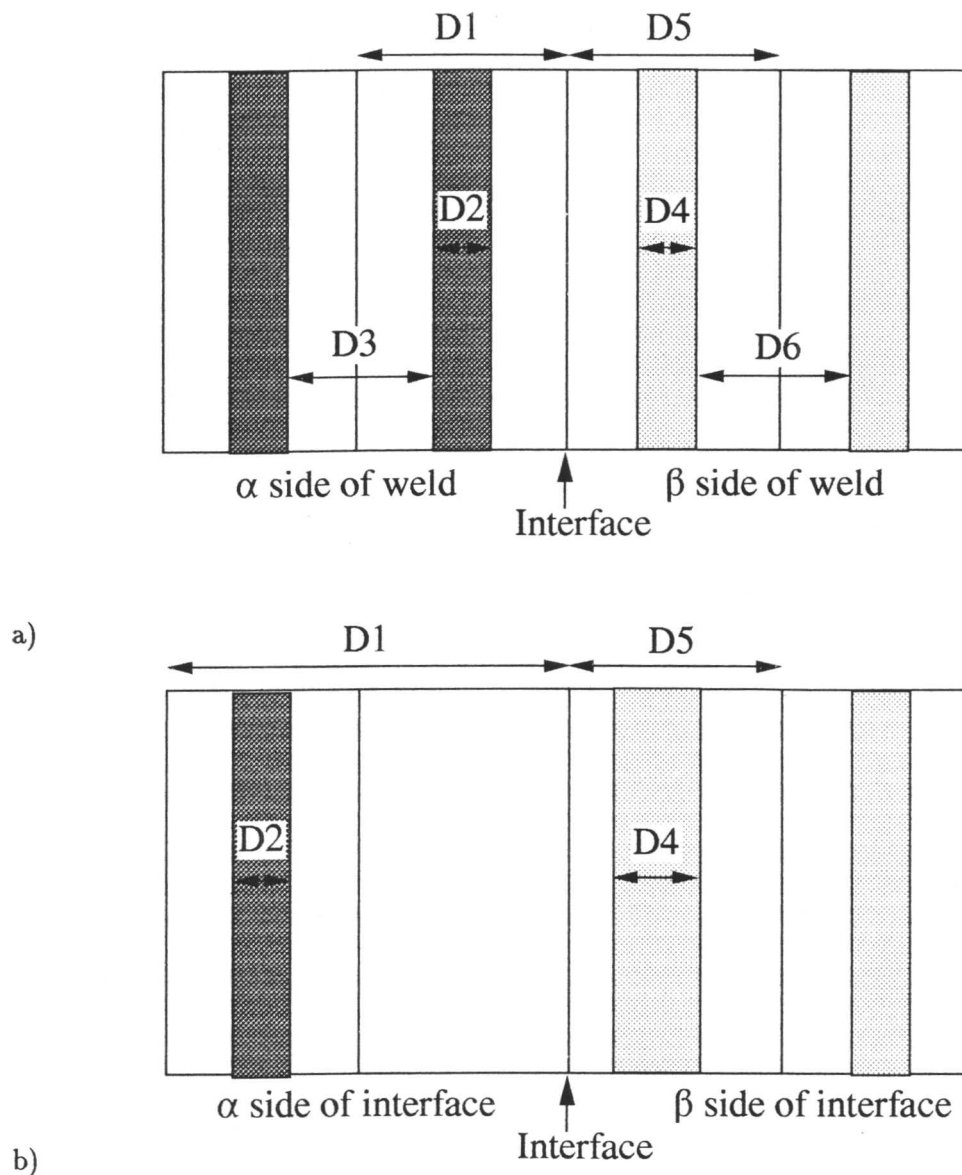


Figure 7.14: a) Initial model dimensions b) Resetting of the model dimensions after dissolution of a particle.

force for diffusion is levelling off. The carbon concentrations in the carbide $x^{B\beta}$ and $x^{A\alpha}$ also vary with carbon concentration as illustrated in Figure 7.17 and predicted by MTDATA plots such as Figure 7.8.

Figure 7.18 illustrates how the decarburised zone width increases with time in a step-like fashion. Although all of the results presented here are from the exponential model, the linear model predicts the same trends.

7.11 Conclusions

Two models were presented in this chapter for the prediction of decarburised zone widths. From the experimental work of Chapter 6, two major requirements of these models were that they account for the precipitation sequences occurring in dissimilar metal welds during tempering and that they predict non-parabolic growth of the decarburised zone. Both of the models



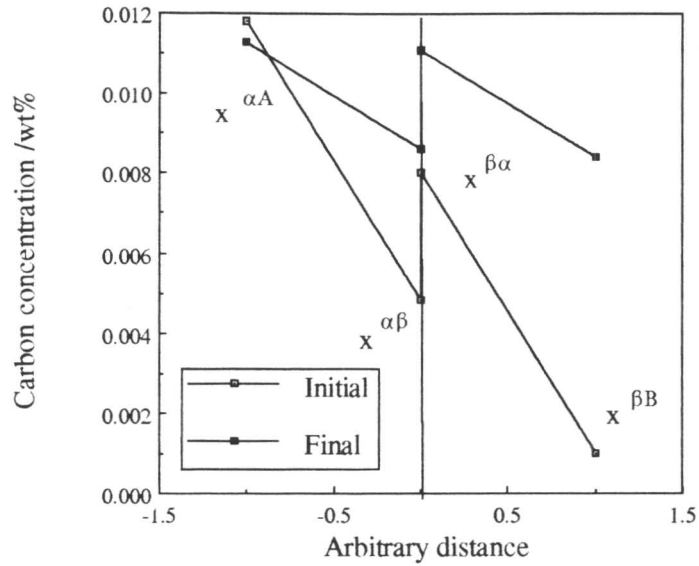


Figure 7.16: Change in carbon concentration gradients : mild steel/ $2\frac{1}{4}$ CrMo, carbide A= Fe_3C , carbide B= $\text{M}_{23}\text{C}_6 \rightarrow \text{Fe}_3\text{C}$ when $\bar{x}_\beta \geq 0.4\text{wt}\%$, 700°C .

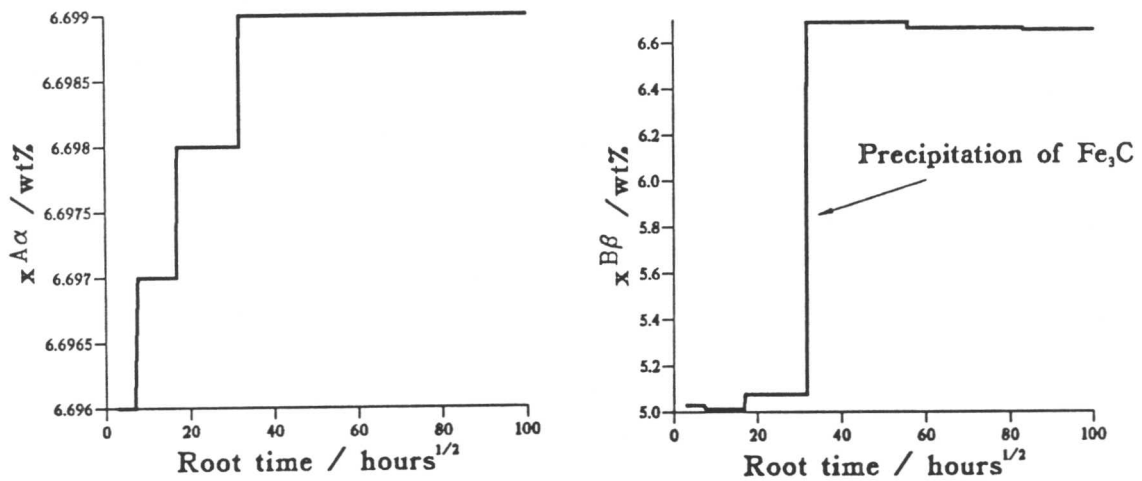


Figure 7.17: Change in $x^{B\beta}$ and $x^{A\alpha}$ with root time : mild steel/ $2\frac{1}{4}$ CrMo, carbide A= Fe_3C , carbide B= $\text{M}_{23}\text{C}_6 \rightarrow \text{Fe}_3\text{C}$ when $\bar{x}_\beta \geq 0.4\text{wt}\%$, 700°C .

successfully meet this criteria.



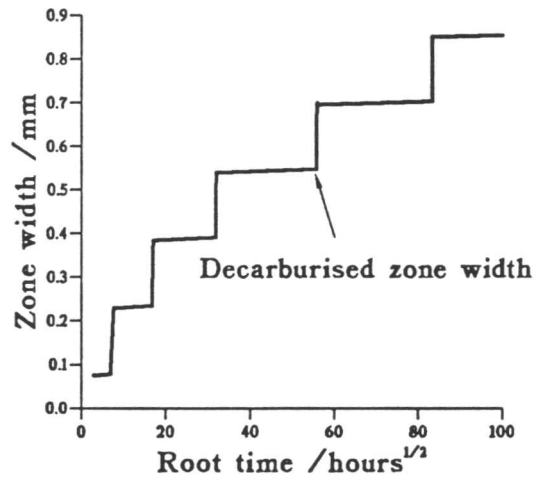


Figure 7.18: Change in decarburised zone width with root time : mild steel/ $2\frac{1}{4}$ CrMo, carbide A= Fe_3C , carbide B= $\text{M}_{23}\text{C}_6 \rightarrow \text{Fe}_3\text{C}$ when $\bar{x}_\beta \geq 0.4\text{wt}\%$, 700°C .

CHAPTER 8

Applications of the model

8.1 Introduction

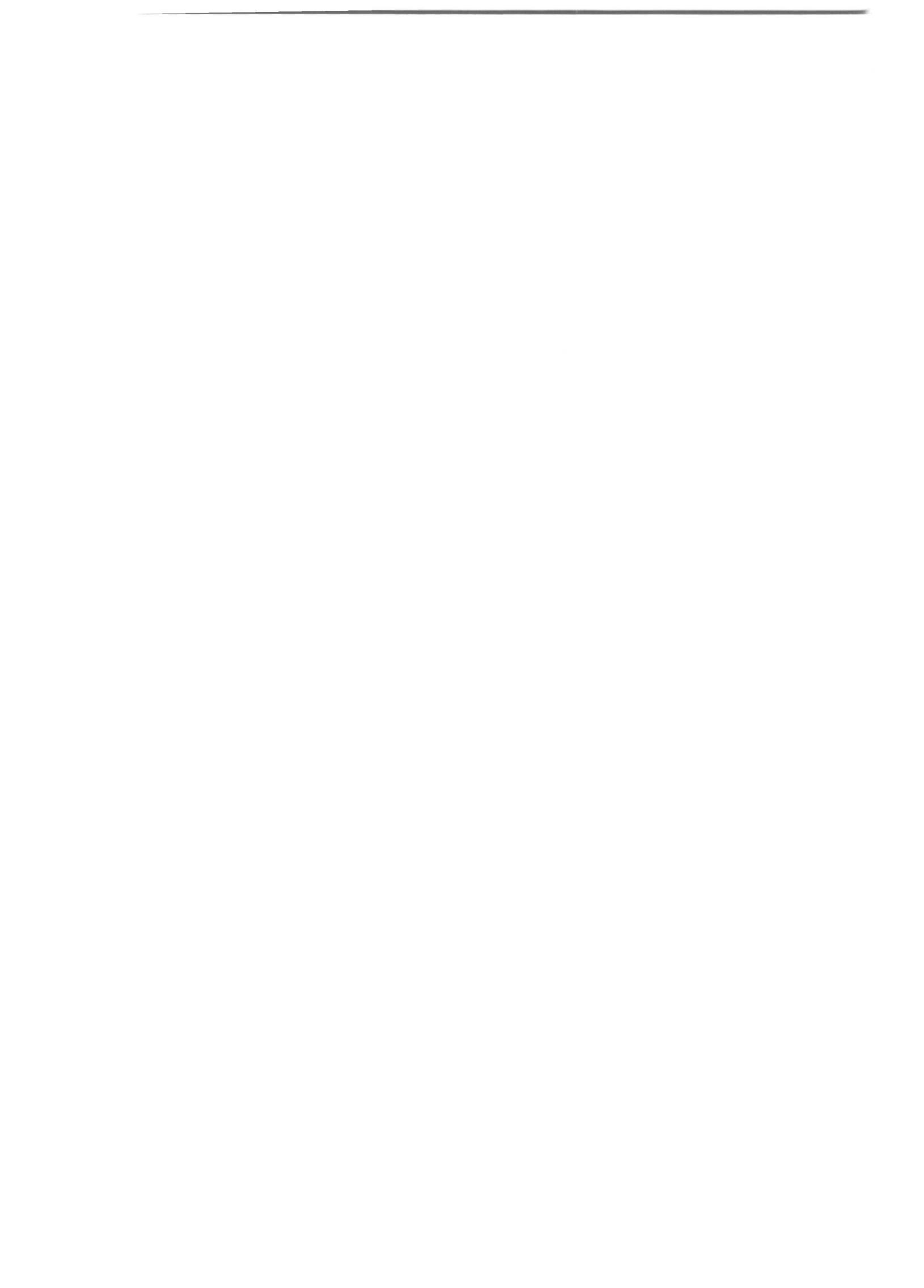
As a result of the experimental work into the diffusion of carbon across dissimilar ferritic/ferritic welds, there were four points that arose that required addressing and modelling:-

- i) The decarburised zone width should show non-parabolic kinetics *i.e.* it should level off on a plot against root time.
- ii) The decarburised zone width should increase with both time and temperature.
- iii) The model should be able to predict the extent of decarburisation with respect to the difference in substitutional alloy content across the welded joint.
- iv) The model should be able to predict the extent of carburisation in relation to the extent of decarburisation.

The work presented here is intended to illustrate how the models cope with these points and to go on to explain how it has found industrial application in the selection of material for dissimilar metal joints.

8.2 Levelling of the decarburised zone

This is probably the most significant result regarding these dissimilar metal joints from the point of view of the manufacturer as it suggests that a maximum decarburised zone width is reached rather than a continual growth over the service life of the weld. The reason for the levelling off is thought to be a result of the change in bulk carbon concentrations of the alloys at the interface. This causes both a change in the carbide that is precipitating and a change in the interfacial carbon concentrations resulting in a levelling of the respective carbon concentration gradients as was illustrated in Figure 7.9. It is therefore necessary to account for these changes in the model, which is achieved via the MTDATA calculations described in the previous chapter. As an illustration of this, plots are presented in Figure 8.1 where the interfacial carbon concentrations $x^{A\alpha}$, $x^{\alpha A}$, $x^{B\beta}$ and $x^{\beta B}$ are kept constant (Figure 8.1a) and are allowed to change according to the equations calculated using MTDATA. These plots show how the decarburised zone widths level off as a result of changes in the equilibrium carbon concentrations owing to a change in the bulk carbon concentration. It should be noted from Figure 8.1 that the decarburised zone width does not start at zero time but at a value



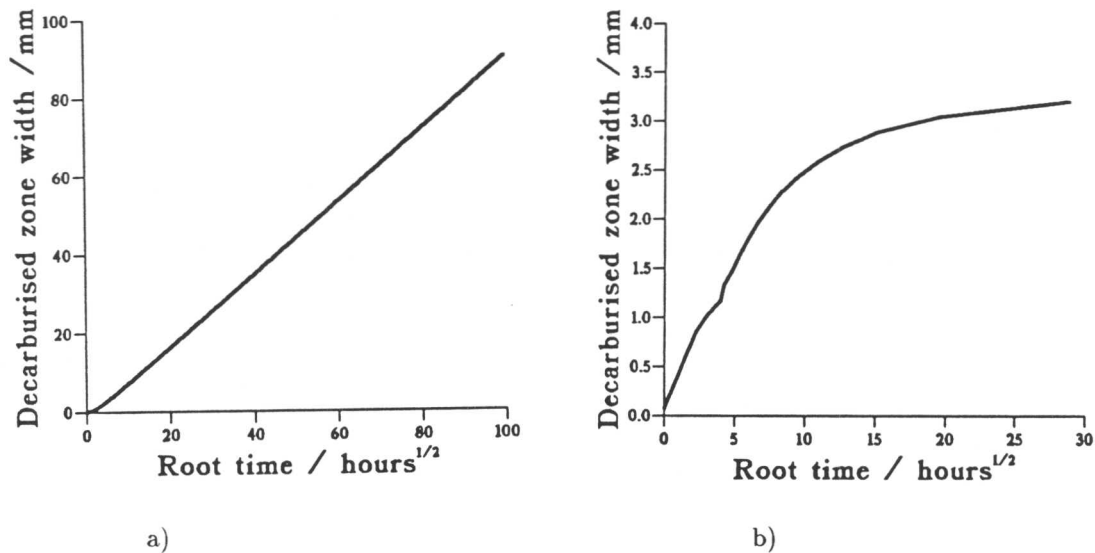


Figure 8.1: Illustration of the effect of a) keeping the equilibrium carbon concentrations constant and b) allowing them to change as a function of the bulk carbon concentration. This calculation was carried out for the mild steel/ $2\frac{1}{4}$ CrMo joint at 700°C using the linear model, $d_{20} = 5\mu\text{m}$, and using the Wagner model to calculate the partition coefficient.

corresponding to z_0^A . The smooth profile is obtained by joining the tops of the steps of a plot such as Figure 7.18.

8.3 Decarburised zone increase with time and temperature

8.3.1 Linear model

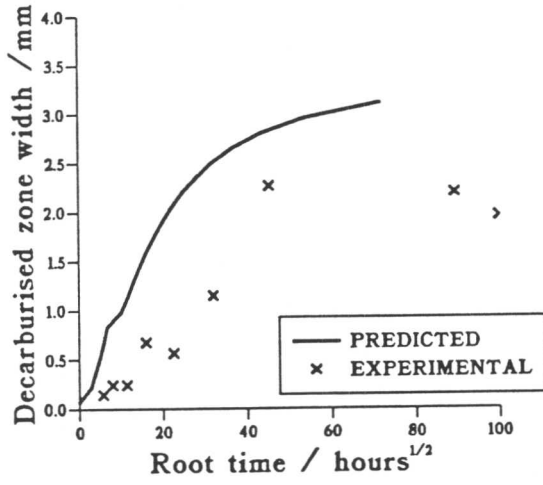
Predicted and experimental values of the decarburised zone width are compared for the linear model in Figure 8.2 for the mild steel/1CrMo, mild steel/ $2\frac{1}{4}$ CrMo joint and the $2\frac{1}{4}$ CrMo/9CrMo joint. These plots illustrate that the linear model successfully predicts an increase in the decarburised zone width with both time and temperature for both these joints. The prediction of the actual decarburised zone width values, although rather high, is fairly accurate, especially at the shorter times.

8.3.2 Problems with the linear model

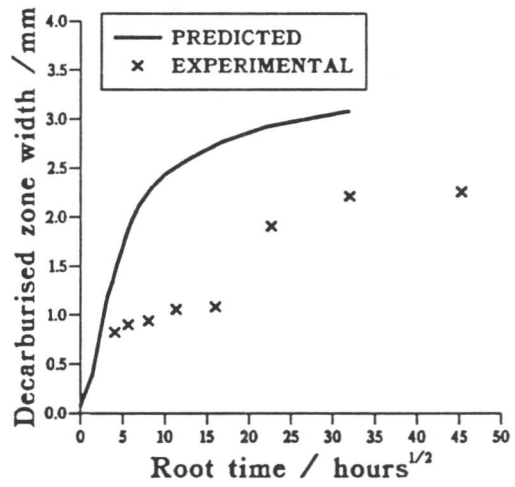
8.3.2.1 Mass balance breakdown

The reason for this is illustrated in Figure 8.3. As each successive particle is dissolved the gradient is instantaneously switched from situation 1 to situation 2 and a certain amount of carbon is apparently created from nowhere. At the shorter times or lower temperatures where few particles have been dissolved, this discrepancy is negligible but is exacerbated as more particles dissolve at longer times or higher temperatures.

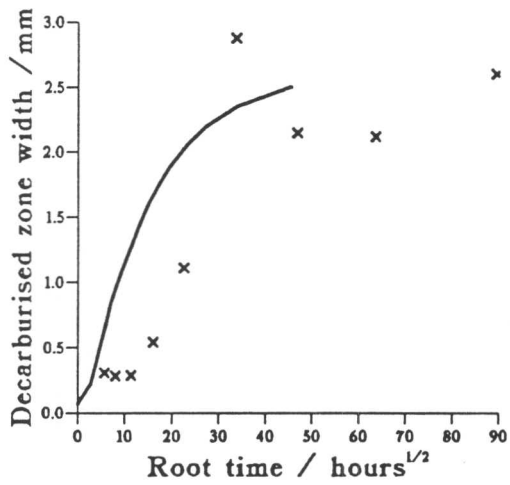




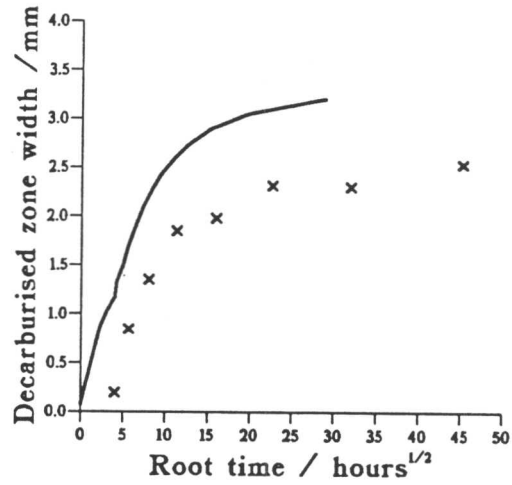
a)



b)



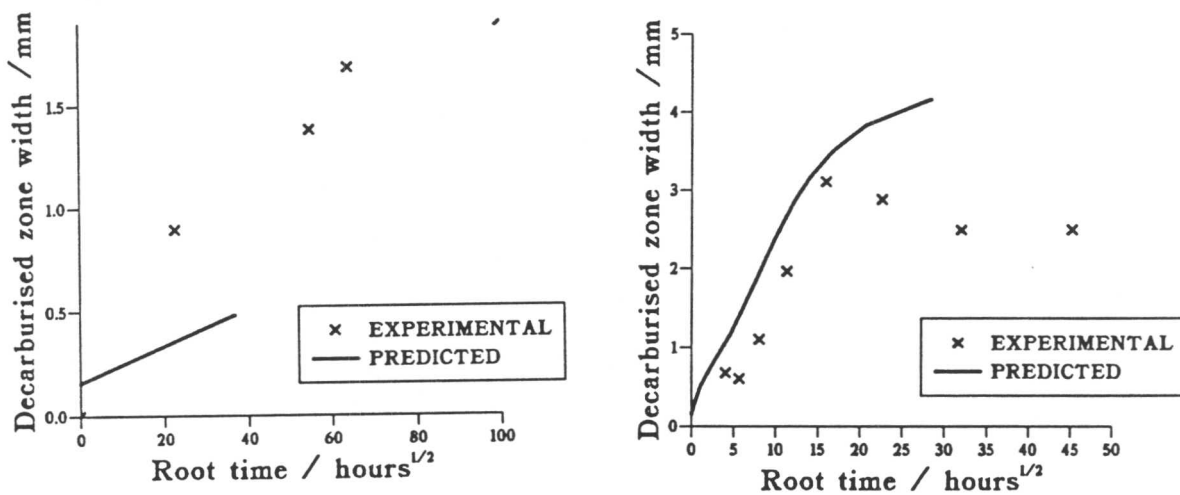
c)



d)

Figure 8.2: Predicted plots for the linear model : Mild steel/1CrMo a) at 620°C b) at 700°C, mild steel/2 $\frac{1}{4}$ CrMo c) at 620°C d) at 700°C, 2 $\frac{1}{4}$ CrMo/9CrMo e) at 620°C f) at 730°C. For all of these calculations the Wagner model was used to calculate the partition coefficient and $d_{20} = 5\mu\text{m}$





e) f)
Figure 8.2: Predicted plots for the linear model : Mild steel/1CrMo a) at 620°C b) at 700°C, mild steel/2 $\frac{1}{4}$ CrMo c) at 620°C d) at 700°C, 2 $\frac{1}{4}$ CrMo/9CrMo e) at 620°C f) at 730°C. For all of these calculations the Wagner model was used to calculate the partition coefficient and $d_{20} = 5\mu m$

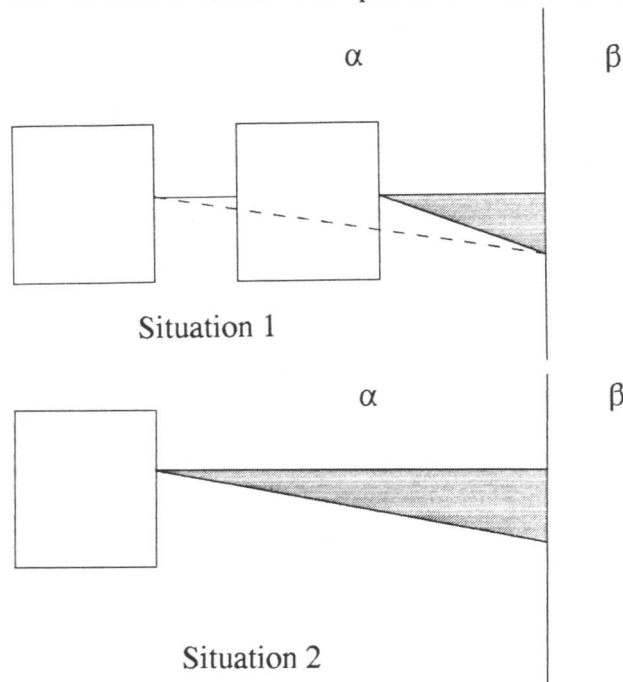


Figure 8.3: Mass balance breakdown in the linear model.

8.3.2.2 Stopping the model

The plots of Figure 8.2 showed that the prediction of the decarburised zone width stops before the time allowed for diffusion has lapsed. (In all these simulations the program was run for 10,000 hours.) If reference is made back to the equations for the calculation of the diffusion



distances:-

$$z_i^A = \sqrt{\frac{2D_\alpha(x^{\alpha A} - x^{\alpha\beta})t}{(x^{A\alpha} - x^{\alpha A})} + z_o^A{}^2} \quad (8.1)$$

$$z_j^B = \sqrt{\frac{2D_\beta(x^{\beta\alpha} - x^{\beta B})t}{(x^{B\beta} - x^{\beta B})} + z_o^B{}^2} \quad (8.2)$$

it can be seen that the model will breakdown if

$$x^{\alpha A} < x^{\alpha\beta}$$

or

$$x^{\beta\alpha} < x^{\beta B}$$

In relation to the relevant carbon concentration gradients, this effectively means that diffusion is no longer going to take place from α to β (Figure 8.4). This results in the model stopping 'prematurely'. The effect of this is most dramatic for the $2\frac{1}{4}$ CrMo/9CrMo joint at 620°C which has stopped after only one particle has been dissolved.

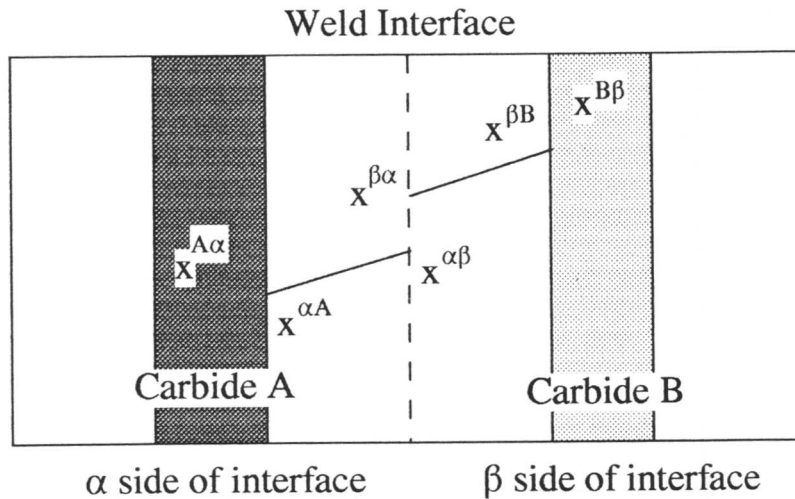


Figure 8.4: Concentration gradients that cause the model to stop prematurely.

8.3.2.3 Problem with the $2\frac{1}{4}$ CrMo/12CrMo joint

The problem with this joint in the linear model is that the model stops before the first particle has dissolved for the reasons mentioned in the previous section. The calculations of $x^{\beta B}$ and $x^{B\beta}$ are proceeding within the limits of the MTDATA calculations but are causing $x^{\beta B}$ to be greater than $x^{\beta\alpha}$ quite quickly. If the values of $x^{\beta B}$ and $x^{B\beta}$ are allowed to remain constant then the plot in Figure 8.5 is obtained which proves that the problem simply lies in



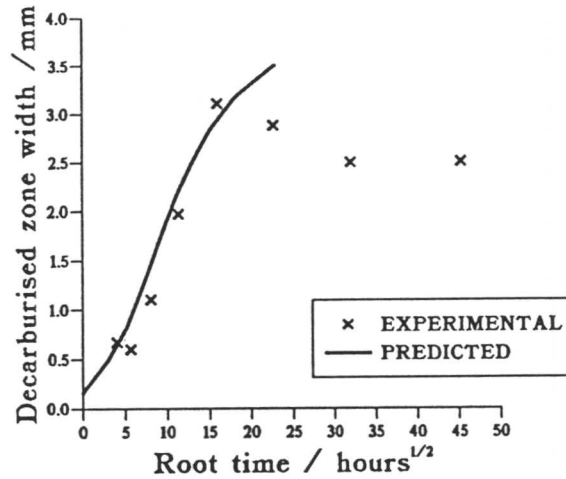


Figure 8.5: $2\frac{1}{4}\text{CrMo}/12\text{CrMo}$ joint at 730°C illustrating the effect of keeping the equilibrium carbon concentrations constant ; $d_{20} = 5\mu\text{m}$, Wagner model used for calculation of k .

the calculations of the equilibrium carbon concentrations and obtaining a value of k for such high chromium concentrations and complex systems.

The conclusion is therefore that, although the linear model gives accurate results for some joints it cannot be relied upon for joints with higher solute concentrations and calculations at longer times and higher temperatures.

8.3.3 Exponential model

The exponential model also predicts an increase in decarburised zone width with both time and temperature as illustrated in Figure 8.6 for the mild steel/ $2\frac{1}{4}\text{CrMo}$ joint at 700°C and 620°C .

In comparison with the experimental data (Figure 8.7) it can be seen that these predictions are slightly low. However, the exponential model does have a major application in that it allows comparisons to be made between different joints.

8.4 Effect of the difference in substitutional alloy concentration

In order to be able to compare alloy systems, the calculations have to be made using the same method for the calculation of the partition coefficient and the same value of the particle size. The exponential model is more sensitive to particle size than the linear model in that the slower kinetics at lower temperatures require a smaller particle size to be set. This is more in keeping with what is observed experimentally. The actual values of the decarburised zone width are then not really relevant as long as a comparison can be made. The exponential model



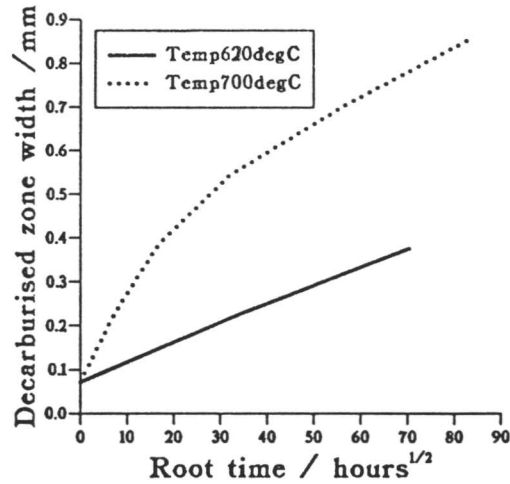


Figure 8.6: Mild steel/ $2\frac{1}{4}$ CrMo joint decarburised zone width predictions using the exponential model ; $d_{20} = 5\mu m$. The Wagner model was used to calculate the partition coefficient.

allows this to be done because it does not suffer from the same problems of mass balance that the linear model does so it can run for all of the systems. The experimental data presented in Chapter 6 revealed the following sequences for the degree of carburisation:

At the post weld heat treatment temperature:-

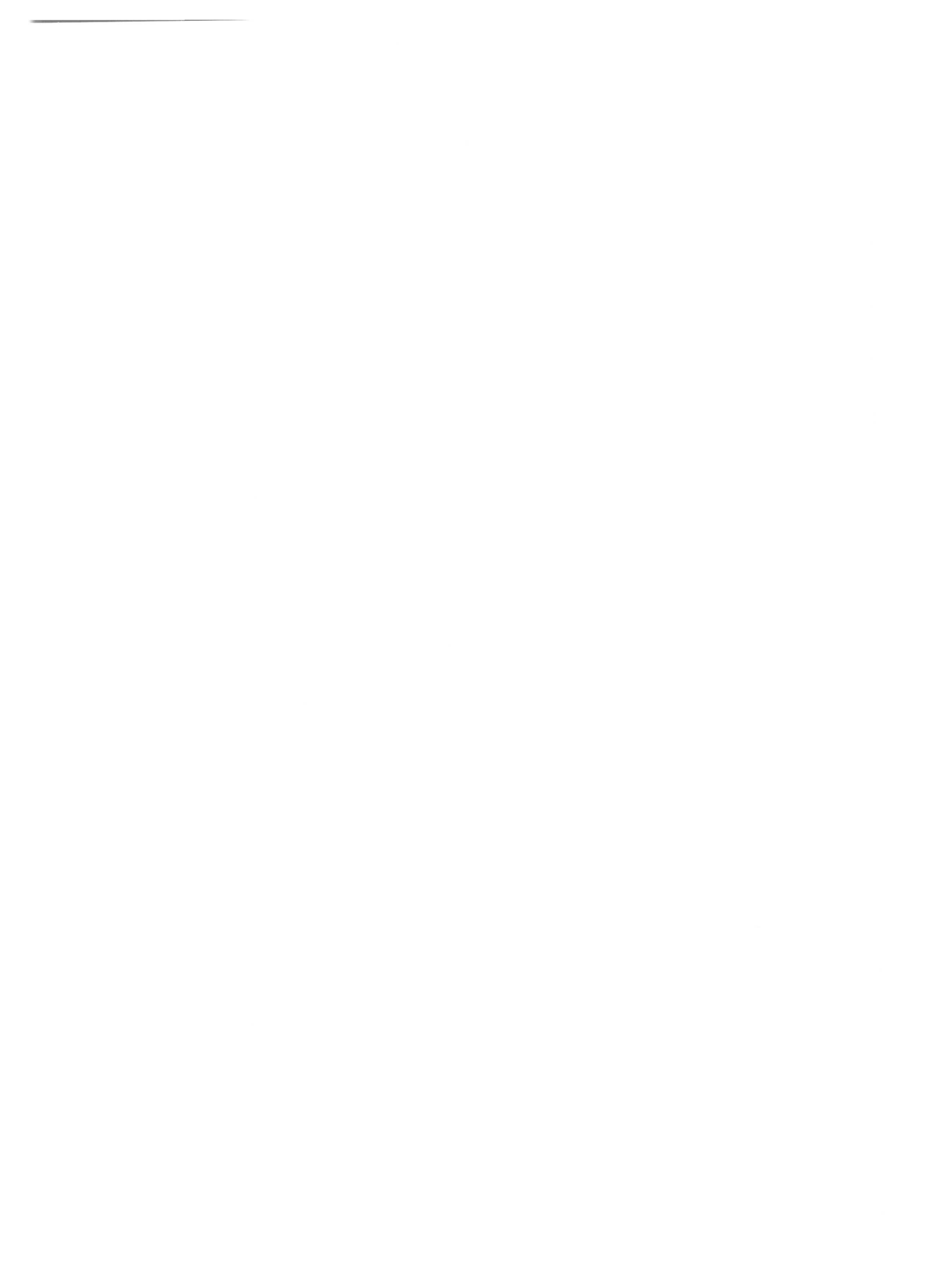
$$2\frac{1}{4}\text{CrMo}/12\text{CrMo} > (2\frac{1}{4}\text{CrMo}/9\text{CrMo} \ \& \ \text{mild steel}/2\frac{1}{4}\text{CrMo}) > \text{mild steel}/1\text{CrMo}$$

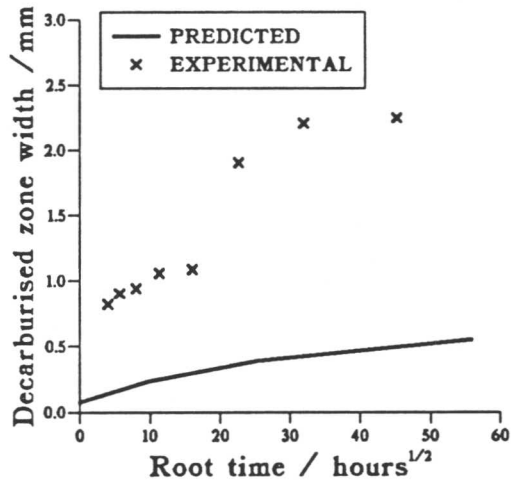
At 620°C:-

$$(\text{mild steel}/2\frac{1}{4}\text{CrMo} \ \text{and} \ \text{mild steel}/1\text{CrMo}) > (2\frac{1}{4}\text{CrMo}/9\text{CrMo} \ \text{and} \ 2\frac{1}{4}\text{CrMo}/12\text{CrMo})$$

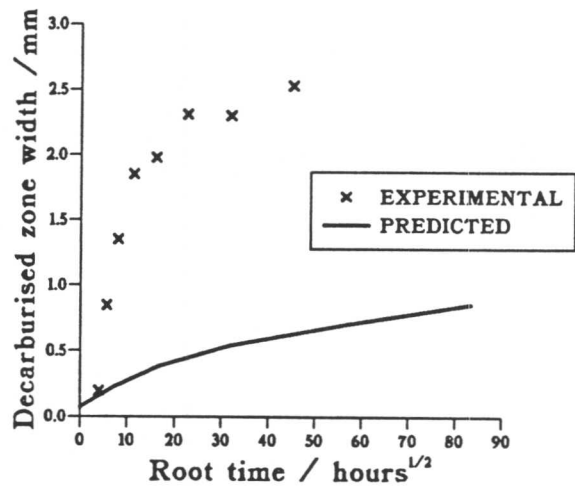
The graphs presented in Figure 8.8 show the calculations made from the exponential model revealing the same types of sequences in the extent of decarburisation.

There are two interesting things to note from these plots. Firstly, the model successfully predicts the change in sequence of the alloys between the two temperatures. It might be expected that the $2\frac{1}{4}$ CrMo/12CrMo and $2\frac{1}{4}$ CrMo/9CrMo would still exhibit higher degrees of decarburisation than either of the mild steel joints at both temperatures. Christoffel and Curran also noted this phenomenon, but were unable to explain it other than to indicate that it was not the absolute difference in alloy content that was important, as might be expected, but the particular alloy combinations involved. In an attempt to try and account for these changes, the initial carbon concentrations at the interface have been plotted for the mild steel/ $2\frac{1}{4}$ CrMo and $2\frac{1}{4}$ CrMo/12CrMo at both temperatures, Figure 8.9. Both joints show steeper gradients at the higher temperature which would be expected as the degree of decarburisation is greater at higher temperatures. However, the mild steel/ $2\frac{1}{4}$ CrMo joint shows steeper

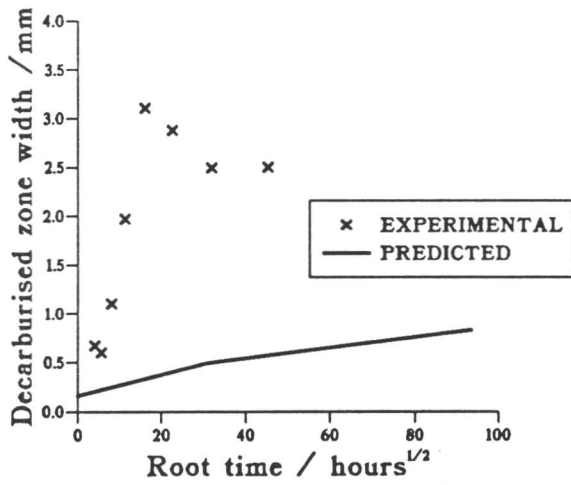




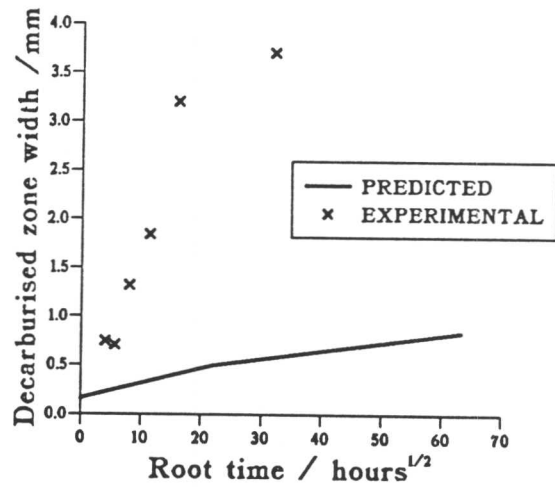
a)



b)

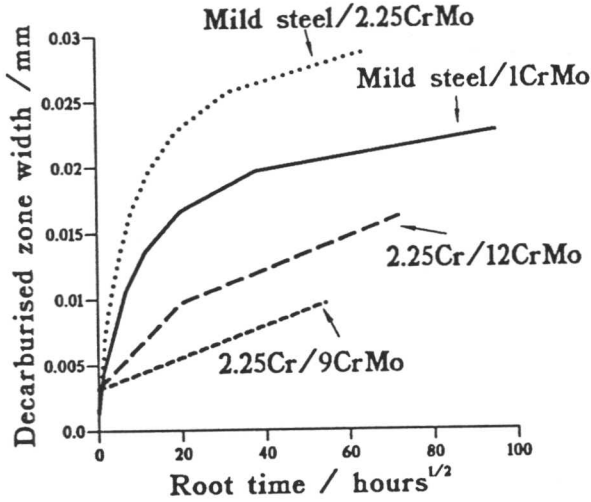


c)

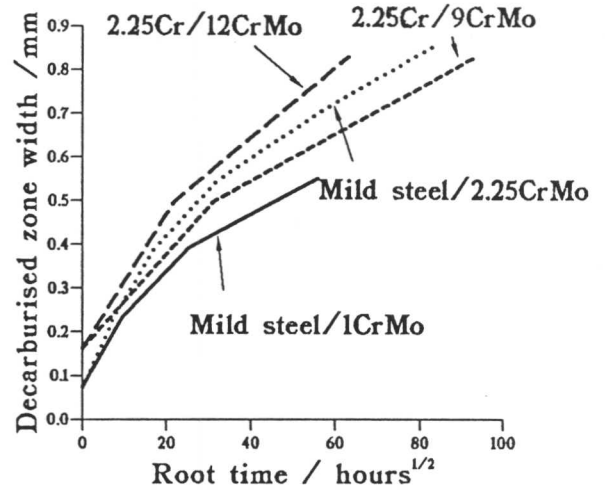


d)

Figure 8.7: Predicted plots for the exponential model at the post weld heat treatment temperature a) Mild steel/1CrMo b) Mild steel/2 $\frac{1}{4}$ CrMo c) 2 $\frac{1}{4}$ CrMo/9CrMo d) 2 $\frac{1}{4}$ CrMo/12CrMo. For all of these calculations the Wagner model was used to calculate the partition coefficient and $d_{20} = 5\mu m$



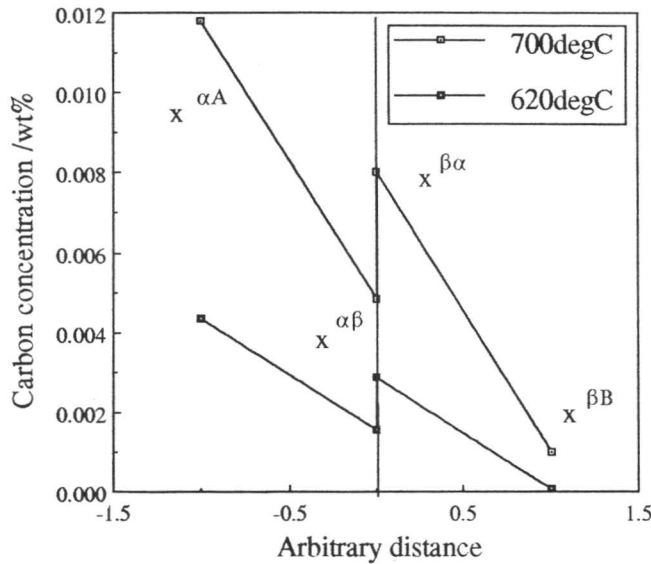
a)



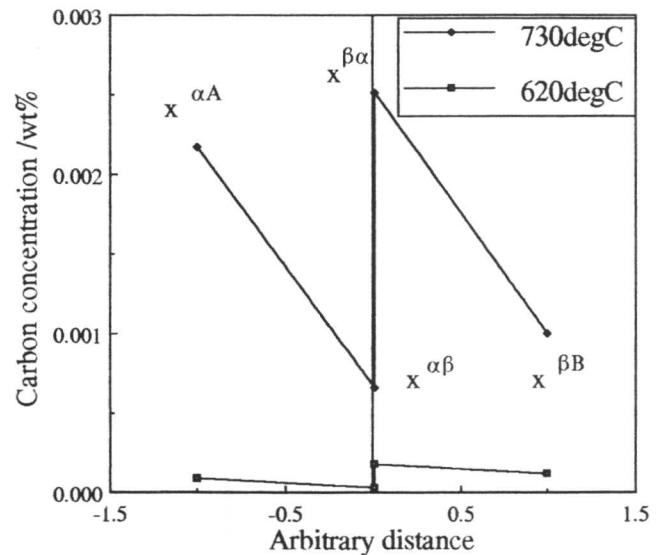
b)

Figure 8.8: Exponential model predictions of the extent of decarburisation at a) 620°C ($d_{20}=0.1\mu m$) and b) the post weld heat treatment temperature of the joints ($d_{20} = 5\mu m$). The partition coefficient was calculated using the Wagner model.

gradients than the 2 $\frac{1}{4}$ CrMo/12CrMo at both temperatures. Also, in all cases $x^{\alpha A} > x^{\beta B}$ except for the 2 $\frac{1}{4}$ CrMo/12CrMo joint at 620°C, where $x^{\alpha A} < x^{\beta B}$. The factors governing the extent of decarburisation would therefore seem to be a complex balance between the type of carbide on either side of the weld interface and the values of $x^{\alpha A}$ and $x^{\beta B}$.



a)



b)

Figure 8.9: Carbon concentration gradients for a) mild steel/2 $\frac{1}{4}$ CrMo at 700°C and 620°C and b) 2 $\frac{1}{4}$ CrMo/12CrMo at 730°C and 620°C

Secondly, the model predicts the crossing over of the plots for the $2\frac{1}{4}\text{CrMo}/9\text{CrMo}$ and mild steel/ $2\frac{1}{4}\text{CrMo}$ joints. It was mentioned in Chapter 6 that it was impossible to determine which of these joints had the greater degree of decarburisation because the plots overlap, Figure 8.10.

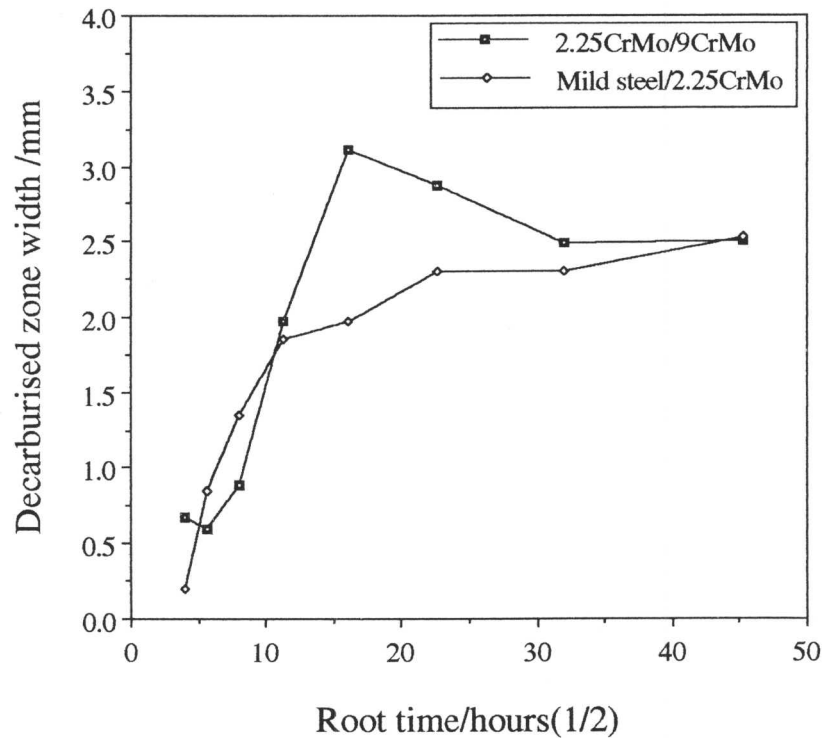


Figure 8.10: Experimental decarburised zone widths for the mild steel/ $2\frac{1}{4}\text{CrMo}$ and $2\frac{1}{4}\text{CrMo}/9\text{CrMo}$ joint at the post weld heat treatment temperature.

If the exponential model is run to longer times the plot of Figure 8.11 is obtained which shows a similar overlapping. This phenomenon was also observed on running the linear model to longer times. The mild steel/ $2\frac{1}{4}\text{CrMo}$ joint is therefore seen to start off more quickly than the $2\frac{1}{4}\text{CrMo}/9\text{CrMo}$ joint but will level out more quickly. This has to be an important consideration in dissimilar metal weld design and the ability of this model to able to predict factors such as this is extremely useful.

8.5 The effect of carburisation

The predicted carburised zone width is shown in Figure 8.12 for the mild steel/ $2\frac{1}{4}\text{CrMo}$ joint at 700°C .

It can be seen that the carburised zone width levels off in a similar manner to the experimental results. There is, however, a slight discontinuity in the graph corresponding to the onset of cementite precipitation where the values of $x^{\beta B}$ and $x^{B\beta}$ are changed. The plot of the predicted decarburised and carburised zone width of Figure 8.13 for this joint indicates that

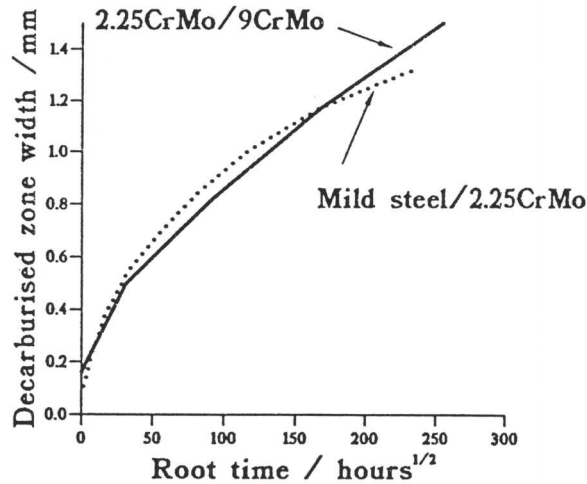


Figure 8.11: Exponential model predictions of the decarburised zone width for the $2\frac{1}{4}$ CrMo/9CrMo and mild steel/ $2\frac{1}{4}$ CrMo joint showing the overlapping of the plots.

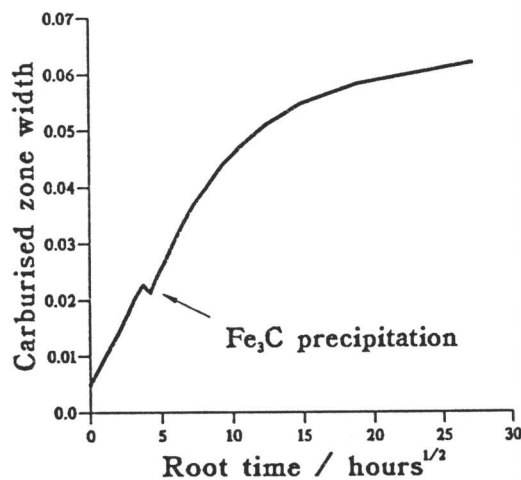


Figure 8.12: Carburisation effect for the mild steel/ $2\frac{1}{4}$ CrMo joint at 700°C.

the carburisation effect is less than the decarburisation effect as was noted experimentally in Figure 6.11.

8.6 Conclusions and further applications of the model

The conclusions from the results of the modelling work presented here are:-

1. The model will predict the non-parabolic kinetics of the decarburisation process. This is a result of allowing the equilibrium carbon concentrations in the ferrite and carbides to change as a function of the bulk carbon concentration.

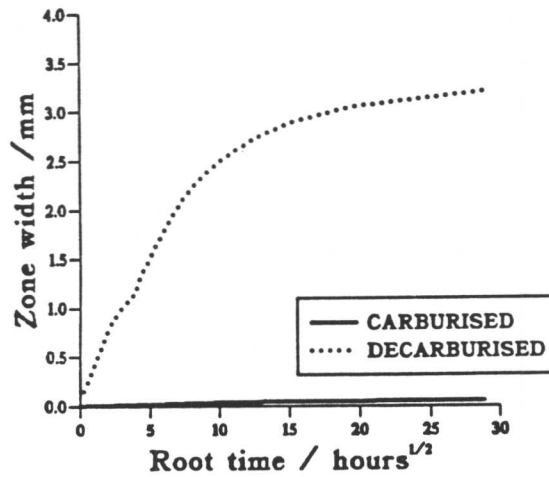


Figure 8.13: Comparison of predicted carburised and decarburised zone widths for the mild steel/ $2\frac{1}{4}$ CrMo joint at 700°C using the linear model.

2. The linear model will predict an ‘upper bound’ for the extent of decarburisation in a joint. However, owing to assumptions made about the mass balance on changing a particle and the difficulty of obtaining accurate thermodynamic data, it is recommended that this model is only used for simple systems and not any system containing more than 9wt% chromium.
3. The exponential model predicts much slower kinetics, but, as a result, predictions can be made for more alloy systems. This means that this model can be used to compare the extent of decarburisation in different alloy systems and those containing higher chromium concentrations. A general rule seems to be that decarburisation is minimised if there is the same type of carbide on either side of the interface *e.g.* $M_{23}C_6$ in the $2\frac{1}{4}$ CrMo/12CrMo joint at 620°C gives less decarburisation than Fe_3C and $M_{23}C_6$ for a mild steel/ $2\frac{1}{4}$ CrMo joint. This also accounts for the reason why the mild steel/ $2\frac{1}{4}$ CrMo joint levels off more quickly than the $2\frac{1}{4}$ CrMo/9CrMo joint at the post weld heat treatment temperature because the carbide type changes to being the same on either side.

Now that the models have been established, further applications for them can be envisaged. The ability to compare the extent of decarburisation in different joints makes the exponential model a useful tool in alloy design for dissimilar metal welds. In fact, this model has already found industrial application in this area. This property of the model can also be extended to actually designing alloys that will produce the smallest decarburised zone widths.

As decarburisation can occur during post weld heat treatment and during subsequent service it should be possible to change the temperature during the calculation and monitor the effect of an initial decarburised zone width on subsequent diffusion.

CHAPTER 9

Conclusions and Further Work

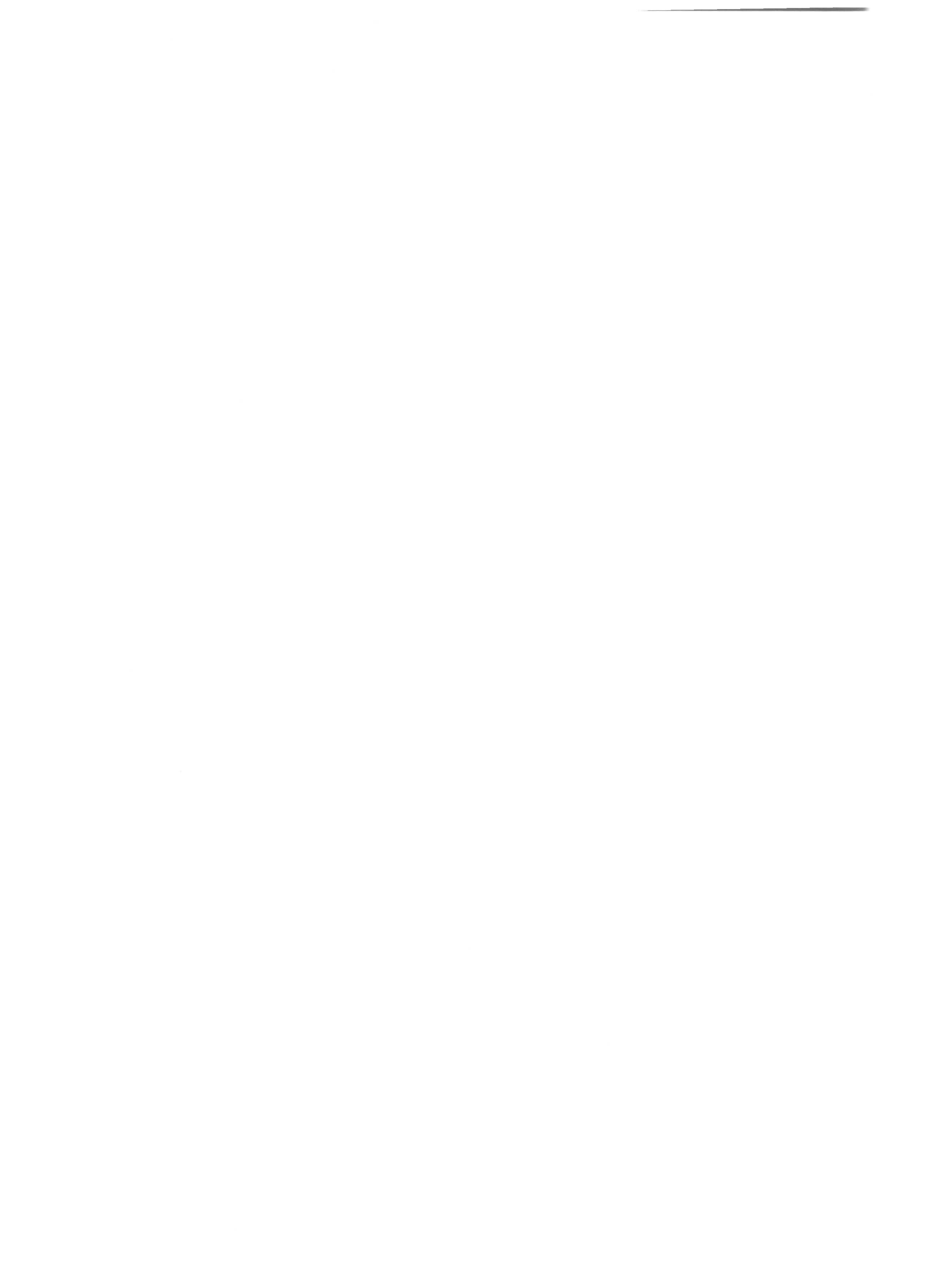
9.1 Conclusions

The aim of this work was to study the diffusion of carbon across dissimilar steel welds and ultimately to be able to model this process in both the austenite and ferrite phase fields. The major conclusions can be summarised as follows:-

1. Modelling of carbon diffusion in austenite can be achieved by the combination of equations to describe diffusion in semi-infinite media. The only limitation to this is the prediction of the partition coefficient, especially in concentrated solutions.
2. Modelling of carbon diffusion in ferrite is more complicated as the carbon available for diffusion is tied up in the form of carbides. Any model for carbon diffusion in ferrite must take this into account.
3. In ferritic/ferritic joints, the decarburised zone widths do not exhibit the expected parabolic kinetics but level off on a plot against root time.
4. The transport of carbon across the weld interface causes a reversion in the normal precipitation sequence.
5. The effect of the change in the bulk carbon concentration on either side of the interface causes the decarburised zone width to level off.
6. Two models have been developed for the prediction of decarburised zone widths, one which assumes a linear carbon concentration gradient and one which assumes an exponential profile.
7. The linear model for the prediction of decarburised zone widths will predict an 'upper bound' for the lower alloy combinations.
8. The exponential model will successfully predict trends in the extent of decarburisation although the actual values tend to be low. This has enabled this model to find industrial application as a tool in materials selection for dissimilar metal welds.
9. A general principle is that the carbon migration at dissimilar ferritic steel joints can be minimised by ensuring that the same kind of carbide is stable on either side of the joint. This phenomenon also explains the deviation from the parabolic rule at long times.

9.2 Further work

Possible further work on dissimilar metal welds could lie in the following areas:-



1. Finding ways of healing the microstructure.
2. Prediction of decarburisation across ferritic/austenitic dissimilar metal welds.

9.2.1 Healing the decarburised microstructure

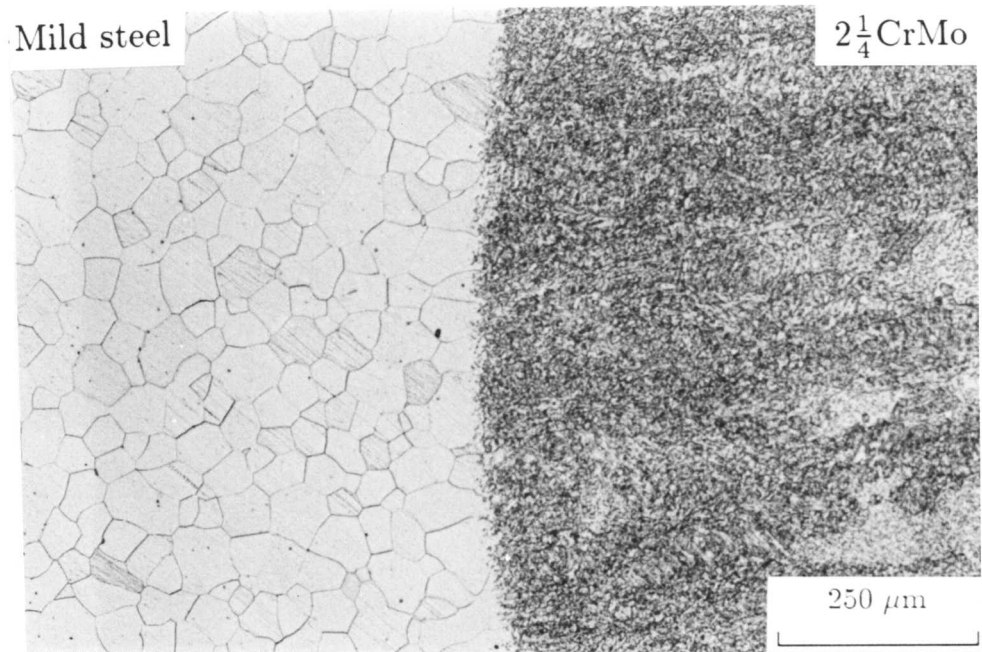
A small study into the feasibility of healing the decarburised microstructures was started during the course of this work. The 'healing' process involves reheating the microstructure into the austenite phase field to dissolve the carbides and then cool to room temperature. The initial trials were carried out on two mild steel/ $2\frac{1}{4}$ CrMo specimens which had received a heat treatment of 4096 hours at 700°C. MTDATA calculations revealed that full dissolution of the carbides should occur at 900°C, so a heat treatment of 1 hour at 950°C was applied to ensure complete dissolution and equilibration of the microstructure. One of the specimens was then quenched into water and the other air cooled to room temperature. The starting microstructure and resultant microstructures are illustrated in Figure 9.1. Hardness profiles across all three joints are provided in Figure 9.2.

It can be seen that the quenched sample, whilst regaining some of its original hardness has cracked at the position corresponding to the peak in the hardness profile. However, the air cooled sample, although still being relatively soft, has a more level profile, indicating that the discontinuity at the interface has decreased. However, more work is required to discover whether other properties such as toughness have recovered.

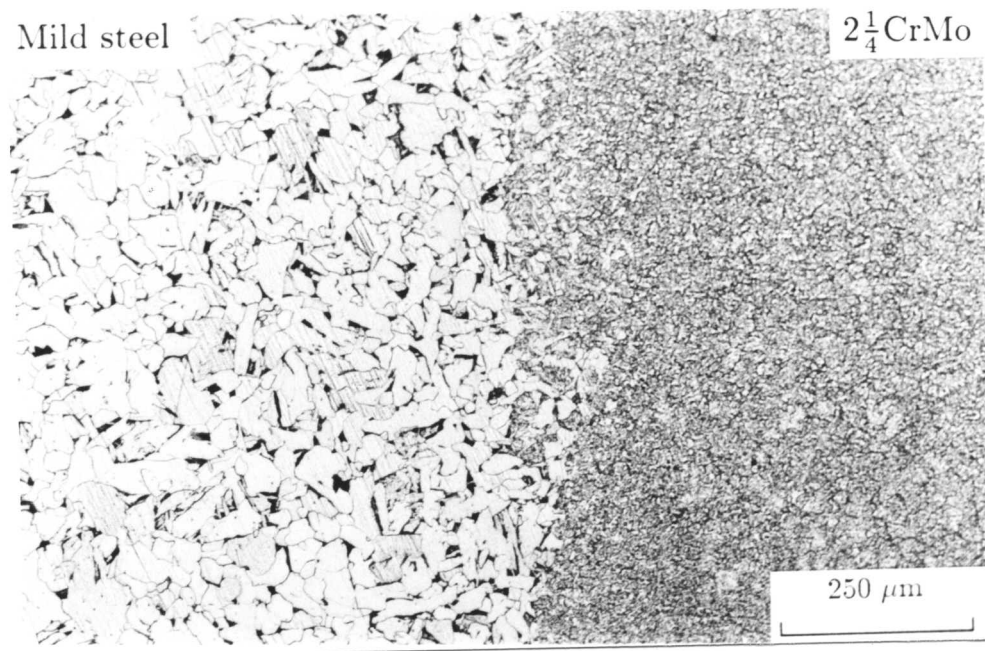
9.2.2 Prediction of decarburisation across ferritic/austenitic joints

The ferritic/austenitic type of dissimilar metal welds, although not studied at all in this work, make up a large proportion of the welds found in power station boilers. Diffusion in this case occurs from the ferrite to the austenitic side of the weld. Using the program for calculating diffusion profiles across austenitic/austenitic joints and combining this with the program for calculating the extent of diffusion in ferritic/ferritic joints, it should be possible to make predictions for the ferritic/austenitic system.





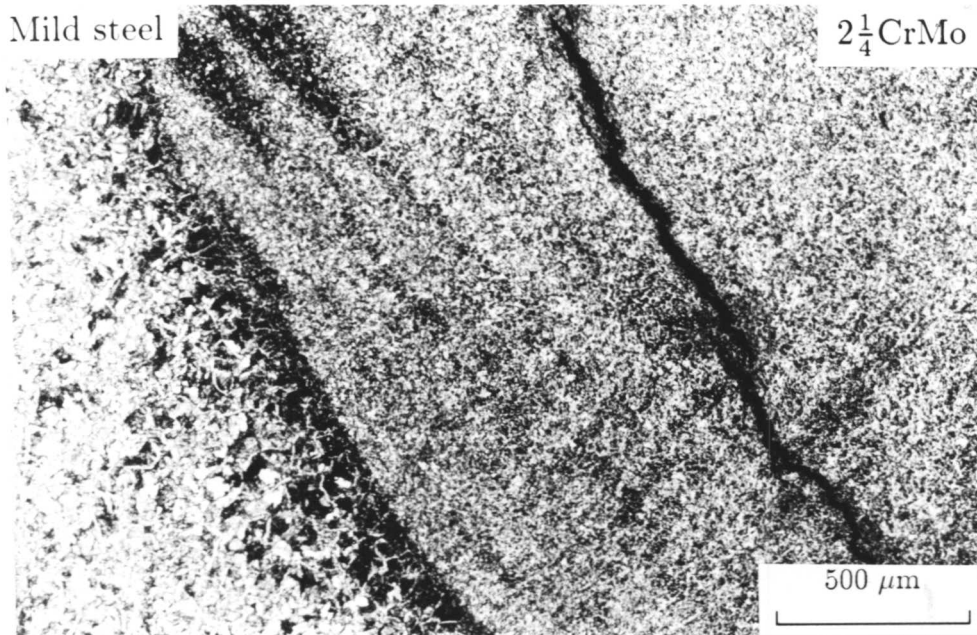
a) Initial microstructure



b) Air cooled microstructure

Figure 9.1: Interface microstructure for the mild steel/ $2\frac{1}{4}\text{CrMo}$ joint a) initial microstructure, b) air cooled microstructure c) quenched microstructure.





c) Quenched microstructure

Figure 9.1: Interface microstructure for the mild steel/ $2\frac{1}{4}$ CrMo joint a) initial microstructure, b) air cooled microstructure c) quenched microstructure.

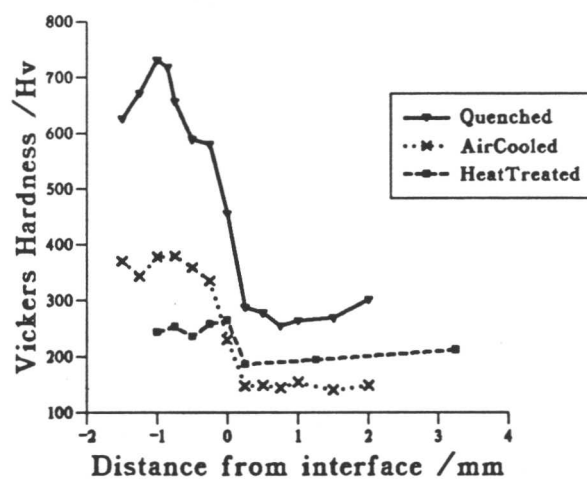


Figure 9.2: Hardness profile across all three joints



References

- Afrouz, A., Collins, M. J. and Pilkington, R., (1983)
Microstructural examination of a 1Cr-0.5Mo steel during creep, *Mater. Tech.*, **10**, 461-464
- Agren, J., (1983)
A note on the theoretical treatment of up-hill diffusion in compound welds, *Metallurgical Transactions*, **15**, 2083-2084
- Andrews, K. W., Dyson, D. J. and Keown, S. R., (1967)
Interpretation of electron diffraction patterns, *Hilger and watts Ltd., London*
- Baganis, E. A., and Kirkaldy, J. S., (1978)
Hardenability concepts with applications to steels, *AIME*, 82-125
- Baker, R. G. and Nutting J., (1959)
JISI, **192**, 257-268
- Balluffi, R. W., Cohen, M. and Averbach, B. L., (1951,)
The tempering of chromium steels, *Trans ASM*, **43**, 497-526
- Bhadeshia, H. K. D. H., (1981(a))
Diffusion of carbon in austenite, *Metal Science*, **15**, 477-484
- Bhadeshia, H. K. D. H., (1981(b))
Driving force for martensitic transformation in steels, *Metal Science*, **15**, 175-177
- Bhadeshia, H. K. D. H., (1981(c))
Thermodynamic extrapolation and martensite-start temperature of substitutionally alloyed steels, *Metal Science*, **15**, 178-180
- Bhadeshia, H. K. D. H., (1985)
Diffusional formation of ferrite in iron and its alloys, *Progress in Materials Science*, **29**, 321-386
- Bhadeshia, H. K. D. H., (1988)
CEGB Internal report, TPRD/L/3236/R87
- Bhadeshia H. K. D. H., (1992)
Bainite in Steels, *Institute of Materials, London*
- Bhadeshia, H. K. D. H, Svensson, L.E. and Gretoft, B., (1986)
Third International Conference on Welding and Performance of Pipelines, published by the Welding Institute, Cambridge, U. K.
- Beech, J. and Warrington, D. H., (1966)
JISI, **204**, 460-469
- Buchmayer, B., Cerjak, H., Witwer, M. and Kirkaldy, J. S., (1989)
Carbon diffusion and microstructure in dissimilar Cr-Mo-V welds and their influence on the mechanical properties, *Recent trends in welding research and technology, Proceedings of the 2nd international conference on trends in welding research*, Gatlinburg, U. S. A., May 1989, 237-242
- Christoffel, R. J., and Curran, R. M., (1956)
Welding Journal, **35(9)**, 457(s)-468(s)
- Darken, L. S., (1949)
Trans. AIME, **180**, 430-438
- Dyson, D. J. and Andrews, K. W., (1964)
The structure and metallurgical significance of the iron-molybdenum carbide Fe_2MoC (M_aC_b), *JISI*, **April**, 325-329
- Fujita, H. and Gosting L. J., (1956)
J. Am. Chem. Soc., **79**, 1099-1108

- Gorton, O. K., (1975)
Fabrication aspects of steels for boiler construction, *Materials In Power Plant*, **Series 3**, 44-51
- Hillert, M., (1959)
Acta. Met., **7**, 653-658
- Hillert, M. and Staffansson, L-I., (1970)
Regular solution model for stoichiometric phases and ionic melts, *Acta Chemica Scandinavia*, **24**, 3618-3626
- Hippesley, C. A., (1981)
Precipitation sequences in the HAZ of $2\frac{1}{4}$ CrMo steel during stress relief heat treatment, *Metal Science*, **April**, 137-147
- Irvine, K. J., Crowe, D. J. and Pickering, F. B., (1960)
The physical metallurgy of 12% chromium steels *JISI*, **August**, 386-405
- Kirkaldy, J. S., (1957)
Diffusion in multicomponent metallic systems, *Canadian Journal of Physics*, **35**, 435-440
- Kirkaldy, J. S., (1958)
Diffusion in multicomponent systems, *Canadian Journal of Physics*, **36**, 899-906
- Kirkaldy, J. S. and Young, D. S., (1987)
Diffusion in the condensed state, *Institute of Metals*, **Book 322**
- Kimmins, S. T., (1989)
G. E. C. Report No. RD/L/3529/R89
- Klueh, R. L. and King, J. F., (1982)
Welding Journal (Research Supplement), **9**, 301-311
- Klueh R. L. and Leitnaker, J. M., (1975)
An analysis of the decarburisation and ageing processes in $2\frac{1}{4}$ CrMo steel, *Met. Trans. A*, **6A**, 1089-2093
- Kucera, J. and Stransky, K., (1982)
Diffusion in iron, iron solid solutions and steels, *Materials Science and Engineering*, **52**, 1-38
- Little E. A., Harries, D. R. and Pickering, F. B., (1978)
Some aspects of the structure property relationships in 12%Cr steels, *Ferritic steels for fast reactor steam generators*, 136-144
- McLellan, R. B., Rudee, M. L. and Ischibachi, T., (1965)
The thermodynamics of dilute interstitial solid solutions with dual site occupancy and its applications to the diffusion of carbon in α -iron, *Trans. Met. Soc. AIME*, **233**, 1938-1948
- MTDATA - Metallurgical and Thermochemical Databank, (1989)
Version 4.30, *National Physical Laboratory, Teddington, Middlesex, U.K.*
- Murphy, M. C. and Branch, G. D., (1968)
Properties and microstructure of 12Cr-Mo-V-Nb creep resisting steel, *JISI*, 266-273
- Nutting, J., (1969)
The physical metallurgy of alloy steels, *JISI*, **June**, 872-893
- Onsager, L., (1945-46)
Ann. N. Y. Acad. Sci., **46**, 241
- Park, L., Fujita, T and Asakura, K., (1980)
Microstructure and creep rupture properties of a low Si-12Cr-Mo-V-Nb steel, *Trans. ISIJ*, **20**, 88-107



- Panton-Kent, R., (1989)
Welding Institute members report, 404-1989, 3-32
- Pickering, F. B. and Vassiliou, A. D., (1980)
 Effect of austenitising temperature on constitution, transformation and tempering of 9Cr1Mo steel, *metals technology, 7(10)*, 409-413
- Pilling, J. and Ridley, N., (1982)
Metallurgical Transactions A, 13A, 557-563
- Porter, D. A. and Easterling, K. E., (1981)
Phase transformations in metals and alloys, Van Nostrand Reinhold
- Ryder R. H., Roberts, D. I., Viswanathan, R. and Prager, M., (1986)
 Dissimilar weld failure analysis and development, *Recent trends in welding research and technology, Proceedings of an international conference on trends in welding research, Gatlinburg, U. S. A., May 1986, 509-513*
- Sanderson, S. J., (1977)
 Secondary hardening and tempering processes for a 9Cr-1Mo steel austenitised in the $\gamma + \delta$ phase field, *Metal Science, 11*, 490-492
- Sikka, V. K., Ward, C.T. and Thomas, K.C., (1983)
Ferritic steels for high temperature applications, Conference proceedings of the ASM ed. Ashok K. Khare, 65-84
- Siller, R. H. and McLellan, R. B., (1969,)
Metallurgical Transactions, 1, 985-990
- Smith, R. and Nutting, J., (1957)
JISI, 187, 314-329
- Stark, J. P., (1980)
 An approximate analytical demonstration of the famous Darken experiment, *Metallurgical Transactions A, 11A*, 1797-1798
- Thomson, R. C. and Bhadeshia, H. K. D. H., (1992)
 Carbide precipitation in 12CrMoV power plant steel, *Met. Trans A, 23A* 1171-1179
- Toft, L. H. and Marsden, R., (1961)
 The structure and properties of 1Cr-0.5Mo steel after service in CEGB power stations, *JISI Special Report, 70*, 276-294
- Trivedi, R. and Pound, G. M., (1967)
Journal of Applied Physics, 38(9), 3569
- Uhrenius, B., (1977)
Scandinavian Journal of Metallurgy, 6, 86-89
- Viswanathan, R. and Dimmer, J., (1985)
Dissimilar weld failure analysis program, EPRI CS 4252
- Wada, T., Wada, H., Elliott, J. F., and Chipman, J., (1972)
 Thermodynamics of the FCC Fe-Mn-C and Fe-Si-C alloys, *Met. Trans., 3*, 1657-1662
- Wada, T., Wada, H., Elliott, J. F., and Chipman, J., (1972)
 Activity of carbon and solubility of carbides in the FCC Fe-Mo-C, Fe-Cr-C and Fe-V-C alloys, *Met. Trans., 3*, 2865-2872
- Wells, C., Batz, W. and Mehl, R. F., (1950)
Trans.AIME, 188, 553-560

Woodhead, J. H. and Quarrell, A. G., (1965)

Role of carbides in low alloy creep resisting steels, *JISI* June 605-620

Yu, J, (1989)

Carbide stability diagrams in $2\frac{1}{4}$ CrMo steels *Met. Trans A*, **20A**, 1561-1564

Appendix I

The differential of the error function

This differential is required when solving the boundary condition of continuous flux across the interface and the derivation of the solution is as follows:-

$$\operatorname{erf}(bz) = \frac{2}{\sqrt{\pi}} \int_0^{bz} \exp\{-x^2\} dx$$

where in this case,

$$b = \frac{1}{2\sqrt{Dt}}$$
$$x = \frac{z}{2\sqrt{Dt}}$$

If $\operatorname{erf}(bz)$ is defined as $f(z)$ then,

$$f(z) = \frac{2}{\sqrt{\pi}} \int_0^{bz} \exp\{-x^2\} dx$$

Also if $y = bz$ then,

$$g(y) = \frac{2}{\sqrt{\pi}} \int_0^y \exp\{-x^2\} dx$$

Therefore, $f(z) = g(y)$, so

$$\frac{\partial f}{\partial z} = \frac{\partial g}{\partial z} = \frac{\partial g}{\partial y} \frac{\partial y}{\partial z}$$

Therefore

$$\frac{\partial f}{\partial z} = \frac{2}{\sqrt{\pi}} \exp\{-x^2\} b$$
$$\frac{\partial \{\operatorname{erf}(bz)\}}{\partial z} = \frac{2}{\sqrt{\pi}} \exp\left\{-\frac{z^2}{4Dt}\right\} \frac{1}{2\sqrt{Dt}}$$
$$\frac{\partial \operatorname{erf}\left\{\frac{z}{2\sqrt{Dt}}\right\}}{\partial z} = \frac{2}{\sqrt{\pi}} \exp\left\{-\frac{z^2}{4Dt}\right\} \frac{1}{2\sqrt{Dt}}$$

Appendix II
**Program listing for calculating diffusion profiles with
austenite on both sides of the interface**



.....
This program is for considering the diffusion couple
with austenite on both sides of the interface
.....

The alpha side of the interface is the high carbon activity side
The theta side of the interface is the low carbon activity side
A1 is the constant calculated from the boundary conditions in Chapter 3
B1 is the constant calculated from the boundary conditions in Chapter 3
CA is the carbon concentration in alpha at some position X after some time T
CG is the carbon concentration in theta at some position X after some time T
CAO is the carbon concentration in the high carbon activity side of the weld distant from the interface
CGO is the carbon concentration in the low carbon activity side of the weld distant from the interface
CAG is the carbon concentration at the weld junction on the alpha side
CGA is the carbon concentration at the weld junction on the theta side
DA is the diffusion coefficient in the alpha component
DG is the diffusion coefficient in the theta component
KTEMP is the absolute temperature
K is the partition coefficient at the interface
THR is the time in hours
T is the time in seconds
W is the carbon carbon interaction energy in austenite
WX1 is the weight percent of element X on the high carbon activity side.
WX2 is the weight percent of element X on the low carbon activity side.
XX1 is the mole fraction of element X on the low carbon activity side.
XX2 is the mole fraction of element X on the high carbon activity side.
X is the distance on either side of the interface in metres
XMM is the distance on either side of the interface in millimetres
.....
.....

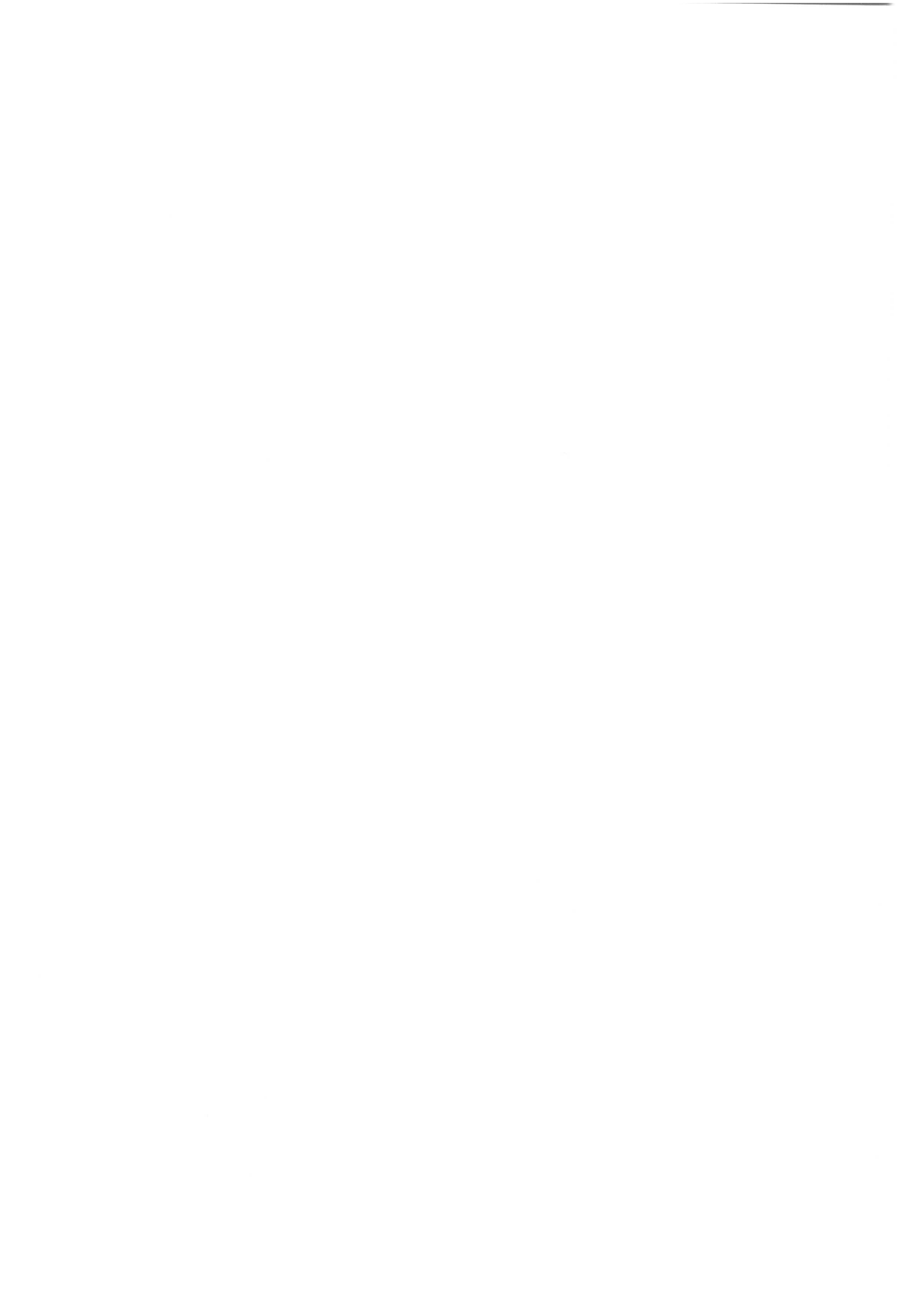
```
IMPLICIT DOUBLE PRECISION(A-H,K,N-Z), INTEGER(I,J,L,M)
DIMENSION D1(30),D2(30),Y1(30),Y2(30),YC1(30),YC2(30)
AVER=2.0
```

Subroutines LOGO, DATA, DATA1 and DATA2 and DDTA all collect and display the data with options to make any changes
Subroutine OMEGA calculates the carbon-carbon interaction energy for each side of the weld

```
CALL LOGO(AVER)
OPEN(2,FILE='AUS.RES')
CALL DATA(KTEMP,THR)
CALL DATA1(WC1,WMN1,WSI1,WNI1,WCR1,WMO1,WW1,WV1,WNB1,WCO1)
CALL DATA2(WC2,WMN2,WSI2,WNI2,WCR2,WMO2,WW2,WV2,WNB2,WCO2)
CALL OMEGA(WC1,WSI1,WMN1,WNI1,WMO1,WCR1,WV1,W1)
CALL OMEGA(WC2,WSI2,WMN2,WNI2,WMO2,WCR2,WV2,W2)
WRITE(*,*)' Is the diffusion driven by: '
WRITE(*,*)' 1. Silicon'
WRITE(*,*)' 2. Chromium'
CALL REEDI(JY)
500 CALL DDTA(WC1,WMN1,WSI1,WNI1,WCR1,WMO1,WW1,WV1,WNB1,WCO1,
& WC2,WMN2,WSI2,WNI2,WCR2,WMO2,WW2,WV2,WNB2,WCO2,KTEMP,THR,W1,W2,JY)
```

Subroutine CON converts the data from weight per cent to mole fraction

```
CALL CON(WC1,WMN1,WSI1,WNI1,WCR1,WMO1,WW1,WV1,WNB1,WCO1,
& XC1,XMN1,XSI1,XNI1,XCR1,XMO1,XW1,XV1,XNB1,XCO1)
```



```

CALL CON(WC2,WMN2,WSI2,WNI2,WCR2,WMO2,WW2,WV2,WNB2,WCO2,
& XC2,XMN2,XSI2,XNI2,XCR2,XMO2,XW2,XV2,XNB2,XCO2)
CAO=XC1
CGO=XC2

```

These equations calculate the initial guesses of CAG and CAG in order that a value of the partition coefficient can be calculated (Section 4.4)

The subroutine DIFFF calculates the diffusion coefficient of carbon in austenite

```

CAG=XC1*0.66D0
CGA=XC2*1.33D0
IF (CAG .LT. CAO) THEN
  CALL DIFFF(W1,CAG,CAO,KTEMP,DA)
ELSE
  CALL DIFFF(W1,CAO,CAG,KTEMP,DA)
ENDIF
IF (CGO .LT. CGA) THEN
  CALL DIFFF(W2,CGO,CGA,KTEMP,DG)
ELSE
  CALL DIFFF(W2,CGA,CGO,KTEMP,DG)
ENDIF

```

The KFUN subroutines calculate the partition coefficient by one of the methods below

```

WRITE(*,*)' For the calculation of partition coefficient;'
WRITE(*,*)' Option 1 = Wagner'
WRITE(*,*)' Option 2 = Uhrenius'
WRITE(*,*)' Option 3 = Wada et al.'
WRITE(*,*)' Option 4 = Experimental value'
WRITE(*,*)' Select the method number to continue.'
CALL REEDI(J)
IF (J .EQ. 1) THEN
  CALL KFUN(CAO,XMN1,XSI1,XNI1,XCR1
& ,XMO1,XCU1,XW1,XV1,XNB1,XCO1,CGO,XMN2,XSI2,XNI2,XCR2
& ,XMO2,XCU2,XW2,XV2,XNB2,XCO2,KTEMP,K)
ELSEIF (J .EQ. 2 .AND. JY .EQ. 1) THEN
  CALL KFUN2(XSI1,CAO,XSI2,CGO,KTEMP,K)
ELSEIF (J .EQ. 2 .AND. JY .EQ. 2) THEN
  CALL KFUN6(XCR1,CAO,XCR2,CGO,KTEMP,K)
ELSEIF (J .EQ. 3 .AND. JY .EQ. 1) THEN
  CALL KFUN4(WSI1,WC1,KTEMP,WC2,WSI2,K)
ELSEIF (J .EQ. 3 .AND. JY .EQ. 2) THEN
  CALL KFUN7(WCR1,WC1,KTEMP,WC2,WCR2,K)
ELSEIF (J .EQ. 5) THEN
  WRITE(*,*)' Input value of k.'
  CALL REED(K)
  IF (K .GT. 1.0D+02 .OR. K .LT. 0.0D0) THEN
    CALL BOUND(K,1.0D+02,0.0D+00)
  ENDIF
ENDIF
100  A1=(CGO+(CAO*DSQRT(DA/DG)))/(K+DSQRT(DA/DG))
CAG=A1
CGA=K*A1
IF (CAG .LT. CAO) THEN
  CALL DIFFF(W1,CAG,CAO,KTEMP,DAN)
ELSE
  CALL DIFFF(W1,CAO,CAG,KTEMP,DAN)
ENDIF

```



```

IF (CGO .LT. CGA) THEN
  CALL DIFFF(W2,CGO,CGA,KTEMP,DGN)
ELSE
  CALL DIFFF(W2,CGA,CGO,KTEMP,DGN)
ENDIF

```

DAN and DGN are the values of the diffusion coefficient produced in the iteration process

```

N=(DA/DAN)

```

This IF-ELSE loop determines whether the iteration continues

```

IF ( N .LT. 1.05 .AND. N .GT. 0.95) THEN
  GOTO 30
ELSE
  DA=DAN
  DG=DGN
  GOTO 100
ENDIF

```

```

30 T=THR*3600

```

This DO loop produces the values of CA and CG at various values of XMM

```

M = 0
DO 40 I = 0,25
  X=I*1.0D-03
  XMM=X*1.0D+03
  A1=(CGO+(CAO*DSQRT(DA/DG)))/(K+DSQRT(DA/DG))
  B1=CAO-A1
  CA=A1+(B1*DERF((X/(2.0*DSQRT(DA*T))))))
  CG=(K*A1)-(DSQRT(DA/DG)*B1*DERF((X/(2.0*DSQRT(DG*T))))))
  CAG=A1
  CGA=K*A1
  NEG=-XMM
  M = M + 1
  D1(M)=XMM
  Y1(M)=CA
  D2(M)=NEG
  Y2(M)=CG

```

All of the calculations are made in mole fraction and subroutine CONVE converts the concentrations back to wt%

```

      CALL CONVE(M,Y1,XMN1,XSI1,XNI1,XCR1,XMO1,XW1,XV1,XNB1,XCO1,
&      YC1)
      CALL CONVE(M,Y2,XMN2,XSI2,XNI2,XCR2,XMO2,XW2,XV2,XNB2,XCO2,
&      YC2)
40 CONTINUE

```

The results are printed to the file AUS.RES in subroutine RESULT, but there is also an option to print to the screen, subroutine RESP or for a plot, subroutine PLOT

```

CALL RESULT(K,DA,DG,T,THR,D1,YC1,D2,YC2,M)
WRITE(*,*) ' Results are in the file AUS.RES '
WRITE(*,*) ' Do you want a screen printout?'
WRITE(*,*) ' 1 ----- YES '
WRITE(*,*) ' 2 ----- NO '
CALL REEDI(LYES)
IF (LYES .EQ. 1) THEN
  CALL RESP(K,CAG,CGA,DA,DG,T,THR,D1,YC1,D2,YC2,M)
ELSE

```



```

      GOTO 80
    ENDIF
80  WRITE(*,*) ' Do you want a plot??'
    WRITE(*,*) ' 1 ----- YES '
    WRITE(*,*) ' 2 ----- NO '
    CALL REEDI(MYES)
    IF (MYES .EQ. 1) THEN
      CALL PLOT(D1,YC1,D2,YC2)
    ELSE
      GOTO 90
    ENDIF
90  WRITE(*,1)
1   FORMAT(' 1 ----- RECALCULATE' /
&    ' 2 ----- QUIT')
    CALL REEDI(IYES)
    IF (IYES .EQ. 1) THEN
      GOTO 500
    ELSEIF (IYES .EQ. 2) THEN
      GOTO 110
    ENDIF
110  END

```

.....

The data routines input the data to the program. Every value is checked to ensure that it lies within the preset bounds for that variable. If it does not the option is given to enter another value or continue with the value inputted, although no guarantee is given for the success of the run!

```

      SUBROUTINE DATA(KTEMP,THR)
      IMPLICIT DOUBLE PRECISION (A-H,K,N-Z), INTEGER(I,J,L,M)
      WRITE(*,8)
8     FORMAT(10X,' Please enter the following information:-')
      WRITE(*,1)
1     FORMAT(10X,' Temperature in Kelvin')
      CALL REED(KTEMP)
      IF (KTEMP .GT. 1700 .OR. KTEMP .LT. 900) THEN
        CALL BOUND(KTEMP,1700.0D0,900D0)
      ENDIF
      WRITE(*,4)
4     FORMAT(10X,' Time in hours')
      CALL REED(THR)
      IF (THR .GT. 1.0D99 .OR. THR .LT. 1.0D-99) THEN
        CALL BOUND(THR,1.0D99,1.0D-99)
      ENDIF
      RETURN
      END

```

.....

```

      SUBROUTINE DATA1(WC1,WMN1,WSI1,WNI1,WCR1,WMO1,WW1,WV1,WNB1,WCO1)
      IMPLICIT DOUBLE PRECISION (A-H,K,N-Z), INTEGER(I,J,L,M)
      WRITE(*,1)
1     FORMAT(10X,' Please enter the following information:-')
      WRITE(*,2)
2     FORMAT(10X,' Carbon conc. in low C activity steel in wt %')
      CALL REED(WC1)

```



```

IF (WC1 .GT. 5 .OR. WC1 .LT. 0.02) THEN
  CALL BOUND(WC1,5.0D0,2.0D-2)
ENDIF
WRITE(*,3)
3  FORMAT(10X,' Manganese conc. in low C activity steel in wt %')
  CALL REED(WMN1)
  IF (WMN1 .GT. 15 .OR. WMN1 .LT. 0.02) THEN
    CALL BOUND(WMN1,15.0D0,2.0D-2)
  ENDIF
  WRITE(*,4)
4  FORMAT(10X,' Silicon conc. in low C activity steel in wt %')
  CALL REED(WSI1)
  IF (WSI1 .GT. 15 .OR. WSI1 .LT. 0.02) THEN
    CALL BOUND(WSI1,15.0D0,2.0D-3)
  ENDIF
  WRITE(*,5)
5  FORMAT(10X,' Nickel conc. in low C activity steel in wt %')
  CALL REED(WNI1)
  IF (WNI1 .GT. 15 .OR. WNI1 .LT. 0.0) THEN
    CALL BOUND(WNI1,15.0D0,0.0D0)
  ENDIF
  WRITE(*,6)
6  FORMAT(10X,' Chromium conc. in low C activity steel in wt %')
  CALL REED(WCR1)
  IF (WCR1 .GT. 15 .OR. WCR1 .LT. 0.0) THEN
    CALL BOUND(WCR1,15.0D0,0.0D0)
  ENDIF
  WRITE(*,7)
7  FORMAT(10X,' Molybdenum conc. in low C activity steel in wt %')
  CALL REED(WMO1)
  IF (WMO1 .GT. 15 .OR. WMO1 .LT. 0.0) THEN
    CALL BOUND(WMO1,15.0D0,0.0D0)
  ENDIF
  WRITE(*,9)
9  FORMAT(10X,' Tungsten conc. in low C activity steel in wt %')
  CALL REED(WW1)
  IF (WW1 .GT. 15 .OR. WW1 .LT. 0.0) THEN
    CALL BOUND(WW1,15.0D0,0.0D0)
  ENDIF
  WRITE(*,10)
10 FORMAT(10X,' Vanadium conc. in low C activity steel in wt %')
  CALL REED(WV1)
  IF (WV1 .GT. 15 .OR. WV1 .LT. 0.0) THEN
    CALL BOUND(WV1,15.0D0,0.0D0)
  ENDIF
  WRITE(*,11)
11 FORMAT(10X,' Niobium conc. in low C activity steel in wt %')
  CALL REED(WNB1)
  IF (WNB1 .GT. 15 .OR. WNB1 .LT. 0.0) THEN
    CALL BOUND(WNB1,15.0D0,0.0D0)
  ENDIF
  WRITE(*,12)
12 FORMAT(10X,' Cobalt conc. in low C activity steel in wt %')
  CALL REED(WCO1)
  IF (WCO1 .GT. 15 .OR. WCO1 .LT. 0.0) THEN

```



```
CALL BOUND(WCO1,15.0D0,0.0D0)
ENDIF
RETURN
END
```

```
.....
.....
SUBROUTINE DATA2(WC2,WMN2,WSI2,WNI2,WCR2,WMO2,WW2,WV2,WNB2,WCO2)
IMPLICIT DOUBLE PRECISION (A-H,K,N-Z), INTEGER(I,J,L,M)
WRITE(*,1)
1  FORMAT(10X,' Please enter the following information:-')
WRITE(*,2)
2  FORMAT(10X,' Carbon conc. in high C activity steel in wt %')
CALL REED(WC2)
IF (WC2 .GT. 5 .OR. WC2 .LT. 0.02) THEN
    CALL BOUND(WC2,5.0D0,2.0D-2)
ENDIF
WRITE(*,3)
3  FORMAT(10X,' Manganese conc. in high C activity steel in wt %')
CALL REED(WMN2)
IF (WMN2 .GT. 15 .OR. WMN2 .LT. 0.02) THEN
    CALL BOUND(WMN2,15.0D0,2.0D-2)
ENDIF
WRITE(*,4)
4  FORMAT(10X,' Silicon conc. in high C activity steel in wt %')
CALL REED(WSI2)
IF (WSI2 .GT. 15 .OR. WSI2 .LT. 0.02) THEN
    CALL BOUND(WSI2,15.0D0,2.0D-2)
ENDIF
WRITE(*,5)
5  FORMAT(10X,' Nickel conc. in high C activity steel in wt %')
CALL REED(WNI2)
IF (WNI2 .GT. 15 .OR. WNI2 .LT. 0.0) THEN
    CALL BOUND(WNI2,15.0D0,0.0D0)
ENDIF
WRITE(*,6)
6  FORMAT(10X,' Chromium conc. in high C activity steel in wt %')
CALL REED(WCR2)
IF (WCR2 .GT. 20 .OR. WCR2 .LT. 0.0) THEN
    CALL BOUND(WCR2,20.0D0,0.0D0)
ENDIF
WRITE(*,7)
7  FORMAT(10X,' Molybdenum conc. in high C activity steel in wt %')
CALL REED(WMO2)
IF (WMO2 .GT. 15 .OR. WMO2 .LT. 0.0) THEN
    CALL BOUND(WMO2,15.0D0,0.0D0)
ENDIF
WRITE(*,9)
9  FORMAT(10X,' Tungsten conc. in high C activity steel in wt %')
CALL REED(WW2)
IF (WW2 .GT. 15 .OR. WW2 .LT. 0.0) THEN
    CALL BOUND(WW2,15.0D0,0.0D0)
ENDIF
WRITE(*,10)
10 FORMAT(10X,' Vanadium conc. in high C activity steel in wt %')
```



```

CALL REED(WV2)
IF (WV2 .GT. 15 .OR. WV2 .LT. 0.0) THEN
  CALL BOUND(WV2,15.0D0,0.0D0)
ENDIF
WRITE(*,11)
11  FORMAT(10X,' Niobium conc. in high C activity steel in wt %')
CALL REED(WNB2)
IF (WNB2 .GT. 15 .OR. WNB2 .LT. 0.0) THEN
  CALL BOUND(WNB2,15.0D0,0.0D0)
ENDIF
WRITE(*,12)
12  FORMAT(10X,' Cobalt conc. in high C activity steel in wt %')
CALL REED(WCO2)
IF (WCO2 .GT. 15 .OR. WCO2 .LT. 0.0) THEN
  CALL BOUND(WCO2,15.0D0,0.0D0)
ENDIF
RETURN
END

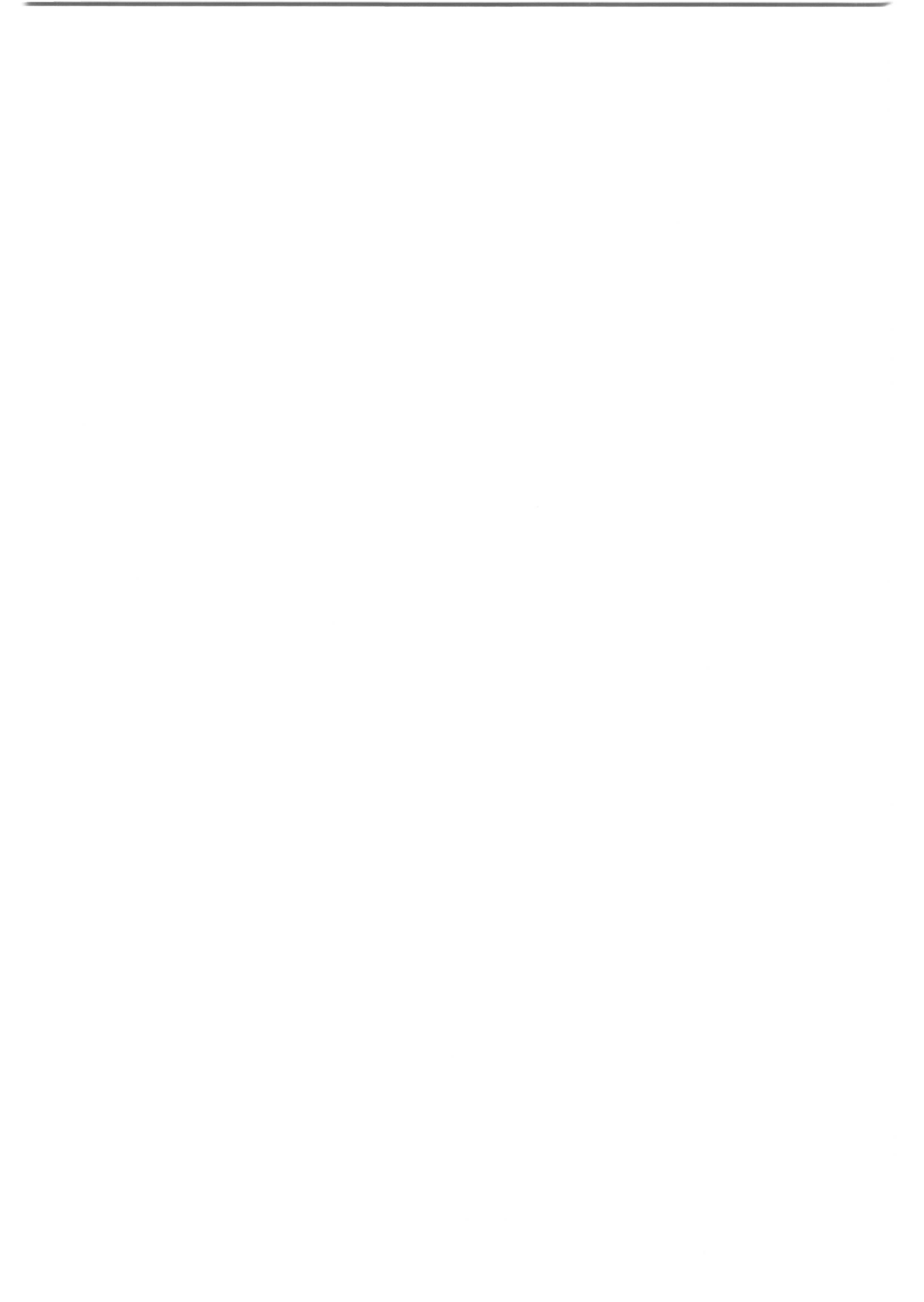
```

.....
.....
This subroutine converts weight percent to mole fraction

```

SUBROUTINE CON(WC,WMN,WSI,WNI,WCR,WMO,WW,WV,WNB,WCO,
&  XC,XMN,XSI,XNI,XCR,XMO,XW,XV,XNB,XCO)
IMPLICIT DOUBLE PRECISION (A-Z)
AC=12.01
AMN=54.94
ASI=28.09
ANI=58.71
ACR=52.00
AMO=95.94
AW=183.85
AV=50.94
ANB=92.91
ACO=58.93
AFE=55.85
ADD=WC+WMN+WSI+WNI+WCR+WMO+WW+WV+WNB+WCO
WFE=100.0D0-ADD
MC=WC/AC
MMN=WMN/AMN
MSI=WSI/ASI
MNI=WNI/ANI
MCR=WCR/ACR
MMO=WMO/AMO
MW=WW/AW
MV=WV/AV
MNB=WNB/ANB
MCO=WCO/ACO
MFE=WFE/AFE
SUM=MC+MMN+MSI+MNI+MCR+MMO+MW+MV+MNB+MCO+MFE
XC=MC/SUM
XMN=MMN/SUM
XSI=MSI/SUM
XNI=MNI/SUM
XCR=MCR/SUM

```



```

XMO=MMO/SUM
XW=MW/SUM
XV=MV/SUM
XNB=MNB/SUM
XCO=MCO/SUM
RETURN
END

```

.....
.....
This is a subroutine to calculate the carbon-carbon interaction energy in austenite as a function of alloy composition. The theory for this program is in Bhadeshia (1981 c).
The answer is in Joules/mol.

```

SUBROUTINE OMEGA(WC,WSI,WMN,WNI,WMO,WCR,WV,W)
DOUBLE PRECISION C(8),P(8),B1,B2,Y(8),T10,T20,B3,XBAR
DOUBLE PRECISION WC,WSI,WMN,WNI,WMO,WCR,WV,W
INTEGER B5,I,U,B4
B3=0.0D+00
C(1)=WC/12.0115D+00
C(2)=WSI/28.09D+00
C(3)=WMN/54.94D+00
C(4)=WNI/58.71D+00
C(5)=WMO/95.94D+00
C(6)=WCR/52.0D+00
C(7)=WV/50.94D+00
C(8)=C(1)+C(2)+C(3)+C(4)+C(5)+C(6)+C(7)
C(8)=100.0D+00-C(8)
C(8)=C(8)/55.84D+00
B1=C(1)+C(2)+C(3)+C(4)+C(5)+C(6)+C(7)+C(8)
DO 107 U=2,7
    Y(U)=C(U)/C(8)
107 CONTINUE
DO 106 U=1,8
    C(U)=C(U)/B1
106 CONTINUE
XBAR=C(1)
XBAR=DINT(10000.0D+00*XBAR)
XBAR=XBAR/10000
B2=0.0D+00
T10=Y(2)*(-3)+Y(3)**2+Y(4)*12+Y(5)*(-9)+Y(6)*(-1)+Y(7)*(-12)
T20=-3*Y(2)-37.5*Y(3)-6*Y(4)-26*Y(5)-19*Y(6)-44*Y(7)
P(2)=2013.0341+763.8167*C(2)+45802.87*C(2)**2-280061.63*C(2)**3
& +3.864D+06*C(2)**4-2.4233D+07*C(2)**5+6.9547D+07*C(2)**6
P(3)=2012.067-1764.095*C(3)+6287.52*C(3)**2-21647.96*C(3)**3-
& 2.0119D+06*C(3)**4+3.1716D+07*C(3)**5-1.3885D+08*C(3)**6
P(4)=2006.8017+2330.2424*C(4)-54915.32*C(4)**2+1.6216D+06*C(4)**3
& -2.4968D+07*C(4)**4+1.8838D+08*C(4)**5-5.5531D+08*C(4)**6
P(5)=2006.834-2997.314*C(5)-37906.61*C(5)**2+1.0328D+06*C(5)**3
& -1.3306D+07*C(5)**4+8.411D+07*C(5)**5-2.0826D+08*C(5)**6
P(6)=2012.367-9224.2655*C(6)+33657.8*C(6)**2-566827.83*C(6)**3
& +8.5676D+06*C(6)**4-6.7482D+07*C(6)**5 +2.0837D+08*C(6)**6
P(7)=2011.9996-6247.9118*C(7)+5411.7566*C(7)**2
& +250118.1085*C(7)**3-4.1676D+06*C(7)**4
DO 108 U=2,7
    B3=B3+P(U)*Y(U)

```



```

      B2=B2+Y(U)
108  CONTINUE
      IF (B2 .EQ. 0.0D+00) GOTO 455
      W=(B3/B2)*4.187
      GOTO 456
455   W=8054.0
456  CONTINUE
      RETURN
      END

```

.....

.....

This subroutine converts from mole fraction to weight percent.

```

      SUBROUTINE CONVE(M,Y,XMN,XSI,XNI,XCR,XMO,XW,XV,XNB,
&    XCO,YC)
      IMPLICIT DOUBLE PRECISION(A-H,K,N-Z), INTEGER(I,J,L,M)
      DIMENSION Y(30),YC(30)
      AC=12.01
      AMN=54.94
      ASI=28.09
      ANI=58.71
      ACR=52.00
      AMO=95.94
      AW=183.85
      AV=50.94
      ANB=92.91
      ACO=58.93
      AFE=55.85
      ADD=Y(M)+XMN+XSI+XNI+XCR+XMO+XW+XV+XNB+XCO
      XFE=1.0D0-ADD
      NC=Y(M)*AC
      MMN=XMN*AMN
      NSI=XSI*ASI
      NNI=XNI*ANI
      NCR=XCR*ACR
      NMO=XMO*AMO
      NW=XW*AW
      NV=XV*AV
      NNB=XNB*ANB
      NCO=XCO*ACO
      NFE=XFE*AFE
      SUM=NC+MMN+NSI+NNI+NCR+NMO+NW+NV+NNB+NCO+NFE
      YC(M)=(NC/SUM)*100
      RETURN
      END

```

.....

.....

This program calculates the Wagner activity coefficients for the calculation of the value of k.
EX is the Wagner interaction parameter for element X
AC is the activity coefficient of carbon
LAC is the log of the activity coefficient

```

      SUBROUTINE KFUN(XC1, XMN1, XSI1, XNI1, XCR1, XMO1, XCU1,
&    XW1, XV1, XNB1, XCO1, XC2, XMN2, XSI2, XNI2, XCR2, XMO2, XCU2
&    , XW2, XV2, XNB2, XCO2, KTEMP, K)

```



```

IMPLICIT DOUBLE PRECISION (A-Z)
EC=8910/KTEMP
EMN=-5070/KTEMP
ESI=4.84-(7370/KTEMP)
ENI=-2.2+(7600/KTEMP)
ECR=24.4-(38400/KTEMP)
EMO=3.855-(17870/KTEMP)
ECU=4200/KTEMP
EW=23.4-(36214/KTEMP)
EV=-24660/KTEMP
ENB=-28770/KTEMP
ECO=2800/KTEMP
LAC1=(XC1*EC)+(XMN1*EMN)+(XSI1*ESI)+(XNI1*ENI)+(XCR1*ECR)+
& (XMO1*EMO1)+(XCU1*ECU)+(XW1*EW)+(XV1*EV)+(XNB1*ENB)+(XCO1*ECO)
LAC2=(XC2*EC)+(XMN2*EMN)+(XSI2*ESI)+(XNI2*ENI)+(XCR2*ECR)+
& (XMO2*EMO2)+(XCU2*ECU)+(XW2*EW)+(XV2*EV)+(XNB2*ENB)+(XCO2*ECO)
AC1=DEXP(LAC1)
AC2=DEXP(LAC2)
K=AC1/AC2
RETURN
END

```

.....

This program calculates the Uhrenius activity coefficients for the determination of the partition coefficient when Si is driving the diffusion.

AY is the activity of carbon

LAY is the log of the carbon activity

YCR, YC, K1 AND K2 are defined in Uhrenius, B., 1977, Scandanavian Journal of Metallurgy, 6, 86-89.

R is the gas constant

```

SUBROUTINE KFUN2(XSI1,XC1,XSI2,XC2,KTEMP,K)
IMPLICIT DOUBLE PRECISION (A-Z)
R=8.314
K1=42140+23.17*KTEMP
K2=126.9
YCR1=XSI1/(1.0-XC1)
YC1=XC1/(1.0-XC1)
LAY1=(R*KTEMP*DLOG(YC1/(1.0-YC1))+(K1*YC1)+(K2*YCR1))
& /(R*KTEMP)
AY1=DEXP(LAY1)
YCR2=XSI2/(1.0-XC2)
YC2=XC2/(1.0-XC2)
LAY2=(R*KTEMP*DLOG(YC2/(1.0-YC2))+(K1*YC2)+(K2*YCR2))
& /(R*KTEMP)
AY2=DEXP(LAY2)
K=(AY1*XC2)/(AY2*XC1)
RETURN
END

```

.....

This program calculates the partition coefficient as given by the data of Wada *et al.*

These equations are for Si driving the diffusion.

```

SUBROUTINE KFUN3(WSI1,WC1,KTEMP,WC2,WSI2,K)

```



```

IMPLICIT DOUBLE PRECISION(A-H,K,N-Z), INTEGER(I,J,L,M)
A1=8.90*WSI1
B1=179.0+A1
C1=(B1/KTEMP)*WC1
AFC1=C1+((0.041+(62.5/KTEMP))*WSI1)
FC1=DEXP(AFC1)
A2=8.90*WSI2
B2=179.0+A2
C2=(B2/KTEMP)*WC2
AFC2=C2+((0.041+(62.5/KTEMP))*WSI2)
FC2=DEXP(AFC2)
K=FC1/FC2
RETURN
END

```

.....
.....
This program calculates the Uhrenius activity coefficients for the determination of the partition coefficient when Cr is driving the diffusion

```

SUBROUTINE KFUN6(XCR1,XC1,XCR2,XC2,KTEMP,K)
IMPLICIT DOUBLE PRECISION (A-Z)
R=8.314
K1=42140+23.17*KTEMP
K2=-339+0.187*KTEMP
YCR1=XCR1/(1.0-XC1)
YC1=XC1/(1.0-XC1)
LAY1=(R*KTEMP*DLOG(YC1/(1.0-YC1)))+(K1*YC1)+(K2*YCR1))
& / (R*KTEMP)
AY1=DEXP(LAY1)
YCR2=XCR2/(1.0-XC2)
YC2=XC2/(1.0-XC2)
LAY2=(R*KTEMP*DLOG(YC2/(1.0-YC2)))+(K1*YC2)+(K2*YCR2))
& / (R*KTEMP)
AY2=DEXP(LAY2)
K=(AY1*XC2)/(AY2*XC1)
RETURN
END

```

.....
.....
This subroutine calculates the partition coefficient according to the data of Wada *et al.* when Cr is driving the diffusion.

```

SUBROUTINE KFUN7(WCR1,WC1,KTEMP,WC2,WCR2,K)
IMPLICIT DOUBLE PRECISION(A-H,K,N-Z), INTEGER(I,J,L,M)
AFC1=2300/KTEMP-2.24+((179/KTEMP)*WC1)-((102/KTEMP)-0.033)*WCR1
FC1=DEXP(AFC1)
AFC2=2300/KTEMP-2.24+((179/KTEMP)*WC2)-((102/KTEMP)-0.033)*WCR2
FC2=DEXP(AFC2)
K=FC1/FC2
RETURN
END

```

.....
.....
This program calculates the effective diffusivity of carbon in austenite, taking account



of the fact that the diffusivity is concentration dependent.
 HH is Planck's constant (Joules/sec)
 KK is Boltzmann's constant (Joules/ Kelvin)
 Z is the co-ordination of an interstitial site
 PSI is the concentration dependance of the diffusion coefficient
 THETA is the number of C atoms/number of Fe atoms
 ACTIV is the activity of carbon in austenite
 R is the gas constant
 X is the mole fraction of carbon
 SIGMA is the site exclusion probability

```

SUBROUTINE DIFFF(W,XBAR,XGAG,T,ANS)
IMPLICIT DOUBLE PRECISION (A-H,K-Y), INTEGER(I,J,Z)
DOUBLE PRECISION DIFF(500), CARB(500)
HH=6.6262D-34
KK=1.38062D-23
Z=12
A5=1.0D+00
R=8.31432D+00
II2=0
DASH=(KK*T/HH)*DEXP(-(21230.0D+00/T))*DEXP(-31.84D+00)
This DO loop specifies the variables for the subroutine TRAPE to evaluate the integral
DO 9 II=1,1000
  CARB(II)=XBAR
  IF (II .GT. 1)GOTO 1
  GOTO 8
1  XINCR=(XGAG-XBAR)/10
  CARB(II)=CARB(II-1)+XINCR
  (CARB(II) .GT. XGAG) GOTO 5
8  X=CARB(II)
  II2=II2+1
  THETA=X/(A5-X)
  CALL LOGS(X,T,W,R,ACTIV)
  ACTIV=DEXP(ACTIV)
  CALL DIV(X,T,W,R,DACTIV)
  DACTIV=DACTIV*ACTIV
  DACTIV=DACTIV*A5/((A5+THETA)**2)
  SIGMA=A5-DEXP((-W)/(R*T))
  PSI=ACTIV*(A5+Z*((A5+THETA)/(A5-(A5+Z/2)*THETA+(Z/2)*
& (A5+Z/2)*(A5-SIGMA)*THETA*THETA)))+(A5+THETA)*DACTIV
  DIFF(II)=DASH*PSI*1.0D-04
9  CONTINUE
5  II3=0

```

TRAPE is a subroutine for integration of a function

```

CALL TRAPE(CARB,DIFF,ANS,II2)
ANS=ANS/(XGAG-XBAR)
RETURN
END

```

.....

This function gives LN(ACTIVITY) of carbon in austenite

```

SUBROUTINE LOGS(X,T,W,R,CT)
DOUBLE PRECISION J,DG,DUM,T,R,W,X,CT
J=1-DEXP(-W/(R*T))
DG=DSQRT(1-2*(1+2*J)*X+(1+8*J)*X*X)

```



```

DUM=5*DLOG((1-2*X)/X)+6*W/(R*T)+((38575.0)-(
& 13.48)*T)/(R*T)
CT=DUM+DLOG(((DG-1+3*X)/(DG+1-3*X))**6)
RETURN
END

```

.....

This function gives the differential of LN(ACTIVITY) of carbon in austenite with respect to X

```

SUBROUTINE DIV(X,T,W,R,DCG)
DOUBLE PRECISION J,DG,DDG,X,T,W,R,DCG
J=1-DEXP(-W/(R*T))
DG=DSQRT(1-2*(1+2*J)*X+(1+8*J)*X*X)
DDG=(0.5/DG)*(-2-4*J+2*X+16*J*X)
DCG=-((10/(1-2*X))+(5/X))+6*((DDG+3)/(DG-1+3*X
& )-(DDG-3)/(DG+1-3*X))
RETURN
END

```

.....

The purpose of this subroutine is to compute the vector of integral values for a given general table of argument and function values

USAGE - CALL TRAPE(X,Y,Z,NDIM)
DESCRIPTION OF PARAMETERS

X - Double precision input vector of argument values

Y - Double precision input vector of function values

Z - The resulting DP vector of integral values

NDIM - The dimension of vectors X,Y,Z. NDIM MAX. 1000

METHOD

Beginning with Z(1)=0, evaluation of vector z is done by means of the trapezoidal rule.

```

.....
SUBROUTINE TRAPE(X,Y,ANS,NDIM)
DOUBLE PRECISION X(1000),Y(1000),AZ(1000)
DOUBLE PRECISION SUM1,SUM2,ANS
SUM2=0.D+00
IF (NDIM-1)4,3,1
INTEGRATION LOOP
1      DO 2 I=2,NDIM
        SUM1=SUM2
        SUM2=SUM2+.5D+00*(X(I)-X(I-1))*(Y(I)+Y(I-1))
2      AZ(I-1)=SUM1
3      AZ(NDIM)=SUM2
        ANS=SUM2
4      RETURN
        END

```

.....

This is a routine for calculating the error function.

```

DOUBLE PRECISION FUNCTION DERF(Y)
IMPLICIT REAL*8(A-H,O-Z)
INTEGER ISW,I
DOUBLE PRECISION P(5),Q(3),P1(8),Q1(7),P2(5),Q2(4)
COEFFICIENTS FOR 0.0 .LE. Y .LT. 0.477
DATA P(1)/-.44422647396874/,
& P(2)/10.731707253648/,

```



```

&      P(3)/15.915606197771/,
&      P(4)/374.81624081284/,
&      P(5)/2.5612422994823D-02/
      DATA Q(1)/17.903143558843/,
&      Q(2)/124.82892031581/,
&      Q(3)/332.17224470532/
COEFFICIENTS FOR .477 .LE. Y .LE. 4.0
      DATA P1(1)/7.2117582508831/,
&      P1(2)/43.162227222057/,
&      P1(3)/152.98928504694/,
&      P1(4)/339.32081673434/,
&      P1(5)/451.91895371187/,
&      P1(6)/300.45926102016/,
&      P1(7)/-1.3686485738272D-07/,
&      P1(8)/.56419551747897/
      DATA Q1(1)/77.000152935229/,
&      Q1(2)/277.58544474399/,
&      Q1(3)/638.98026446563/,
&      Q1(4)/931.35409485061/,
&      Q1(5)/790.95092532790/,
&      Q1(6)/300.45926095698/,
&      Q1(7)/12.782727319629/
COEFFICIENTS FOR 4.0 .LT. Y
      DATA P2(1)/-.22695659353969/,
&      P2(2)/-4.9473091062325D-02/,
&      P2(3)/-2.9961070770354D-03/,
&      P2(4)/-2.2319245973418D-02/,
&      P2(5)/-2.7866130860965D-01/
      DATA Q2(1)/1.0516751070679/,
&      Q2(2)/.19130892610783/,
&      Q2(3)/1.0620923052847D-02/,
&      Q2(4)/1.9873320181714/
CONSTANTS
      DATA XMIN/1.0D-8/,XLARGE/5.6875D0/
      DATA SSQPI/.56418958354776/
FIRST EXECUTABLE STATEMENT
      X = Y
      ISW = 1
      IF (X.GE.0.0D0) GO TO 5
          ISW = -1
          X = -X
5          IF (X.LT..477D0) GO TO 10
          IF (X.LE.4.0D0) GO TO 25
          IF (X.LT.XLARGE) GO TO 35
          RES = 1.D0
          GO TO 50
ABS(Y) .LT. .477, EVALUATE APPROXIMATION FOR ERF
10          IF (X.LT.XMIN) GO TO 20
          XSQ = X*X
          XNUM = P(5)
          DO 15 I=1,4
              XNUM = XNUM*XSQ+P(I)
15          CONTINUE
          XDEN = ((Q(1)+XSQ)*XSQ+Q(2))*XSQ+Q(3)
          RES = X*XNUM/XDEN

```



```

                GO TO 50
20             RES = X*P(4)/Q(3)
                GO TO 50
.477 .LE. ABS(Y) .LE. 4.0 EVALUATE APPROXIMATION FOR ERF
25             XSQ = X*X
                XNUM = P1(7)*X+P1(8)
                XDEN = X+Q1(7)
                DO 30 I=1,6
                    XNUM = XNUM*X+P1(I)
                    XDEN = XDEN*X+Q1(I)
30             CONTINUE
                RES = XNUM/XDEN
                GO TO 45
4.0 .LT. ABS(Y), EVALUATE APPROXIMATION FOR ERF
35             XSQ = X*X
                XI = 1.0D0/XSQ
                XNUM = P2(4)*XI+P2(5)
                XDEN = XI+Q2(4)
                DO 40 I=1,3
                    XNUM = XNUM*XI+P2(I)
                    XDEN = XDEN*XI+Q2(I)
40             CONTINUE
                RES = (SSQPI+XI*XNUM/XDEN)/X
45             RES = RES*DEXP(-XSQ)
                RES = 1.0D0-RES
50             IF (ISW.EQ.-1) RES = -RES
                DERF = RES
                RETURN
                END

```

```

.....
                DOUBLE PRECISION FUNCTION DERFC(A)
                DOUBLE PRECISION A,DERF
                DERFC=1.0D+00-DERF(A)
                RETURN
                END

```

.....

.....

This subroutine reads in a double precision number and checks that a character string has not been input

```

                SUBROUTINE REED(A)
                IMPLICIT DOUBLE PRECISION(A-H,K,N-Z), INTEGER(I,J,L,M)
996             READ(*,*,ERR=999)A
                GOTO 998
999             WRITE(*,997)
997             FORMAT(10X,' Your input is incorrect, please try again.')


```

 GOTO 996
998 RETURN
 END

```


```

.....

.....

This routine checks that the input value is an integer

```

                SUBROUTINE REEDI(I)

```



```

INTEGER I
996 READ(*,*,ERR=999)I
    GOTO 998
999 WRITE(*,997)
997 FORMAT(10X,' Your input is incorrect, please try again.')
```

.....
.....
This routine checks that the input data is within the bounds for that variable

```

SUBROUTINE BOUND(A,B,C)
IMPLICIT DOUBLE PRECISION(A-H,K,N-Z), INTEGER(I,J,L,M)
2 WRITE(*,1)B,C
1 FORMAT(10X,' Your input is out of bounds'/
& 12X,' The limits are 'D12.4,' to ', D12.4///  

& 12X,' Please input a new value or type 999 to continue with'/
& 12X,' your dubious choice of input! ')
CALL REED(D)
IF (D .EQ. 999)GOTO 3
    A=D
    IF (A .LT. C .OR. A .GT. B)GOTO 2
3 RETURN
END
```

.....
.....
This subroutine prints out all of the input data and gives the option to change any of the variables

```

SUBROUTINE DDTA(WC1,WMN1,WSI1,WNI1,WCR1,WMO1,WW1,WV1,WNB1,WCO1,
& WC2,WMN2,WSI2,WNI2,WCR2,WMO2,WW2,WV2,WNB2,WCO2,KTEMP,THR,W1,W2,JY)
IMPLICIT DOUBLE PRECISION(A-H,K,N-Z), INTEGER(I,J,L,M)
200 WRITE(*,300)WC1,WMN1,WSI1,WNI1,WCR1,WMO1,WW1,WV1,WNB1,WCO1,
& WC2,WMN2,WSI2,WNI2,WCR2,WMO2,WW2,WV2,WNB2,WCO2
WRITE(*,400)KTEMP,THR,W1,W2
300 FORMAT(
& 10X' The current values that have been inputed are:-'/
& 10X' Low C activity side of the weld'/
& 10X' 1. C ',F8.3,10X,' wt %'/
& 10X' 2. Mn ',F8.3,10X,' 3. Si ',F8.3/
& 10X' 4. Ni ',F8.3,10X,' 5. Cr ',F8.3/
& 10X' 6. Mo ',F8.3,10X,' 7. W ',F8.3/
& 10X' 8. V ',F8.3,10X,' 9. Nb ',F8.3/
& 10X' 10. Co ',F8.3 /
& 10X' High C activity side of the weld'/
& 10X' 11. C ',F8.3,10X,' wt %'/
& 10X' 12. Mn ',F8.3,10X,' 13. Si ',F8.3/
& 10X' 14. Ni ',F8.3,10X,' 15. Cr ',F8.3/
& 10X' 16. Mo ',F8.3,10X,' 17. W ',F8.3/
& 10X' 18. V ',F8.3,10X,' 19. Nb ',F8.3/
& 10X' 20. Co ',F8.3)
400 FORMAT(10X,' 21. Temperature in Kelvin ',F8.3/
& 10X' 22. Time in hours ',F8.3/
& 10X' Carbon-carbon interaction energy in alpha ',D12.4/
& 10X' Carbon-carbon interaction energy in theta ',D12.4/)
```



```

WRITE(*,*)' Is the diffusion driven by: '
WRITE(*,*)' 1. Silicon'
WRITE(*,*)' 2. Chromium'
CALL REEDI(JY)
IF ( WSI1 .LT. WSI2 .AND. JY .EQ. 1) THEN
462   WRITE(*,462)
      FORMAT(10X,'*****WARNING*****'
/
&      10X,' The Si values that you have input are incorrect'/
&      10X,' Please change them.')
```

```

ENDIF
IF ( WCR2 .LT. WCR1 .AND. JY .EQ. 2) THEN
463   WRITE(*,463)
      FORMAT(10X,'*****WARNING*****'
/
&      10X,' The Cr values that you have input are incorrect'/
&      10X,' Please change them.')
```

```

ENDIF
WRITE(*,124)
124  FORMAT(10X,' Do you wish to change any of this input?'20X,/
&      10X,' (Choose the item number, or 0 to continue) ')
CALL REEDI(JYES)
IF (JYES .EQ. 0) THEN
  RETURN
ENDIF
IF (JYES .EQ. 1) GOTO 1
IF (JYES .EQ. 2) GOTO 2
IF (JYES .EQ. 3) GOTO 3
IF (JYES .EQ. 4) GOTO 4
IF (JYES .EQ. 5) GOTO 5
IF (JYES .EQ. 6) GOTO 6
IF (JYES .EQ. 7) GOTO 7
IF (JYES .EQ. 8) GOTO 8
IF (JYES .EQ. 9) GOTO 9
IF (JYES .EQ. 10) GOTO 10
IF (JYES .EQ. 11) GOTO 11
IF (JYES .EQ. 12) GOTO 12
IF (JYES .EQ. 13) GOTO 13
IF (JYES .EQ. 14) GOTO 14
IF (JYES .EQ. 15) GOTO 15
IF (JYES .EQ. 16) GOTO 16
IF (JYES .EQ. 17) GOTO 17
IF (JYES .EQ. 18) GOTO 18
IF (JYES .EQ. 19) GOTO 19
IF (JYES .EQ. 20) GOTO 20
IF (JYES .EQ. 21) GOTO 21
IF (JYES .EQ. 22) GOTO 22
1    WRITE(*,100)
100  FORMAT(10X,' Carbon conc. in low C activity steel in wt %')
CALL REED(WC1)
IF (WC1 .GT. 5 .OR. WC1 .LT. 0.02) THEN
  CALL BOUND(WC1,5.0D0,2.0D-2)
ENDIF
GOTO 200
2    WRITE(*,102)
102  FORMAT(10X,' Manganese conc. in low C activity steel in wt %')
```



```

CALL REED(WMN1)
IF (WMN1 .GT. 15 .OR. WMN1 .LT. 0.02) THEN
    CALL BOUND(WMN1,15.0D0,2.0D-2)
ENDIF
GOTO 200
3   WRITE(*,103)
103  FORMAT(10X,' Silicon conc. in low C activity steel in wt %')
    CALL REED(WSI1)
    IF (WSI1 .GT. 15 .OR. WSI1 .LT. 0.02) THEN
        CALL BOUND(WSI1,15.0D0,2.0D2)
    ENDIF
    GOTO 200
4   WRITE(*,104)
104  FORMAT(10X,' Nickel conc. in low C activity steel in wt %')
    CALL REED(WNI1)
    IF (WNI1 .GT. 15 .OR. WNI1 .LT. 0.0) THEN
        CALL BOUND(WNI1,15.0D0,0.0D0)
    ENDIF
    GOTO 200
5   WRITE(*,105)
105  FORMAT(10X,' Chromium conc. in low C activity steel in wt %')
    CALL REED(WCR1)
    IF (WCR1 .GT. 20 .OR. WCR1 .LT. 0.0) THEN
        CALL BOUND(WCR1,15.0D0,0.0D0)
    ENDIF
    GOTO 200
6   WRITE(*,106)
106  FORMAT(10X,' Molybdenum conc. in low C activity steel in wt %')
    CALL REED(WMO1)
    IF (WMO1 .GT. 15 .OR. WMO1 .LT. 0.0) THEN
        CALL BOUND(WMO1,15.0D0,0.0D0)
    ENDIF
    GOTO 200
7   WRITE(*,107)
107  FORMAT(10X,' Tungsten conc. in low C activity steel in wt %')
    CALL REED(WW1)
    IF (WW1 .GT. 15 .OR. WW1 .LT. 0.0) THEN
        CALL BOUND(WW1,15.0D0,0.0D0)
    ENDIF
    GOTO 200
8   WRITE(*,108)
108  FORMAT(10X,' Vanadium conc. in low C activity steel in wt %')
    CALL REED(WV1)
    IF (WV1 .GT. 15 .OR. WV1 .LT. 0.0) THEN
        CALL BOUND(WV1,15.0D0,0.0D0)
    ENDIF
    GOTO 200
9   WRITE(*,109)
109  FORMAT(10X,' Niobium conc. in low C activity steel in wt %')
    CALL REED(WNB1)
    IF (WNB1 .GT. 15 .OR. WNB1 .LT. 0.0) THEN
        CALL BOUND(WNB1,15.0D0,0.0D0)
    ENDIF
    GOTO 200
10  WRITE(*,110)

```



```

110  FORMAT(10X,' Cobalt conc. in low C activity steel in wt %')
      CALL REED(WCO1)
      IF (WCO1 .GT. 15 .OR. WCO1 .LT. 0.0) THEN
          CALL BOUND(WCO1,15.0D0,0.0D0)
      ENDIF
11  WRITE(*,111)
111  FORMAT(10X,' Carbon conc. in high C activity steel in wt %')
      CALL REED(WC2)
      IF (WC2 .GT. 5 .OR. WC2 .LT. 0.02) THEN
          CALL BOUND(WC2,5.0D0,2.0D-2)
      ENDIF
      GOTO 200
12  WRITE(*,112)
112  FORMAT(10X,' Manganese conc. in high C activity steel in wt %')
      CALL REED(WMN2)
      IF (WMN2 .GT. 15 .OR. WMN2 .LT. 0.02) THEN
          CALL BOUND(WMN2,15.0D0,2.0D-2)
      ENDIF
      GOTO 200
13  WRITE(*,113)
113  FORMAT(10X,' Silicon conc. in high C activity steel in wt %')
      CALL REED(WSI2)
      IF (WSI2 .GT. 15 .OR. WSI2 .LT. 0.02) THEN
          CALL BOUND(WSI2,15.0D0,2.0D-2)
      ENDIF
      GOTO 200
14  WRITE(*,114)
114  FORMAT(10X,' Nickel conc. in high C activity steel in wt %')
      CALL REED(WNI2)
      IF (WNI2 .GT. 15 .OR. WNI2 .LT. 0.0) THEN
          CALL BOUND(WNI2,15.0D0,0.0D0)
      ENDIF
      GOTO 200
15  WRITE(*,115)
115  FORMAT(10X,' Chromium conc. in high C activity steel in wt %')
      CALL REED(WCR2)
      IF (WCR2 .GT. 20 .OR. WCR2 .LT. 0.0) THEN
          CALL BOUND(WCR2,20.0D0,0.0D0)
      ENDIF
      GOTO 200
16  WRITE(*,116)
116  FORMAT(10X,' Molybdenum conc. in high C activity steel in wt %')
      CALL REED(WMO2)
      IF (WMO2 .GT. 15 .OR. WMO2 .LT. 0.0) THEN
          CALL BOUND(WMO2,15.0D0,0.0D0)
      ENDIF
      GOTO 200
17  WRITE(*,117)
117  FORMAT(10X,' Tungsten conc. in high C activity steel in wt %')
      CALL REED(WW2)
      IF (WW2 .GT. 15 .OR. WW2 .LT. 0.0) THEN
          CALL BOUND(WW2,15.0D0,0.0D0)
      ENDIF
      GOTO 200
18  WRITE(*,118)

```



```

118  FORMAT(10X,'Vanadium conc. in high C activity steel in wt %')
      CALL REED(WV2)
      IF (WV2 .GT. 15 .OR. WV2 .LT. 0.0) THEN
          CALL BOUND(WV2,15.0D0,0.0D0)
      ENDIF
      GOTO 200
19    WRITE(*,119)
119  FORMAT(10X,' Niobium conc. in high C activity steel in wt %')
      CALL REED(WNB2)
      IF (WNB2 .GT. 15 .OR. WNB2 .LT. 0.0) THEN
          CALL BOUND(WNB2,15.0D0,0.0D0)
      ENDIF
      GOTO 200
20    WRITE(*,120)
120  FORMAT(10X,' Cobalt conc. in high C activity steel in wt %')
      CALL REED(WCO2)
      IF (WCO2 .GT. 15 .OR. WCO2 .LT. 0.0) THEN
          CALL BOUND(WCO2,15.0D0,0.0D0)
      ENDIF
      GOTO 200
21    WRITE(*,121)
121  FORMAT(10X,' Temperature in Kelvin')
      CALL REED(KTEMP)
      IF (KTEMP .GT. 1700 .OR. KTEMP .LT. 900) THEN
          CALL BOUND(KTEMP,1700.0D0,900D0)
      ENDIF
      GOTO 200
22    WRITE(*,122)
122  FORMAT(10X ' Time in hours')
      CALL REED(THR)
      IF (THR .GT. 1.0D99 .OR. THR .LT. 1.0D-99) THEN
          CALL BOUND(THR,1.0D99,1.0D-99)
      ENDIF
      GOTO 200
      RETURN
      END

```

.....
.....
This subroutine prints out the logo at the head of the program

```

      SUBROUTINE LOGO(AVER)
      IMPLICIT DOUBLE PRECISION (A-Z)
      WRITE(*,1)
1     FORMAT(/)
      WRITE(*,2)
2     FORMAT(
&    10X,' *****')
      WRITE(*,3)
3     FORMAT(10X,' **',44X,'**')
      WRITE(*,3)
      WRITE(*,4)AVER
4     FORMAT(10X,' **',
&    ' CARBON DIFFUSION IN AUSTENITIC JOINTS ** ',/
&    10X,' **',44X,'**'/
&    8X' ** (Version ',F3.1,') ** ')

```



```

WRITE(*,3)
WRITE(*,3)
WRITE(*,3)
WRITE(*,5)
5  FORMAT(10X,'**',2X,' by ',
&    '**',)
WRITE(*,3)
WRITE(*,6)
6  FORMAT(10X,'**',2X,' J. M. Race & H. K. D. H. Bhadeshia ',
&    '**',)
WRITE(*,3)
WRITE(*,7)
7  FORMAT(10X,'**',2X,' University of Cambridge ',
&    '**',)
WRITE(*,3)
WRITE(*,8)
8  FORMAT(10X,'**',2X,' NEI Parsons Ltd. ',
&    '**',)
WRITE(*,3)
WRITE(*,3)
WRITE(*,2)
RETURN
END

```

.....

.....

This subroutine prints the results to the file AUS.RES.

```

SUBROUTINE RESULT(K,DA,DG,T,THR,D1,YC1,D2,YC2,M)
IMPLICIT DOUBLE PRECISION (A-H,K,N-Z), INTEGER(I,J,L,M)
DIMENSION D1(30),YC1(30),D2(30),YC2(30)
WRITE(2,6)T,THR
6  FORMAT(' TIME, SECONDS =',D8.2, ' HOURS =',F5.0///
&    ' MM CA -XMM CG ')
DO 10 I=1,M
WRITE(2,22)D1(I),YC1(I),D2(I),YC2(I)
10 CONTINUE
22  FORMAT(4D12.4,I4)
WRITE(2,60)DA,DG,K
60  FORMAT(' DIFFUSION COEFFICIENT DA, =',D12.4/
&    ' DIFFUSION COEFFICIENT DG, =',D12.4/
&    ' PARTITION COEFFICIENT =',F12.4//)
RETURN
END

```

.....

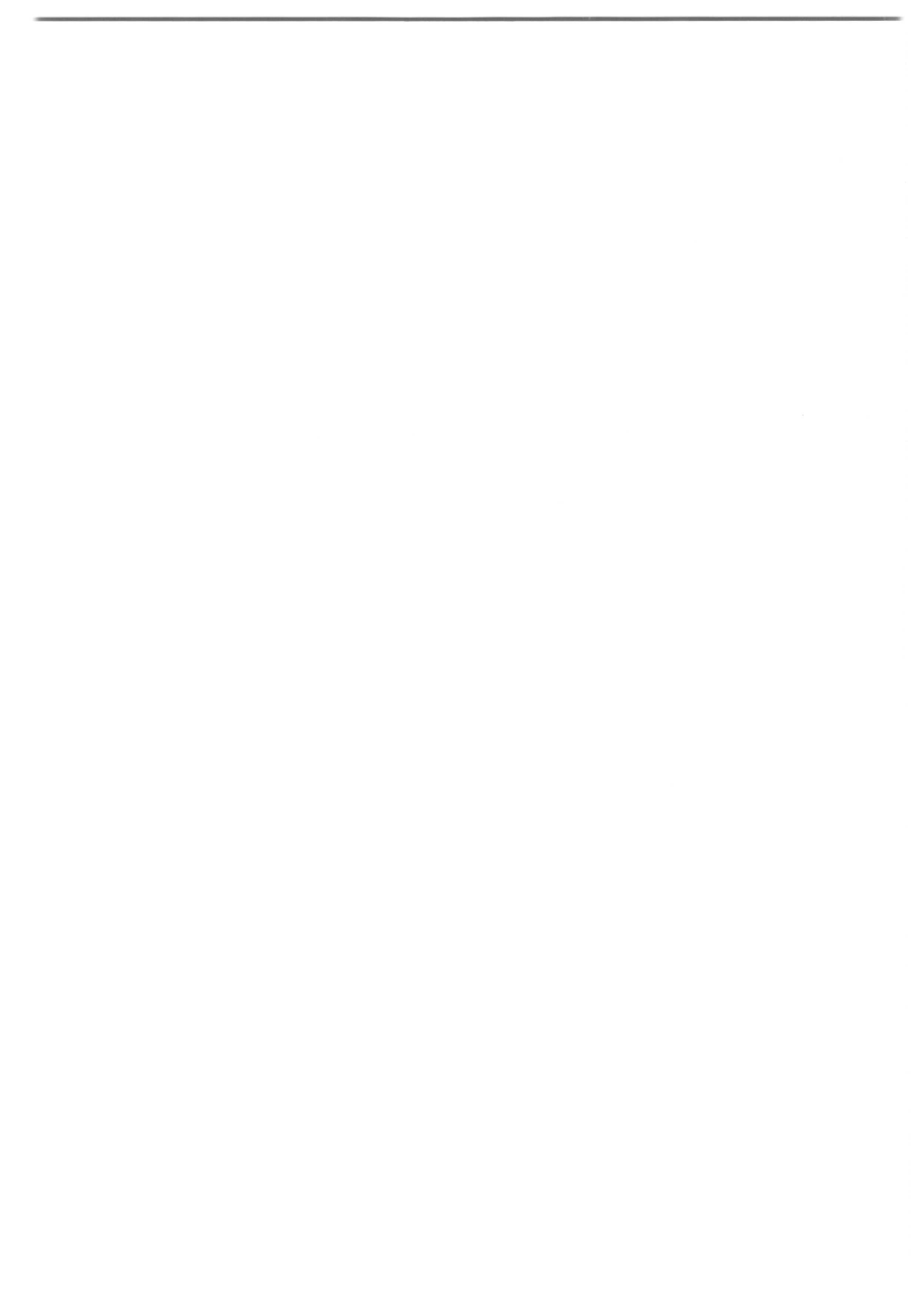
.....

This subroutine prints the results to the screen

```

SUBROUTINE RESP(K,CAG,CGA,DA,DG,T,THR,D1,YC1,D2,YC2,M)
IMPLICIT DOUBLE PRECISION (A-H,K,N-Z), INTEGER(I,J,L,M)
DIMENSION D1(30),YC1(30),D2(30),YC2(30)
WRITE(*,6)T,THR
6  FORMAT(' TIME, SECONDS =',D8.2, ' HOURS =',F5.0/
&    ' MM CA -XMM CG ')
DO 10 I=1,M
WRITE(*,22)D1(I),YC1(I),D2(I),YC2(I)

```



```

10 CONTINUE
WRITE(*,7)
7 FORMAT(/)
22 FORMAT(4D12.4,I4)
WRITE(*,60)DA,DG,K,CAG,CGA
60 FORMAT(' DIFFUSION COEFFICIENT DA, =',D12.4/
& ' DIFFUSION COEFFICIENT DG, =',D12.4/
& ' PARTITION COEFFICIENT =',F12.4/
& ' CAG=',D12.4/
& ' CGA=',D12.4/)
RETURN
END

```

.....

This subroutine produces a plot using NAG graphics routines

```

SUBROUTINE PLOT(D1,YC1,D2,YC2)
IMPLICIT DOUBLE PRECISION (A-H,K,N-Z), INTEGER(I,J,L,M)
DIMENSION D1(30),YC1(30),D2(30),YC2(30)
MAX = 26
CALL XXXXXX
CALL J06VAF(1,6)
CALL J06WAF
OPEN (6,FILE='AUS2.ERR')
CALL J06XDF(1,2,1,1)
CALL J06XDF(2,3,1,1)
CALL J06XDF(3,4,1,1)
CALL J06YMF(1)
IF (YC2(26) .LT. YC1(1)) THEN
    YMIN=YC2(26)*0.8
ELSEIF (YC1(1) .LT. YC1(26)) THEN
    YMIN=YC1(1)*0.8
ELSE
    YMIN=YC1(26)*0.8
ENDIF
IF (YC1(26) .GT. YC2(1)) THEN
    YMAX=YC1(26)*1.2
ELSEIF (YC2(1) .GT. YC2(26)) THEN
    YMAX=YC2(1)*1.2
ELSE
    YMAX=YC2(26)*1.2
ENDIF
CALL J06WBF(-25.0D0,25.0D0,YMIN,YMAX,1)
CALL J06ACF
CALL J06YMF(2)
CALL J06CCF(D1,YC1,MAX,2,10)
234 FORMAT(1X,4D12.4)
CALL J06CCF(D2,YC2,MAX,2,10)
CALL J06YAF(0,YC1(1))
CALL J06YCF(0,YC2(1))
CALL J06YMF(1)
CALL J06AEF
CALL J06YMF(3)
CALL J06AJF(2,'Carbon concentration /wt%')
CALL J06AHF('CARBON CONCENTRATION PROFILE ')

```



```
CALL J06AJF(1,'Distance from interface /mm')  
CALL J06WZF  
RETURN  
END
```

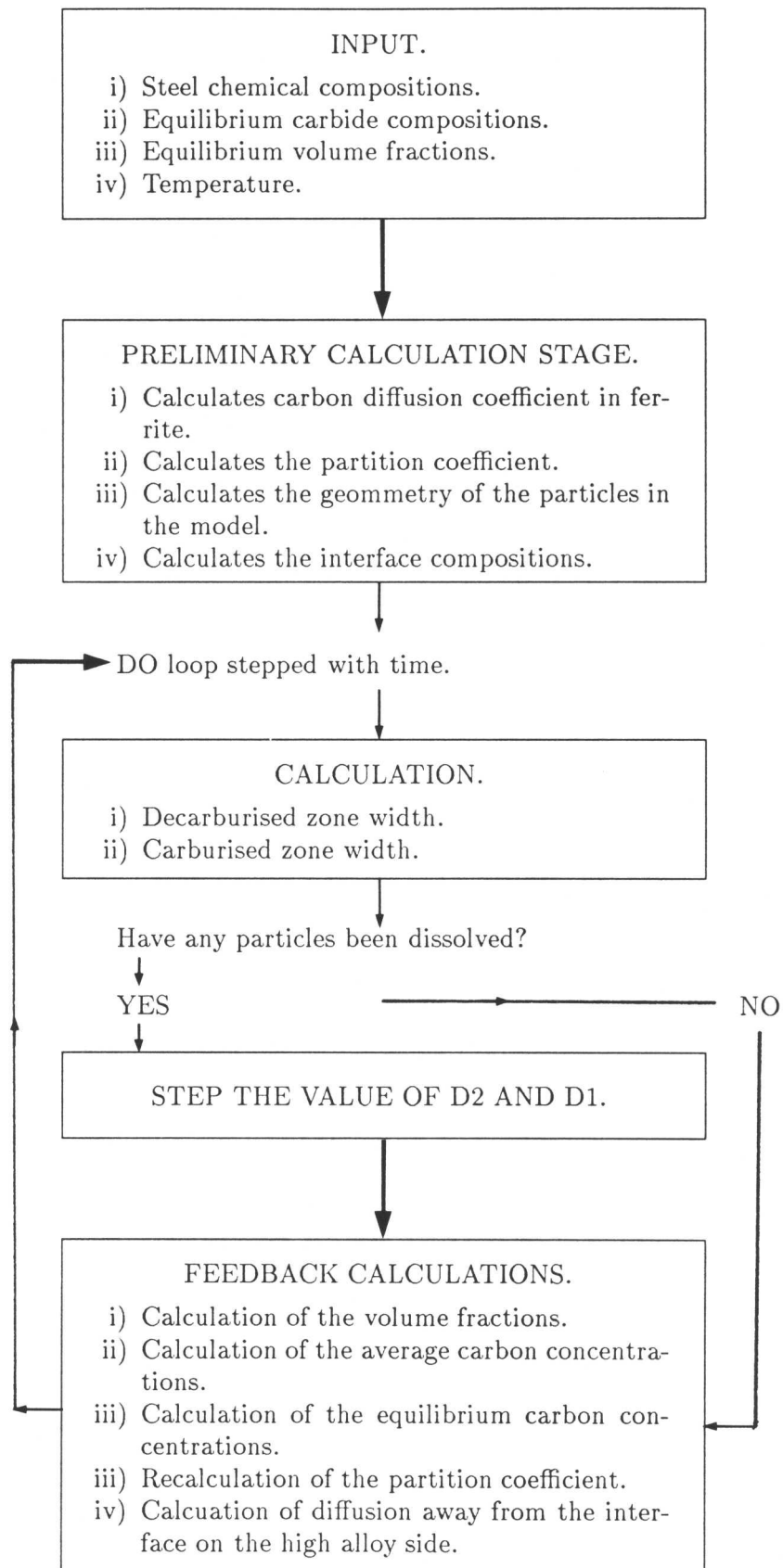
.....
.....



Appendix III
Program listing for calculating decarburised zone widths
with ferrite on both sides of the interface



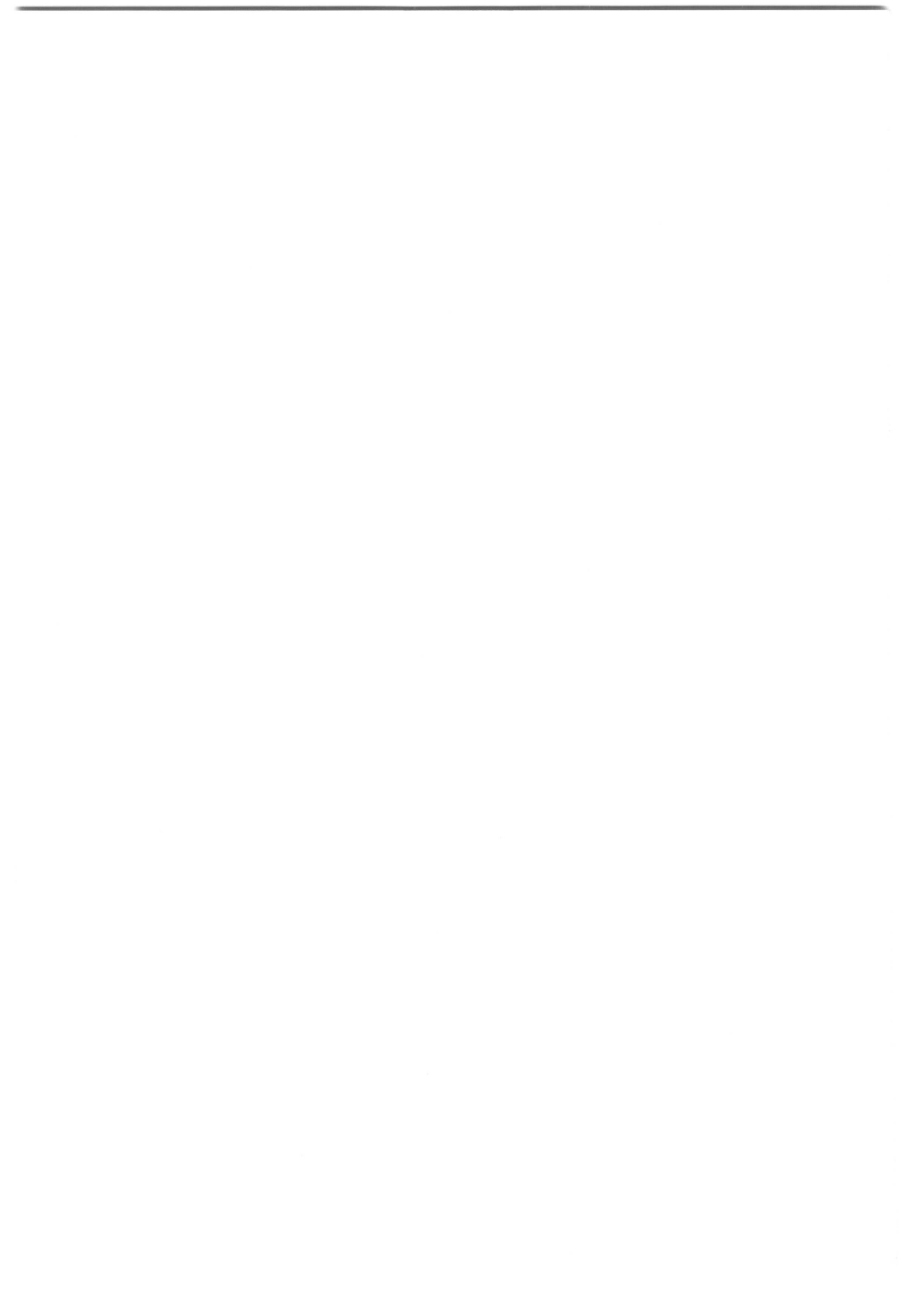
The Ferrite Model – Flow diagram.





.....
This program is a particulate model for the diffusion of carbon across dissimilar metal joints
in the ferrite phase field.
The nomenclature is described as follows:-
.....

ATHR is the root of the time in hours
AVER is the version number.
BA is the number of the dissolving particle on the high carbon activity side
BB is the number of the dissolving particle on the low carbon activity side
CBARA is the average carbon concentration in the high carbon activity slice (\bar{x}_α)
CBARB is the average carbon concentration in the low carbon activity slice (\bar{x}_β)
CZW is the carburised zone width (η^β)
DA is the diffusion coefficient in the high carbon activity side.
DB is the diffusion coefficient in the low carbon activity side.
DZW is the decarburised zone width (η^α)
D1 is the slab size on the high carbon activity side of the interface
D10 is the initial slab size on the high carbon activity side of the interface
D2 is the particle size on the high carbon activity side
D20 is the initial particle size on the high carbon activity side
D3 is the interparticle spacing on the high carbon activity side
D4 is the particle size on the low carbon activity side of the interface
D40 is the initial particle size on the low carbon activity side of the interface
D5 is the slab size on the low carbon activity side
D6 is the interparticle spacing on the low carbon activity side
D60 is the interparticle spacing on the low carbon activity side
K is the partition coefficient.
KTEMP is the absolute temperature
T is the time in hours
TSEC is the time in seconds
VFEA is the equilibrium volume fraction on the high carbon activity side (calculated from MTDATA)
VFEB is the equilibrium volume fraction on the low carbon activity side (calculated from MTDATA)
VFA is the volume fraction of carbide at time T on the high carbon activity side (v_α)
VFB is the volume fraction of carbide at time T on the low carbon activity side (v_β)
WAAL is the concentration of carbon in the carbide in equilibrium with the matrix on the high
carbon activity side /wt% ($x^{A\alpha}$)
WAAL0 is the initial value of WAAL when T=0
WALA is the concentration of carbon in the matrix in equilibrium with carbide on the high
carbon activity side /wt% ($x^{\alpha A}$)
WALA0 is the initial value of WALA when T=0
WALBE is the carbon concentration at the weld junction in the high carbon activity side /wt% ($x^{\alpha\beta}$)
WBBE is the concentration of carbon in the carbide in equilibrium with the matrix on the low
carbon activity side /wt% ($x^{B\beta}$)
WBBE0 is the initial value of WBBE when T=0
WBEAL is the carbon concentration at the weld junction in the low carbon activity side /wt% ($x^{\beta\alpha}$)
WBEB is the concentration of carbon in the matrix in equilibrium with carbide on the low
carbon activity side /wt% ($x^{\beta B}$)
WBEB0 is the initial value of WBEB *i.e.* when T=0
WX1 is the weight percent of element X on the high carbon activity side.
WX2 is the weight percent of element X on the low carbon activity side.
XX1 is the mole fraction of element X on the high carbon activity side.
XX2 is the mole fraction of element X on the low carbon activity side.
ZIA is the distance of the particle from the interface at the end of the time step on the
high carbon activity side (z_i^A)
ZIAS is the square root of ZIA.
ZJB is the distance of the particle from the interface at the end of the time step on the low



carbon activity side(z_j^B)
 ZOA is the distance of the particle from the interface at the start of the time step on the
 high carbon activity side (z_o^A)
 ZOB is the distance of the particle from the interface at the start of the time step on the low
 carbon activity side (z_o^B)

.....
 The subroutines for reading and displaying the data are the same as for the previous model and will
 not be repeated in this listing


```

      IMPLICIT DOUBLE PRECISION (A,C-I,K,M-S,U-Z)
      DOUBLE PRECISION TSEC
      INTEGER J,L,BA,T,BB,JM
      AVER=1.1
  
```

Subroutines LOGO, DATA1-3 and DDTA all collect and display the data with options to make any changes

```

      CALL LOGO(AVER)
      CALL DATA1(WC1,WMN1,WSI1,WNI1,WCR1,WMO1,WW1,WV1,WNB1,WCO1)
      CALL DATA2(WC2,WMN2,WSI2,WNI2,WCR2,WMO2,WW2,WV2,WNB2,WCO2)
      CALL DATA3(KTEMP,WALAE,WBEBE,WAAL,WBEE,VFEA,VFEB)
500    CALL DDTA(WC1,WMN1,WSI1,WNI1,WCR1,WMO1,WW1,WV1,WNB1,WCO1,
      &    WC2,WMN2,WSI2,WNI2,WCR2,WMO2,WW2,WV2,WNB2,WCO2,KTEMP,WALA,
      &    WBEB,WAAL,WBEE,VFEA,VFEB)
  
```

Subroutine CON converts the data from weight per cent to mole fraction

```

      CALL CON(WC1,WMN1,WSI1,WNI1,WCR1,WMO1,WW1,WV1,WNB1,WCO1,
      &    XC1,XMN1,XSI1,XNI1,XCR1,XMO1,XW1,XV1,XNB1,XCO1)
      CALL CON(WC2,WMN2,WSI2,WNI2,WCR2,WMO2,WW2,WV2,WNB2,WCO2,
      &    XC2,XMN2,XSI2,XNI2,XCR2,XMO2,XW2,XV2,XNB2,XCO2)
  
```

Subroutine DIFF calculates the diffusion coefficient of carbon in ferrite.

```

      CALL DIFF(KTEMP,DA)
      CALL DIFF(KTEMP,DB)
  
```

The KFUN subroutines calculate the partition coefficients by one of the methods below.

```

      WRITE(*,*)' For the calculation of partition coefficient;'
      WRITE(*,*)' Method 1 = Wagner'
      WRITE(*,*)' Method 2 = Wada et al'
      CALL REEDI(J)
      IF (J .EQ. 1) THEN
          CALL KFUN1(XC1,XMN1,XSI1,XNI1,XCR1,XMO1,XW1,XV1,XNB1,XCO1,
      &    XC2,XMN2,XSI2,XNI2,XCR2,XMO2,XW2,XV2,XNB2,XCO2,KTEMP,K)
      ELSEIF (J .EQ. 2) THEN
          CALL KFUN2(WCR1,WC1,KTEMP,WC2,WCR2,K)
      ENDIF
  
```

The distances D1-D6 are calculated from the inputed value of the particle size and the volume fraction.

.....
 High carbon activity side - setting up the dimensions of the model

```

      XY=5.0D-06
      D2=XY
      D20=D2
      D10=D20/VFA
      D1=D10
  
```



```

D3=(D1-D2)
ZOA=D3/2
ZIA=ZOA
WALA=WALAE
WAAL=WAALE

```

.....

Low carbon activity side - setting up the dimensions of the model

```

D4=XY
D40=D4
D5=D4/VFB
D6=(D5-D4)
D60=D6
ZOB=D6/2+D4
ZJB=ZOB
WBEB=WBEBE
WBBE=WBBEE

```

The calculations are made of the interface concentrations using equations (7.12) and (7.13) for the linear model

```

WALBE=((ZOA*WALA)+(ZOB*WBEB))/((K*ZOB)+ZOA)
WBEAL=K*WALBE
T=0
BA=0
BB=0
JT=0
JA=0
JM=0
WRITE(*,32)

```

32 FORMAT(2X'ATHR', 'DMW',8X,'BA')

This DO loop calculates the distance of the carbide from the interface ZIA at various times T and then recalculates the values of the distances and the average carbon concentration and volume fractions.

```

DO 30 T=0,10000
  JT=JT+1
  TSEC=T*3600

```

The values of ZIA and ZJB are calculated using the equations (7.7) and (7.8)

```

ZIAS=((2.0D0*DA*(WALA-WALBE)*TSEC)/(WAAL-WALA))+ZOA**2
ZIA=DSQRT(ZIAS)
ZJBS=(DB*((WBEAL-WBEB)/(WBBE-WBEB))*TSEC*2.0D0)+ZOB**2
ZJB=DSQRT(ZJBS)
DZW=(ZIA-ZOA)+(ZOA)+(BA*D10)
CZW=(ZJB-ZOB)+((BB+1)*D40)

```

The calculated values of DZW and CZW are converted to millimetres

```

DZW=DZW*1.0D+03
CZW=CZW*1.0D+03
D6=D60-(ZJB-ZOB)
ATHR=(TSEC/3600)**0.5
IF (TSEC .EQ. 0.0) THEN
  WRITE(*,31)ATHR,DZW,BA
ENDIF

```

This IF-ELSE loop checks to see if any particles have been dissolved in which case it goes

onto the next particle

```

IF ((ZIA-ZOA) .GE. (D20*(BA+1)))THEN
  BA=BA+1
  D1=D10*(BA+1)
  D2=D20*(BA+1)
  JA=1
  VFA=(D2/D1)
  VFB=(D4/D5)
  CBARA=(WAAL*VFA + (WALA*(1.0-VFA)))
  CBARB=(WBEB*VFB + (WBEB*(1.0-VFB)))
ELSE
  D2=(D20*(BA+1))-(ZIA-ZOA)
  D4=(D40*(BB+1))+(ZJB-ZOB)
  VFA=(D2/D1)
  VFB=(D4/D5)

```

The average carbon concentrations on either side of the weld are calculated using equations (7.48) and (7.49)

```

CBARA=(WAAL*VFA + (WALA*(1.0-VFA)))
CBARB=(WBEB*VFB + (WBEB*(1.0-VFB)))

```

If a particle has just been dissolved then the interface concentrations are recalculated using the SUBROUTINE INTER

```

IF (JA .EQ. 1) THEN
  CALL INTER(WALA,WAAL,CBARA,WBEB,WBEB,CBARB,ZJB,ZIA,
&           K,WALBE,WBEAL,JM)
  IF (JM .EQ. 1) GOTO 501
  JA=0
  WRITE(*,31)ATHR,DZW,BA
ENDIF

```

This IF statement checks to see whether the space between particles on the low carbon activity side has been filled with carbide

```

IF ((ZJB-ZOB) .GT. (D60*(BB+1))) THEN
  BB=BB+1
  D5=D5*(BB+1)
ENDIF
ENDIF

```

This IF routine checks that the space between the carbides has not been filled as a result of diffusion away from the interface

```

IF ((D60-ZH) .LT. D6)) THEN
  CALL BACK(DB,WBEB,WBEBE,TSEC,WBEE,D6,CBARB,DELC)
ENDIF
B=WALA-WALBE
B2=-B
CALL CON(CBARA,WMN1,WSI1,WNI1,WCR1,WMO1,WW1,WV1,WNB1,WCO1,
&        XC1,XMN1,XSI1,XNI1,XCR1,XMO1,XW1,XV1,XNB1,XCO1)
CALL CON(CBARB,WMN2,WSI2,WNI2,WCR2,WMO2,WW2,WV2,WNB2,WCO2,
&        XC2,XMN2,XSI2,XNI2,XCR2,XMO2,XW2,XV2,XNB2,XCO2)

```

A new value of the partition coefficient is calculated as a result of the changing carbon concentrations

```

IF (J .EQ.1) THEN
  CALL KFUN1(XC1,XMN1,XSI1,XNI1,XCR1,XMO1,XW1,XV1,XNB1,XCO1,
&          XC2,XMN2,XSI2,XNI2,XCR2,XMO2,XW2,XV2,XNB2,XCO2,KTEMP,K)

```



```

ELSEIF (J .EQ. 2) THEN
    CALL KFUN2(WCR1,CBARA,KTEMP,CBARB,WCR2,K)
ENDIF
ATHR=(TSEC/3600)**0.5
31    FORMAT(2D12.4,I4)
30    CONTINUE
    WRITE(*,50)
50    FORMAT(///)
    WRITE(*,*)'Type 0 to amend data or 1 to quit'
    CALL REEDI(L)
    IF (L .EQ. 0) THEN
        GOTO 500
    ELSEIF (L .EQ. 1) THEN
        GOTO 501
    ENDIF
    STOP
501    END

```

.....

This subroutine calculates the changes in the equilibrium carbon concentrations as a result of the change in carbon concentrations. The equations are calculated by fitting curves to data calculated using MTDATA. These equations are for the 9Cr/2 $\frac{1}{4}$ CrMo joint at 620°C. The rest of the equations are given at the end of this appendix.

```

SUBROUTINE INTER(WALA,WAAL,CBARA,WBEB,WBEBE,CBARB,ZJB,ZIA,
&    K,WALBE,WBEAL,JM)
IMPLICIT DOUBLE PRECISION(A-I,K-Z)
INTEGER JM
WALA=3.5189D-05*(10**(5.138*CBARA))
WAAL=5.0834-(0.49266*CBARA)+(3.1529*CBARA**2)-24.958
&    *(CBARA**3)+62.901*(CBARA**4)
WBEB=2.2060D-04-(2.731D-04*CBARB)+
&    (2.2857D-04*(CBARB**2))
WBEBE=8.6412-(0.22853*DLOG10(CBARB))
WALBE=((ZIA*WALA)+(ZJB*WBEB))/((K*ZJB)+ZIA)
WBEAL=K*WALBE
IF (WALA .LT. WALBE .OR. WBEAL .LT. WBEBE) THEN
    JM=1
    GOTO 44
ENDIF
44    RETURN
END

```

.....

This subroutine calculates the amount of diffusion that is occurring away from the interface on the high alloy side.

DEFC is the amount of carbon that has diffused from slice 1 to slice 2 on the high alloy side

```

SUBROUTINE BACK(DB,WBEB,WBEBE,TSEC,WBEE,D6,CBARB,DELC,ZH)
IMPLICIT DOUBLE PRECISION (A-Z)
ZH=DSQRT(((2*DB*(WBEB-WBEBE)*TSEC)/(WBEBE-WBEE)+(D6**2))
DEFC=(D6-ZH)*(WBEE-WBEBE)
CBARB=CBARB-DEFC
RETURN
END

```


.....

 This is a subroutine to calculate the Wagner activity coefficient. EX is
 the Wagner interaction parameter between element X and carbon, ϵ_{ij}

```

SUBROUTINE KFUN1(XC1,XMN1,XSI1,XNI1,XCR1,XMO1,XW1,XV1,XNB1,
&   XCO1,XC2,XMN2,XSI2,XNI2,XCR2,XMO2,XW2,XV2,XNB2,XCO2,KTEMP,K)
IMPLICIT DOUBLE PRECISION (A-Z)
EC=8910/KTEMP
EMN=-5070/KTEMP
ESI=4.84-(7370/KTEMP)
ENI=-2.2+(7600/KTEMP)
ECR=24.4-(38400/KTEMP)
EMO=3.855-(17870/KTEMP)
EW=23.4-(36114/KTEMP)
EV=-24660/KTEMP
ENB=-28770/KTEMP
ECO=2800/KTEMP
LAC1=(XC1*EC)+(XMN1*EMN)+(XSI1*ESI)+(XNI1*ENI)+(XCR1*ECR)+
&   (XMO1*EMO)+(XW1*EW)+(XV1*EV)+(XNB1*ENB)+(XCO1*ECO)
AC1=DEXP(LAC1)
LAC2=(XC2*EC)+(XMN2*EMN)+(XSI2*ESI)+(XNI2*ENI)+(XCR2*ECR)+
&   (XMO2*EMO)+(XW2*EW)+(XV2*EV)+(XNB2*ENB)+(XCO2*ECO)
AC2=DEXP(LAC2)
K=AC1/AC2
RETURN
END

```

.....

 This subroutine calculates the partition coefficient from the empirical
 equations of Wada *et al.* (1972)
 AFC is the natural logarithm of the activity coefficient
 FC is the activity coefficient

```

SUBROUTINE KFUN2(WCR1,WC1,KTEMP,WC2,WCR2,K)
IMPLICIT DOUBLE PRECISION(A-H,K,N-Z), INTEGER(I,J,L,M)
AFC1=2300/KTEMP-2.24+((179/KTEMP)*WC1)-((102/KTEMP)-0.033)*WCR1
FC1=DEXP(AFC1)
AFC2=2300/KTEMP-2.24+((179/KTEMP)*WC2)-((102/KTEMP)-0.033)*WCR2
FC2=DEXP(AFC2)
K=FC1/FC2
RETURN
END

```

.....

 This subroutine calculates the diffusion coefficient of carbon in ferrite
 as described in Section (7.3) using the model due to McLellan *et al.* (1965)
 DOTO is the diffusion coefficient for carbon atoms jumping from an octahedral to
 an octahedral site via a tetrahedral site
 DTOT is the diffusion coefficient for carbon atoms jumping from a tetrahedral to
 a tetrahedral site via an octahedral site
 DTT is the diffusion coefficient for carbon atoms jumping from a tetrahedral to
 a tetrahedral site
 D is the diffusion coefficient of carbon in ferrite



PHI and F are as defined in McLellan *et al.* (1965)

```
SUBROUTINE DIFF(KTEMP,D)
DOUBLE PRECISION R,KTEMP,PHI,DOTO,DTT,F,D
R=8.314
PHI=1.0D0-1.0/(0.5D0*DEXP(7.2D03*4.184/(R*KTEMP))
& *DEXP(4.4D0)+1.0D0)
DOTO=3.3D-07*DEXP(-19.3D03*4.184D0/(R*KTEMP))
DTT=3.0D-4*DEXP(-14.7D03*4.184D0/(R*KTEMP))
F=0.86D0
D= PHI*DOTO+(1.0D0-PHI)*F*DTT+(1.0D0-PHI)
& *(1.0D0-F)*DOTO
RETURN
END
```

.....



.....
Subroutine INTER for the other joints studied
.....

Mild steel/2 $\frac{1}{4}$ CrMo at 730°C
.....

```
      SUBROUTINE INTER(WALA,WAAL,CBARA,WBEB,WBBE,CBARB,ZJB,ZIA,  
&      K,WALBE,WBEAL,JM)  
      IMPLICIT DOUBLE PRECISION(A-I,K-Z)  
      INTEGER JM  
      WALA=(1.1004D-02)+(4.5057D-03*CBARA)-  
&      (4.2857D-03*CBARA**2)  
      WAAL=6.7006-(3.3143D-02*CBARA)+(5.714D-02*CBARA**2)  
      IF (CBARB .LT. 0.4) THEN  
          WBEB=5.6098D-04*(10**(2.9965*CBARB))  
          WBBE=5.1090-(1.1479*CBARB)+(3.3126*CBARB**2)  
      ELSE  
          WBEB=(4.6043D-03)+(6.7886D-03*CBARB)-(1.8571D-03*CBARB**2)  
          WBBE=6.8311-(0.45905*CBARB)+(0.29452*CBARB**2)  
      ENDIF  
      WALBE=((ZIA*WALA)+(ZJB*WBEB))/(ZIA+(K*ZJB))  
      WBEAL=K*WALBE  
      IF (WALA .LT. WALBE .OR. WBEAL .LT. WBEB) THEN  
          JM=1  
          GOTO 44  
      ENDIF  
44     RETURN  
      END
```

.....
Mild steel/2 $\frac{1}{4}$ CrMo at 620°C
.....

```
      SUBROUTINE INTER(WALA,WAAL,CBARA,WBEB,WBBE,CBARB,ZJB,ZIA,  
&      K,WALBE,WBEAL,JM)  
      IMPLICIT DOUBLE PRECISION(A-I,K-Z)  
      INTEGER JM  
      WALA=(3.6078D-03)+(4.3603D-03*CBARA)-(4.714D-03*CBARA**2)  
      WAAL=6.7006-(5.5714D-02*CBARA)+(8.5714D-02*CBARA**2)  
      IF (CBARB .LT. 0.35) THEN  
          WBEB=2.543D-05*(10**(5.7632*CBARB))  
          WBBE=5.1696-(1.5866*CBARB)+(3.9714*CBARB**2)  
      ELSE  
          WBEB=3.6619D-03+(3.7685D-03*(DLOG10(CBARB)))  
          WBBE=6.7469-(0.17175*CBARB)+(6.1824D-02*CBARB**2)  
      ENDIF  
      WALBE=((ZIA*WALA)+(ZJB*WBEB))/((K*ZJB)+ZIA)  
      WBEAL=K*WALBE  
      IF (WALA .LT. WALBE .OR. WBEAL .LT. WBEB) THEN  
          JM=1  
          GOTO 44  
      ENDIF  
44     RETURN  
      END
```



.....
.....
Mild steel/1CrMo at 700°C
.....

```
      SUBROUTINE INTER(WALA,WAAL,CBARA,WBEB,WBBE,CBARB,ZJB,ZIA,  
&      K,WALBE,WBEAL,JM)  
      IMPLICIT DOUBLE PRECISION(A-I,K-Z)  
      INTEGER JM  
      WALA=(1.1004D-02)+(4.5057D-03*CBARA)-(4.2857D-03*CBARA**2)  
      WAAL=6.7006-(3.3143D-02*CBARA)+(5.714D-02*CBARA**2)  
      IF (CBARB .LT. 0.3) THEN  
          WBEB=-5.5371D-04+(3.6744D-02*CBARB)-(1.013D-02*CBARB**2)  
          WBBE=4.9424+(0.45291*CBARB)  
      ELSE  
          WBEB=(6.1877D-03)+(1.539D-02*CBARB)-(9.1372D-03*CBARB**2)  
          WBBE=6.7857-(0.46469*CBARB)+(0.52338*CBARB**2)  
      ENDIF  
      WALBE=((ZIA*WALA)+(ZJB*WBEB))/((K*ZJB)+ZIA)  
      WBEAL=K*WALBE  
      IF (WALA .LT. WALBE .OR. WBEAL .LT. WBEB) THEN  
          JM=1  
          GOTO 44  
      ENDIF  
44     RETURN  
      END
```

.....
.....
Mild steel/1CrMo at 620°C
.....

```
      SUBROUTINE INTER(WALA,WAAL,CBARA,WBEB,WBBE,CBARB,ZJB,ZIA,  
&      K,WALBE,WBEAL,JM)  
      IMPLICIT DOUBLE PRECISION(A-I,K-Z)  
      INTEGER JM  
      WALA=(3.6078D-03)+(4.3603D-03*CBARA)-(4.714D-03*CBARA**2)  
      WAAL=6.7006-(5.5714D-02*CBARA)+(8.5714D-02*CBARA**2)  
      IF (CBARB .LT. 0.1) THEN  
          WBEB=2.5017D-04+(1.2517D-04*CBARB)+(1.5444D-03*CBARB**2)  
          WBBE=4.9588+(0.42104*CBARB)  
      ELSE  
          WBEB=(1.4114D-03)+(5.7409D-03*CBARB)-(2.8689D-03*CBARB**2)  
          WBBE=6.6328-(0.13215*DLOG10(CBARB))  
      ENDIF  
      WALBE=((ZIA*WALA)+(ZJB*WBEB))/((K*ZJB)+ZIA)  
      WBEAL=K*WALBE  
      IF (WALA .LT. WALBE .OR. WBEAL .LT. WBEB) THEN  
          JM=1  
          GOTO 44  
      ENDIF  
44     RETURN  
      END
```



2 $\frac{1}{4}$ CrMo/9CrMo at 730°C

```
.....  
SUBROUTINE INTER(WALA,WAAL,CBARA,WBEB,WBBE,CBARB,ZJB,ZIA,  
& K,WALBE,WBEAL,JM)  
IMPLICIT DOUBLE PRECISION(A-I,K-Z)  
INTEGER JM  
WALA=1.4854D-03*(10**(2.10*CBARA))  
WAAL=5.0441-(0.24299*CBARA)+(0.49609*(CBARA**2))  
WBEB=2.2632D-03-(1.3115D-03*CBARB)+(4.5924D-03*(CBARB**2))  
WBBE=8.6538-0.24565*DLOG10(CBARB)  
WALBE=((ZIA*WALA)+(ZJB*WBEB))/((K*ZJB)+ZIA)  
WBEAL=K*WALBE  
IF (WALA .LT. WALBE .OR. WBEAL .LT. WBEB) THEN  
    JM=1  
    GOTO 44  
ENDIF  
44 RETURN  
END
```

2 $\frac{1}{4}$ CrMo/12CrMo at 730°C

```
.....  
SUBROUTINE INTER(WALA,WAAL,CBARA,WBEB,WBBE,CBARB,ZJB,ZIA,  
& K,WALBE,WBEAL,JM)  
IMPLICIT DOUBLE PRECISION(A-I,K-Z)  
INTEGER JM  
WALA=1.4854D-03*(10**(2.10*CBARA))  
WAAL=5.0441-(0.24299*CBARA)+(0.49609*(CBARA**2))  
WBEB=1.0847D-03-(7.0130D-05*CBARB)+(2.7296D-03*(CBARB**2))  
WBBE=5.4254+(0.34275*DLOG10(CBARB))  
WALBE=((ZIA*WALA)+(ZJB*WBEB))/(ZIA+(K*ZJB))  
WBEAL=K*WALBE  
IF (WALA .LT. WALBE .OR. WBEAL .LT. WBEB) THEN  
    JM=1  
    GOTO 44  
ENDIF  
44 RETURN  
END
```

2 $\frac{1}{4}$ CrMo/12CrMo at 620°C

```
.....  
SUBROUTINE INTER(WALA,WAAL,CBARA,WBEB,WBBE,CBARB,ZJB,ZIA,  
& K,WALBE,WBEAL,JM)  
IMPLICIT DOUBLE PRECISION(A-I,K-Z)  
INTEGER JM  
WALA=3.5189D-05*(10**(5.138*CBARA))  
WAAL=5.0834-(0.49266*CBARA)+(3.1529*CBARA**2)-24.958*(CBARA**3)+  
& 62.901*(CBARA**4)  
WBEB=2.9018D-04-(1.1251D-03*CBARB)+(1.4576D-03*(CBARB**2))  
WBBE=5.4562+(0.42155*DLOG10(CBARB))
```



```
WALBE=((ZIA*WALA)+(ZJB*WBEB))/((K*ZJB)+ZIA)
WBEAL=K*WALBE
IF (WALA .LT. WALBE .OR. WBEAL .LT. WBEB) THEN
    JM=1
    GOTO 44
ENDIF
44  RETURN
END
```

.....
